Distribution Agreement

Signature:

______________________________ ______________

Fadi Emad Pulous Date

Integrin Signaling in the Vascular Endothelium

By

Fadi Emad Pulous
Doctor of Philosophy

Graduate Division of Biological and Biomedical Sciences
Cancer Biology

____
Brian Petrich, Ph.D.
Advisor

____
Andrew Kowalczyk, Ph.D.
Committee Member

____
Melissa Gilbert-Ross, Ph.D.
Committee Member

____
Renhao Li, Ph.D.
Committee Member

____
Adam Marcus, Ph.D.
Committee Member

Accepted:

____
Lisa A. Tedesco, Ph.D.
Dean of the James T. Laney School of Graduate Studies

____
Date

Integrin Signaling in the Vascular Endothelium

By:

Fadi Emad Pulous
B.A., Vanderbilt University, 2013

Advisor: Brian G. Petrich, Ph.D.

An abstract of
A dissertation submitted to the Faculty of the
James T. Laney School of Graduate Studies of Emory University
in partial fulfillment of the requirements for the degree of
Doctor of Philosophy
in Graduate Division of Biological and Biomedical Sciences
Cancer Biology
2019

Abstract

Integrin Signaling in the Vascular Endothelium

By: Fadi Emad Pulous

Understanding the mechanisms by which endothelial cells (ECs) coordinate vascular growth and maintenance has been essential in efforts to modulate EC function in disease states. ECs interact with the ECM through integrin adhesion receptors which are required for EC migration and proliferation. The upregulation of integrin affinity for extracellular ligands, integrin activation, depends on the binding of talin, a cytoskeletal adaptor, to the β integrin tail. EC talin1 is essential for embryonic angiogenesis in mice. Here, I utilized inducible, EC-specific murine models to delete talin1 or induce the expression of an integrin-activation deficient mutant, talin1 L325R to investigate the role of talin and talin-dependent integrin activation in postnatal angiogenesis and in the maintenance of established vessels.

Inducible deletion of talin1 during early postnatal development resulted in vascular hemorrhage, impaired angiogenesis and lethality. Expression of talin1 L325R in ECs during postnatal development impaired retinal angiogenesis but lethality or vascular hemorrhage were not observed in Tln1 L325R mice. However, Tln1 L325R mice were smaller at weaning and throughout adulthood. Interestingly, subcutaneous B16-F0 melanomas grew more slowly in Tln1 L325R mice and showed a marked reduction in tumor angiogenesis. These data indicate that talin-dependent integrin activation is indispensable for postnatal developmental and pathological angiogenesis.

To investigate the role of talin expression in established blood vessels, EC talin deletion was induced in adult mice. EC talin1 deletion caused death 16-20 days after deletion associated with leaky intestinal vasculature. Intestinal ECs of Tln1 EC-KO mice formed cyst-like structures that were detached from neighboring cells with disorganized adherens junctions. Tln1 deletion in cultured ECs promoted cytoskeletal contraction, adherens junction disorganization and diminished barrier function. Genetic and pharmacological experiments suggested that talin was functioning to maintain barrier function primarily by activating β1 integrin.

These results provide important novel insights into how EC integrin activation contributes to blood vessel development and integrity. Future studies building upon this work should reveal new strategies to therapeutically target integrin signaling in order to modulate blood vessel growth and EC barrier function.

Integrin Signaling in the Vascular Endothelium

By:

Fadi Emad Pulous
B.A., Vanderbilt University, 2013

Advisor: Brian G. Petrich, Ph.D.

A dissertation submitted to the Faculty of the
James T. Laney School of Graduate Studies of Emory University
in partial fulfillment of the requirements for the degree of
Doctor of Philosophy
in Graduate Division of Biological and Biomedical Sciences
Cancer Biology
2019

Acknowledgements

Without a doubt, my dissertation would not have come to fruition without the never-ending support, love and sacrifice of my wife, Lesley. A smart, compassionate and incredible woman who has moved far from home and family to accommodate my career development without hesitation. The many nights I have come home to a healthy meal are innumerable but far more integral to the receipt of my terminal degree has been the emotional support and love that has been endless. Thank you so very much for what you have and continue to do for our family. To the Burnett family, thank you for being a tremendous source of encouragement and for letting me be a part of your family.

To my family: thank you for your immovable care and love during this sometimes-tenuous journey. I will never be able to express sufficient gratitude for my parents who have moved half-way across the world from our roots to provide my sisters and me with every possibly avenue for success. Their hard work and sacrifice is a constant motivation at all times. To my sisters Vian and Mimi; one of the most uplifting and motivating aspects of the last 5.5 years has been watching you grow into such smart, caring young women. There is no shortage of entertainment, love and support when I am with you or just talking to you from a distance and for that I will always be grateful.

To my extended family who have supported me from the great state of Michigan all the way to my cousins who I grew up with in Nashville: I am so proud and humbled to call you my aunts, uncles, cousins and grandparents because without your motivating support over the last years, I would not be where I am today. Absence does indeed make the heart grow fonder and I cherish the time we spend together when I am away from the lab in Nashville or Michigan and I look forward to what the future holds for all of us. To my Nana Ferial, I love you very much and you are an inspiration to our entire family. To my family who is no longer with me today: My Nana Marie, my Gedos Odeesh and Sulaiman, and my Uncle Adnan. Not a day goes by where I do not remember you and the times we shared together.

To my friends, Alex, Tim, Pat, Chen, Ed and to those who I have not listed because of space/formatting issues: You have all made the last 5.5 years immeasurably easier thanks to the laughter we've shared along the way. We've made a lot of memories and I know there are more to come.

Last, but certainly not least I would like to thank my advisor and friend, Dr. Brian Petrich. You took a chance on your first PhD student with his sub-par undergrad tenure and through careful guidance have helped me find my way into an academic career. I have been purposeful in my acknowledgements to not depict my training with any negative connotation because to insinuate that I have received anything other than positive support, rigorous scientific training and a valued friendship through these last years would be dishonest. Thank you for taking a chance on me and for helping me become the scientist I am today.

Table of Contents

List of Figures

Figure 4.3: GFP-HTR proximity biotinylation coupled with mass spectrometry identifies known talin-interacting proteins as well as novel interactors

List of Abbreviations

EC: Endothelial cell

HSC: Hematopoietic stem cell

FGF2: Fibroblast growth factor 2

VEGF: Vascular endothelial growth factor

TGF-β: Transforming growth factor beta

Eph-B4: EphrinB4

Eph2: Ephrin2

Blood Brain Barrier: BBB

VEGF-A: Vascular endothelial growth factor A

VEGFR-2: Vascular endothelial growth factor 2

FGFR: Fibroblast growth factor receptor

TIE-1: Tyrosine kinase with immunoglobulin-like and EGF-like domains 1

TIE-2: Tyrosine kinase with immunoglobulin-like and EGF-like domains 2

ANG-2: Angiopoientin-2

ANG-1: Angiopoientin-1

VE-cad: Vascular endothelial cadherin

ECD: Extracellular domain

DLL-NOTCH: Delta-like ligand – NOTCH

DLL4: Delta-like ligand 4

ECM: Extracellular matrix

MMPs: Matrix metalloproteinases

FAs: Focal adhesions

AJs: Adherens junctions

TGFβR: Transforming growth factor beta receptor

TNF-α: Tumor necrosis factor alpha

VE-PTP: Vascular endothelial protein tyrosine phosphatase

Rap1: Ras-proximate protein 1

PI3K: Phosphatidylinositol-3 kinase

MAPK: Mitogen activated protein kinase

FAK: Focal adhesion kinase

DiYF: Tyrosine 747 to Phenylalanine / Tyrosine 759 to Phenylalanine

LPS: Lipopolysaccharide

HUVEC: human umbilical vein endothelial cell

MP: membrane proximal

MD: membrane distal

FERM: 4.1 protein, ezrin, radixin and moesin

PIPKγ: PtdInsP kinase Iγ

MEFs: Mouse embryonic fibroblasts

GFP: Green fluorescent protein

P1: postnatal day 1

P3: postnatal day 3

LLC: Lewis lung carcinoma

Pod: Podocalyxin

FAJs: Focal adherens junctions

HDMVECs: Human dermal microvascular endothelial cells

ZO-1: Zonula occludens 1

shRNA: short hairpin RNA

THD: Talin head domain

GFP-THD: GFP-tagged talin head domain

BRB: Blood retinal barrier

GVB: Gut vascular barrier

EBD: Evans blue dye

GFP-HTR: GFP-talin head-turboID-talin rod

GFP-TID: GFP-turboID

GFP-Tln1: GFP-talin1

GFP-VH: GFP-vinculin head

Chapter 1. Introduction

1.1 Development of the Cardiovascular System

During embryonic development, the *de novo* formation of the mammalian circulatory system facilitates the many distinct mechanisms regulating tissue and organ specification and function[1,2]. In the extraembryonic yolk sac mesoderm, hemangioblasts, precursors of early endothelial and hematopoietic stem cells (ECs and HSCs), organize into cellular clusters termed blood islands[3]. Blood islands further differentiate in response to soluble growth factors such as fibroblast growth factor 2 (FGF-2) and vascular endothelial growth factor (VEGF) into angioblasts that will ultimately give rise to an endothelium[4,5]. In response to these secreted factors, angioblasts coordinate their individual migration to specific sites within the embryo where they adhere to neighboring cells to form loosely aggregated tubes. These early endothelial cells form an initial monolayer wherein the apical face of ECs forms a barrier separating blood cell progenitors from the extravascular space. Concurrently, the mesoderm gives rise to pre-endocardial tubes which develop into the aorta while migratory angioblasts differentiate into cardinal veins[6]. At this stage, blood begins to flow caudally from the heart through the dorsal aorta and circulates back through the posterior cardinal vein. This early cardiovascular system is the first organ to develop in the mammalian embryo and its development to this stage is dependent on vasculogenesis (Figure 1.1), the *de novo* formation of new vasculature from endothelial cell precursors. Later embryonic development and postnatal vascular growth is mediated largely through angiogenesis, a process by which pre-existing vessels give rise to new micro-vessels through endothelial cell sprouting, migration and stabilization[7].

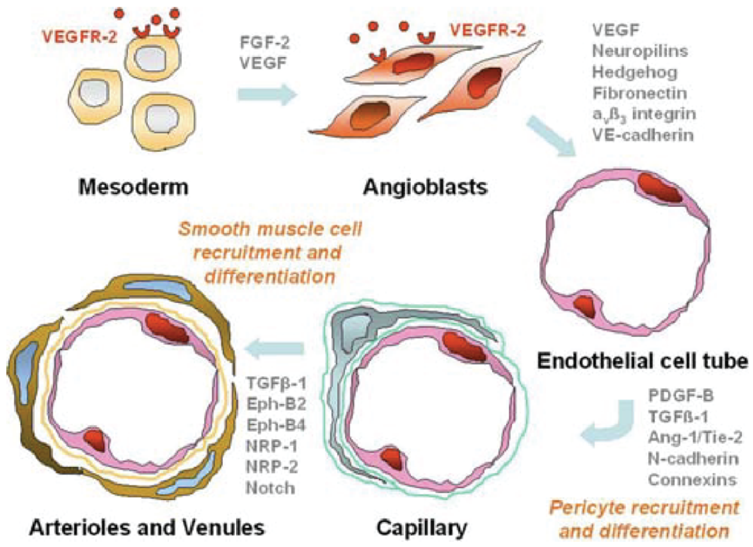

License #4698961124567

Figure 1.1. Vasculogenesis and early EC tube formation

Adapted[7] from Ribatti et al. Vasculogenesis is the *de novo* formation of blood vessels from endothelial precursors (angioblasts). VEGF/FGF-2 signaling drives EC-speciation while a number of adhesion molecules such as integrins and cadherins cooperate with growth factor (VEGF, FGF, Angiopoientin) to form the earliest endothelial tubes. In later embryonic development, Ephrin, TGF-β and Notch signaling drive arterio-venous specification.

1.1.1 Vascular Structure, Organization and Physiological Function

The formation of the vascular network in the early stages of embryonic development is driven predominantly through vasculogenesis while the development of specialized organ-specific networks in later development and postnatal life are largely driven by angiogenesis[4]. Crudely, the blood vascular network acts a conduit for the transport of blood cells, immune cells and other soluble components to peripheral tissues. The cardiovascular system can be differentiated into two interconnected networks of arterial and venous blood vessels, wherein the former carry oxygenated blood to peripheral tissue whereas the latter returns deoxygenated blood to the heart[8, 9]. The arterio-venous systems are connected through a network of microvascular capillaries (Figure 1.2) where gas and nutrient exchange occurs and deoxygenated blood enters venous circulation for return to the heart [10]. Regardless of arterial, venous or microvascular origin, blood vessels are, in general, structured similarly with a tunica intima, the innermost layer of the vessel which is comprised of a monolayer of endothelial cells atop a basement membrane, the tunica media, a middle layer comprised predominantly of connective tissue such as smooth muscle cells, and the tunica externa, an external layer of connective tissue and innervations that stabilize the vessel (Figure 1.2) [8]. Differences in the thickness of connective tissue of the tunica externa exist across more specialized vascular beds. Crucially, it's the function of collective and individual ECs that drive the growth, development and differentiation of vascular beds. Intriguingly, the specification of vasculature into their arterio-venous fates is in part genetically determined prior to the onset of vessel formation[11].

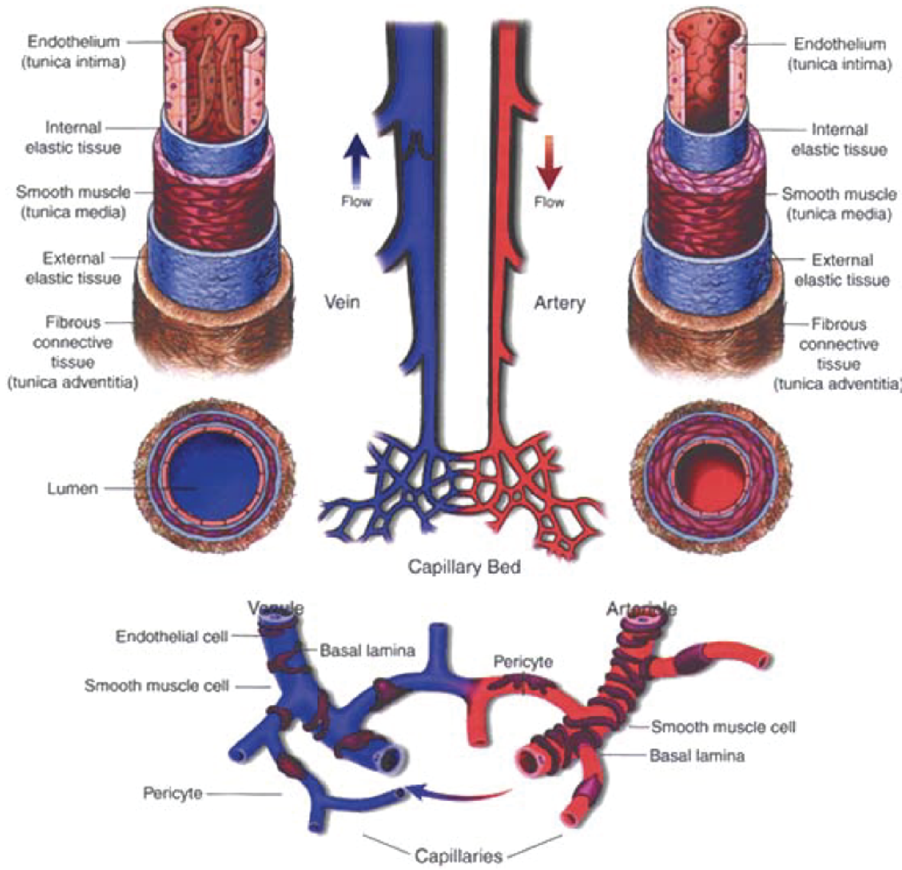

License #4698921334822

Figure 1.2. Arterio-Venous system and vessel structure

Adapted from Torres-Vasquez et al[10]. Vascular organization can be stratified into 3 distinct vessel types: arteries, veins and capillaries. Arteries deliver oxygenated blood away from the heart to distal organs where gas and nutrient exchange takes place in highly dense microvascular capillary beds after which deoxygenated blood is delivered back to the heart through the venous network. Vascular structure is fairly similar across these vessels types: a monolayer of ECs forms the innermost layer of the vessel, smooth muscle cells make up the tunica media and fibrous connective tissue makes up the outermost layer, the tunica adventitia.

Early work in this field characterized a molecular expression pattern that differentiated across venous and arterial ECs[12]. During embryonic angiogenesis, ECs which upregulate the expression of EphrinB4 (Eph-B4) transmembrane receptor differentiated into venous ECs whereas ECs expressing the Eph-B4 ligand, Eph2, had arterial fates [12]. Through elegant lineage tracing experiments in zebrafish, Zhong and colleagues described the mechanism by which hemogenic ECs regulate the expression of these markers in a NOTCH signaling-dependent fashion [13]. This early specialization highlights the tightly regulated differentiation and specialization required to form organ-specific vascular networks. Additionally, microvascular ECs exhibit a higher level of differentiation across different organs to reflect their specialized functions [14, 15]. An example of this can be found in capillary endothelium which has been stratified into three classes: continuous endothelium (lung, brain), fenestrated endothelium (intestine, kidney) and sinusoidal endothelium (liver, bone marrow) (Figure 1.3). Whereas continuous endothelium contains a tightly packed monolayer of ECs forming a tight vascular barrier, fenestrated and sinusoidal contain distinct pores and structures which facilitate the passage of molecules and blood cells. This differential permeability is critical in maintaining organ-specific function such as continuous endothelium in the blood-brain barrier (BBB), fenestrated endothelium which drives absorption and reabsorption in the glomerular capillaries and sinusoidal endothelium of the bone marrow which permits blood cell extravasation in homeostasis and disease [16, 17]. Dysregulation of the vascular barrier is prominent in a number of pathophysiologies associated with cancer, diabetes, hypertension and cardiovascular disease[18-20]. In addition to regulating the vascular barrier in health and disease, new blood vessel growth must also be tightly regulated in the aforementioned pathologies as well as during wound healing. During wound healing, damaged vessels respond to inflammatory cytokines and growth factors, in coordination with other cells such as epithelial cells and fibroblasts, to re-vascularize the injured tissue and promote closure of the wound. As will be discussed in a later chapter, mature vasculature is largely quiescent with ECs rarely proliferating[21] but in contexts like the tumor microenvironment, soluble factors instigate the proliferation of ECs during sprouting angiogenesis resulting in the formation of a leaky, immature vascular network[22, 23]. This unstable network amplifies and promotes tumor progression in a number of ways with many of the mechanisms that promote physiological wound healing co-opted to trigger unregulated tumor angiogenesis. It is therefore important to better understand the known regulatory mechanisms controlling angiogenesis in healthy and disease states especially as they relate to the development of a vascular network with a functional vascular barrier.

1.1.2 Regulation of New Blood Vessel Growth

In this section, I will discuss the intertwined but distinct mechanisms which drive the growth of new blood vessels during embryonic and postnatal development. As previously discussed, early work established the importance of vasculogenic growth factor signaling mediated by the VEGF[24, 25], FGF [5] and transforming growth factor beta (TGF-β) [26, 27] signaling in the establishment of early endothelial tubes that give rise to the vascular network. Deletion of VEGF-A [28, 29] or its major receptor, vascular endothelial growth factor 2 (VEGFR-2) [24, 25] is embryonic lethal at E8.5 due to severely underdeveloped embryonic vasculature. Knockout of FGF-2 or its receptor fibroblast growth factor receptor (FGFR)is especially important in the instruction

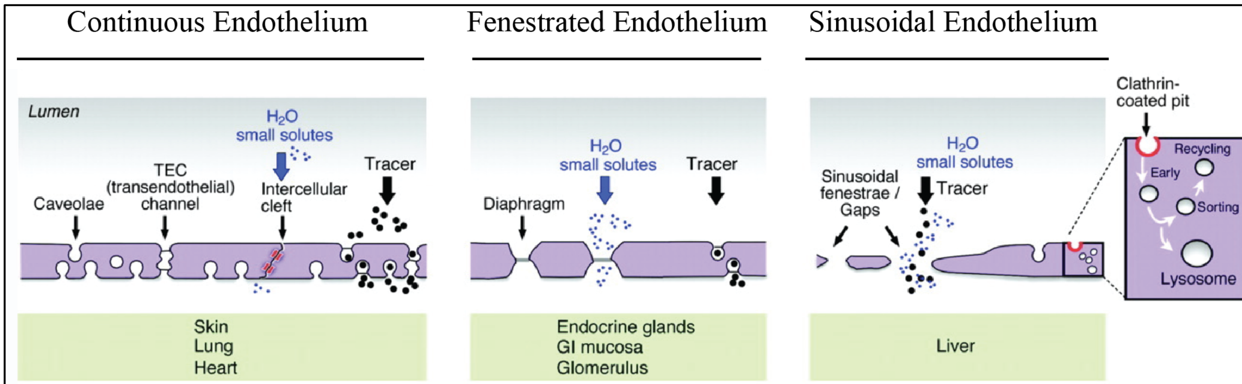

License #4698981103879

Figure 1.3. Endothelial heterogeneity and vascular permeability

Adapted from Aird et al[14,15]. Capillaries regulate the transfer of solutes, gases and fluids from the blood into surrounding tissue. There are 3 structurally and functionally distinct endothelium across all vascular beds: (1) continuous endothelium wherein permeability occurs primarily through intercellular clefts formed by adherens and tight junctions or transcellularly through caveolae (2) fenestrated endothelium which contain fenestrations, transcellular pores with diaphragms approximately 70 nm in diameter, as well as intercellular junctions giving them increased permeability relative to continuous endothelium (3) sinuosoidal endothelium which contain larger (100-200 nm) fenestrations lacking diaphragms and characterized by a discontinuous basement membrane- these capillaries possess high levels of clathrin-coated pits which play a crucial role in receptor-mediated endocytosis.

of pluripotent endothelial cell differentiation. VEGF and FGF signaling during vasculogenesis promote endothelial cell migration, proliferation and adhesion to neighboring ECs [7]. Ablation of TGF-β [26, 27] and PDGF-β[30-32] signaling in angioblasts stunts the maturation of endothelial cell tubes which require heterotypic interactions with mural cells like pericytes as well as smooth muscle to stabilize. The TIE-ANG signaling system also plays a critical role in the maturation of endothelial tubes into blood vessels by coordinating the recruitment of mural cells to stabilize the new vessel. Deletion of the tyrosine kinase with immunoglobulin-like and EGF-like domain receptor 1 or 2 (TIE-1 and TIE-2), which bind angiopoientin-2 (ANG-2) or angiopointin-1 (ANG-1), respectively, results in late embryonic mortality due to cardiovascular defects[33-36]. Growth factor signaling at this early developmental stage also requires the formation of EC-EC contacts between neighboring cells through cell-surface adhesion molecules. One specific example of this relationship was identified in the discovery of the crucial requirement of the endothelial-specific vascular endothelial cadherin (VE-cad) in embryogenesis[37-40]. VE-cad is a transmembrane protein that is expressed on the surface of all ECs as early as E7.5[28]. VE-cad molecules between neighboring ECs interact through a homophilic interaction between the VE-cad extracellular domains (ECD) to tether cells to one another as the VE-cad cytoplasmic tail is indirectly linked to the actin cytoskeleton through its interaction with the p120-catenin complex[41-43]. Curiously, early studies using VE-cad$^{-/-}$ mice revealed that while ECs can form inter-endothelial junctions, likely in part through other adhesion molecules like the Occludin family of tight junction proteins, these embryos were unable to form a vascular plexus resulting in early embryonic lethality[38]. P120 catenin which binds the cytoplasmic domain of VE-cad and stabilizes VE-cad at cell junctions is indispensable for embryonic angiogenesis as its deletion results in insufficient microvascular development and early lethality[44-46]. These data highlight the importance of EC-EC adhesion in the developing embryo.

Many of the growth factors and signaling pathways that regulate vasculogenesis early in the embryo also play an important role in later embryonic development and postnatal angiogenesis. Key signaling pathways which drive the initial stages of sprouting angiogenesis include VEGF, ANG-Tie and Delta-like ligand-Notch (DLL-NOTCH). Crudely, these pathways operate in similar fashion in pathological angiogenesis, but the differences will be highlighted in a later chapter especially in the context of dysregulated EC adhesion. During physiological contexts of sprouting angiogenesis such as wound healing, VEGF-A signaling instigates angiogenesis in two ways: 1) VEGFR-2 on ECs promotes cytoskeletal reorganization which loosens the otherwise tight cell-cell connections between ECs thus increasing local vessel permeability[47, 48] 2) in coordination with DLL-NOTCH signaling to induce the stochastic selection of a tip EC[49-52] which detaches from neighboring ECs and migrates into the ECM (Figure 1.4). In the first step, detachment of neighboring ECs and increased EC ANG-2 secretion accommodates EC migration and induces detachment of pericytes from the sprouting vessel, respectively. Concurrently, VEGF-A sensing by ECs promotes delta like ligand 4 (DLL4) expression on tip ECs. Neighboring ECs upregulate the DLL4 receptor, NOTCH, to become stalk cells which do not individually sprout, but rather proliferate behind the migrating tip EC and drive growth of the sprouting vessel. It is important to note that while tip and stalk ECs possess distinct gene signatures during this process, these changes are terminal in nature as stalk ECs in one context of sprouting angiogenesis may go on to become tip ECs in later situations.

To navigate the extracellular matrix (ECM), tip EC VEGF signaling drives the secretion

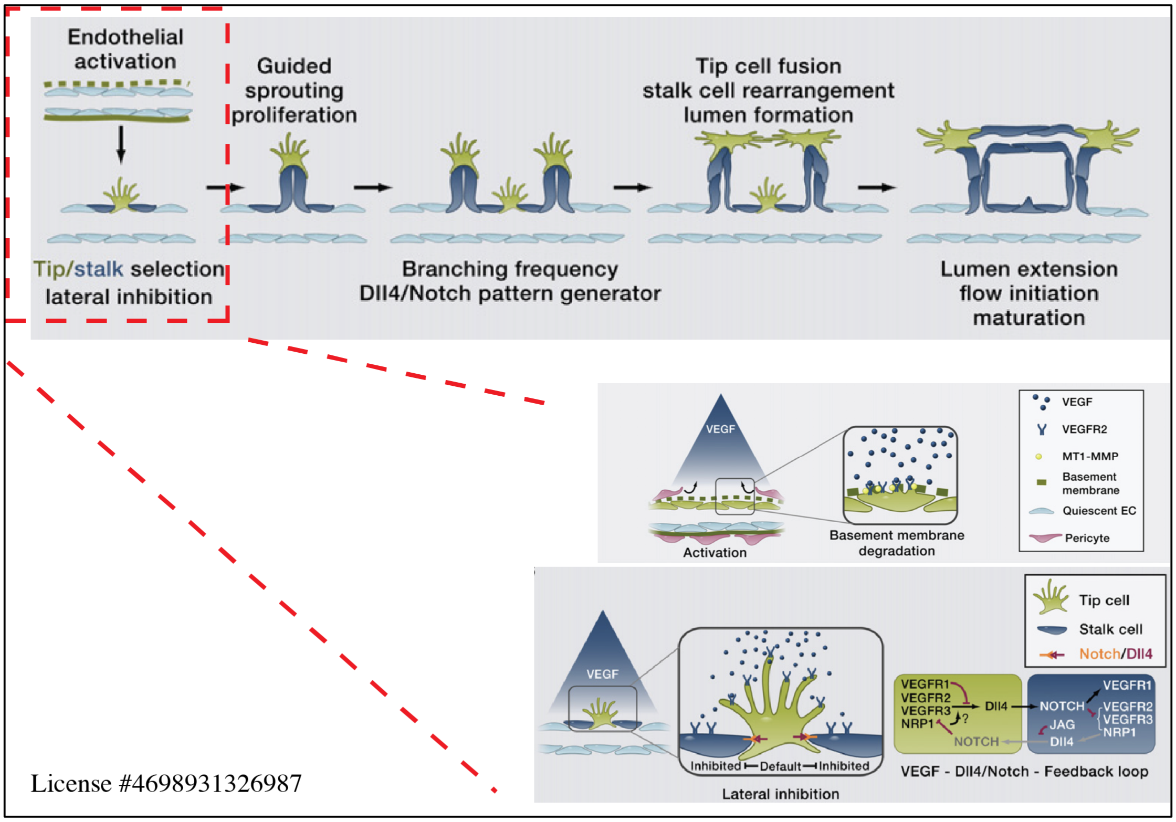

Figure 1.4. Sprouting angiogenesis and tip cell selection

Adapted from Potente et al[23]. Steps of Vessel Sprouting: (1) EC activation and tip/stalk cell selection (2) tip cell migration and stalk cell proliferation (3) branching coordination (4) stalk elongation, tip cell fusion and lumen formation (5) perfusion and vessel maturation. Inset: Secreted VEGF stimulates ECs via VEGFR-2 which promotes MMP secretion by ECs and detachment from basement membrane. VEGF and Delta-Notch signaling coordinate tip-stalk cell specification in a process termed lateral inhibition.

of matrix metalloproteinases (MMPs) which degrade the ECM and permit EC migration[53, 54]. Migration through the ECM is mediated by the integrin family of transmembrane adhesion receptors which bind various components of the ECM such as fibronectin, collagen and laminin at sites termed focal adhesions (FAs)[55]. Integrins exist as heterodimeric pairings of one of 18 α and 9 β subunits and it is these pairings that dictate specificity to the aforementioned matrix components[56, 57]. Importantly, integrins are linked through the β-integrin cytoplasmic tail to the actin cytoskeleton therefore acting as the mechanical tether between the ECM and the cytoskeleton[58-60]. The adhesive interactions between sprouting tip ECs then regulate the formation of a lumen and ultimately stabilize in a manner that accommodates blood perfusion in a process termed anastomosis[61]. During later embryonic and postnatal development, the vascular network undergoes extensive pruning and remodeling of newly formed vessels[62, 63]. This general process resolves redundant smaller vessels and immature sprouts by retraction of these undeveloped vessels. Crucially, while secreted factors instigate sprouting angiogenesis, the signaling pathways downstream of these agonists coordinate changes in adhesive interactions of ECs with neighboring cells as well as with the ECM to accomplish new vessel growth[48]. Thus, it is the dynamic relationship of the endothelium with its local microenvironment which drives angiogenesis in the embryo, wound healing and pathological conditions. However, as the vascular network fully forms, the mechanisms regulating now quiescent endothelium must be regulated to maintain the homeostatic function of the circulatory system.

1.1.3 Vascular Homeostasis and Barrier Function

Once the vascular network is established and circulation is established, mature blood vessels function in the delivery of nutrients, gas exchange and blood cells throughout the body. Established vasculature differs from newly developing vasculature not only in its appearance and organization but also, as a result, in their molecular signatures. Unlike angiogenic endothelium, a mature endothelium is largely quiescent. EC proliferation occurs at a slow rate[21] as ECs derive queues to maintain this quiescent state through the adhesive interactions at EC-EC contacts and EC-ECM contacts. One example of this regulation can be seen in the signaling pathways downstream of stable EC-EC contacts also called adherens junctions (AJs). The trans-interactions between VE-cad at AJs has two-fold importance in mature vessels: 1) it functions as a physical barrier and regulates paracellular vascular permeability[37-39] 2) it directly interacts with VEGFR2[64, 65 66]and transforming growth factor beta receptor (TGFβR) to inhibit downstream mitogenic pathways[67]. Therefore, it is important to consider the relative contributions of VE-cad in its physical role in the barrier as well as its requirement in mediating signaling pathways to promote contact-inhibition induced proliferation. In the presence of pro-inflammatory and pro-angiogenic agonists, vascular permeability increases as ECs contract to accommodate the weakening of the barrier which requires the disassembly of AJs[68, 69] (Figure 1.5). Cues such as VEGF, Thrombin and tumor necrosis factor alpha (TNF-α) induce reversible cytoskeletal reorganization[70] and the internalization of VE-cad from the cell membrane through phosphorylation of the cytoplasmic tail[71].

Similar to the manner by which AJs contribute to vascular stability and barrier function, integrins anchor the endothelium to the basement membrane and their downstream integrin signaling promotes anti-apoptotic and pro-survival queues[55, 72]. The most well-studied integrin classes in ECs engage ECM components by binding directly to number of distinct ECM

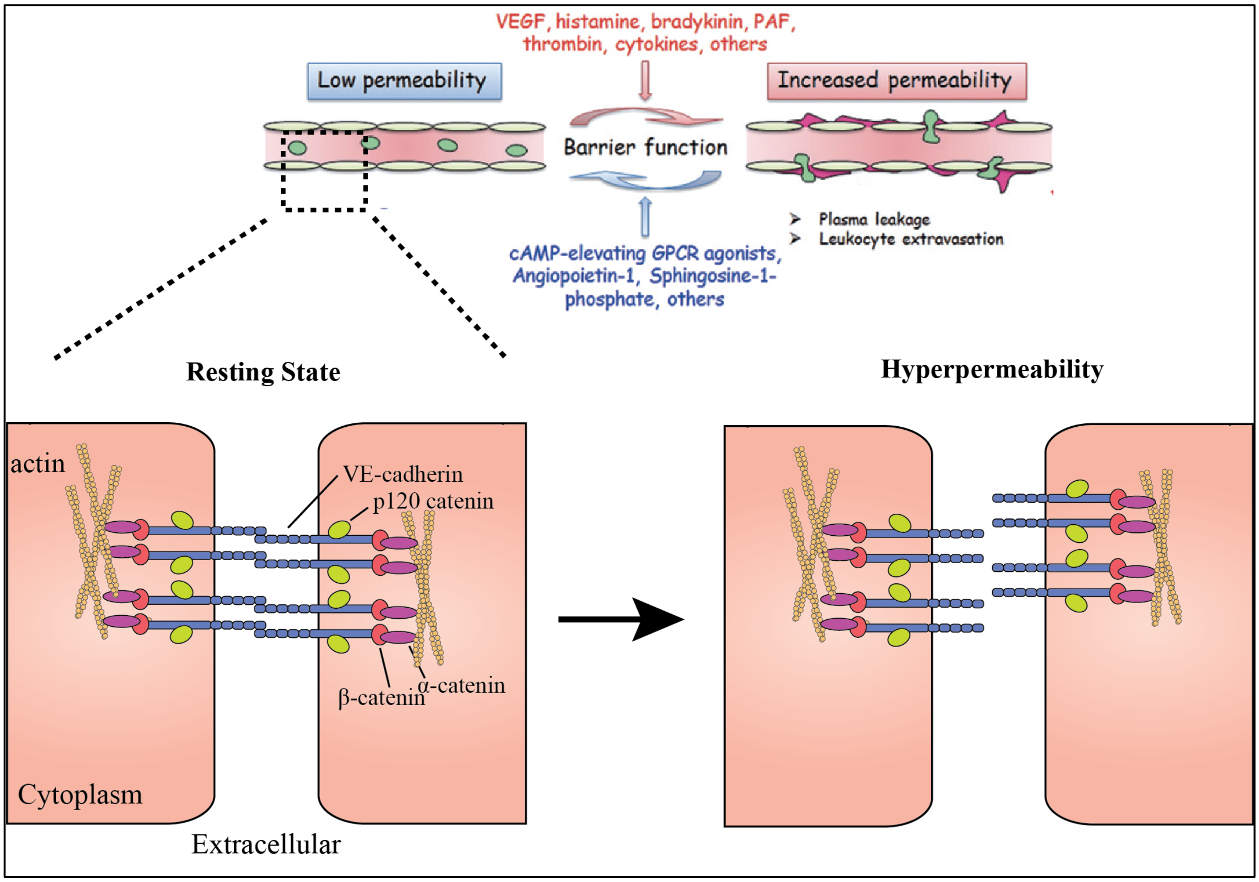

Figure 1.5. Regulation of vascular permeability by adherens junctions

Adapted from Rho et al.[68] Pulous et al.[69] Secretion of permeability-altering factors occurs during a number of diseases such as diabetes, chronic inflammation and cancer. The endothelium senses a number of these factors that either diminish barrier function and increase permeability (red factors) or those that enhance barrier function creating a tight barrier (blue). Changes in permeability are preceded by disassembly of cell-cell adhesions, of note and pictured here is the adherens junction. In resting states, VE-cad molecules form tight transcellular interactions which inhibit the flow of solutes between neighboring cells. But in pathophysiological contexts, these interactions are disrupted and junctions disassembled accommodating heightened leak through the intercellular space.

components including but limited to fibronectin, collagen, laminin and vitronectin. While the role of these receptors in angiogenesis has been extensively studied and will be reviewed in a later chapter, integrin function in the context of barrier regulation has only more recently begun to be appreciated. In general, akin to the changes in AJ stability in response to soluble agonists like VEGF which induce cytoskeletal contraction, integrins sense this increased tension and reorganize accordingly. Eloquent studies whereby deletion of β1, β3, or β5 integrin is induced in postnatal endothelium or established vasculature has suggested that different subunits play complicated roles in several models of agonist induced-permeability which will be highlighted in detail in a later chapter. Integrins coordinate with growth factor signaling and Ang-Tie signaling to regulate these responses as well[73, 74]. Crucially, the roles of cell-cell and cell-matrix adhesion signaling are integral to the stability of established vasculature and in the regulation of the vascular barrier in pathological contexts. Therefore, it is critical to understand how exactly the endothelium becomes activated in pathological conditions and how these signaling pathways induce functional changes in cell adhesion receptors to this end.

1.2 Endothelial Cell Adhesion in Disease

Many inflammatory and pro-angiogenic agonists which instigate sprouting angiogenesis are implicated in barrier regulation. ECs respond to these extracellular cues to restrict or promote the passage of circulating components into tissue. The responses to these queues require both physical changes in AJs and molecular signaling downstream of junctional disassembly that precedes a weakened barrier. The permeability of this barrier can be regulated through both transcellular and paracellular mechanisms. Whereas transcellular permeability is dependent on

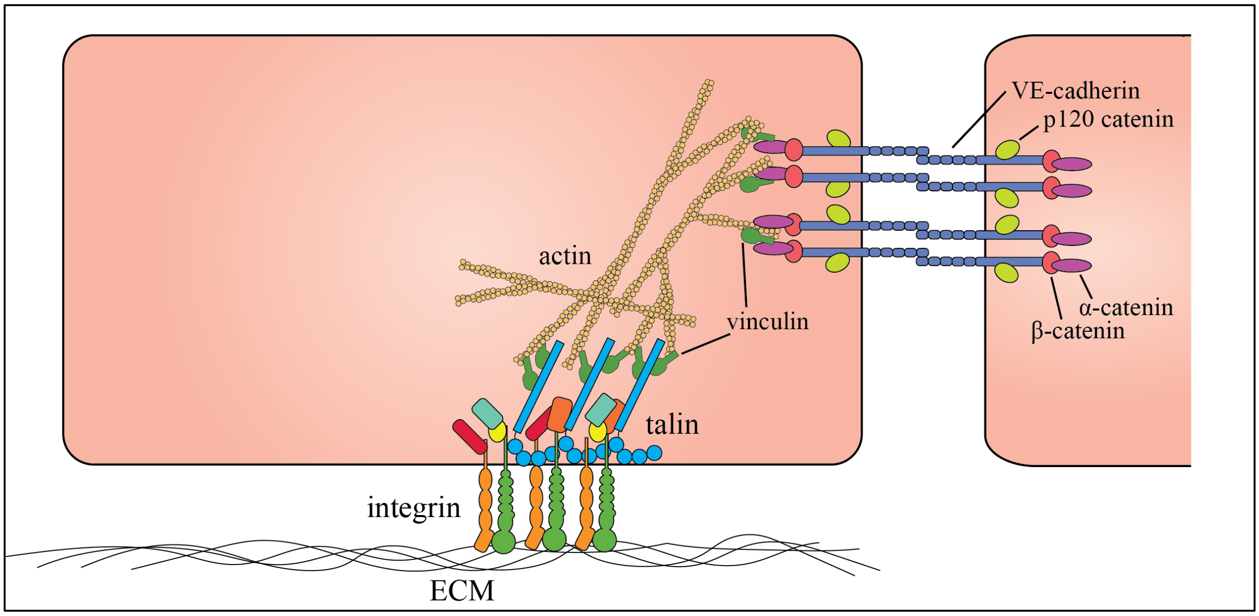

Figure 1.6. EC adhesions are linked through the cytoskeleton.

Adapted from Pulous et al.[69] Focal adhesions are made up of the integrin family of proteins and tether the basal side of the cell to the basement membrane. The cytoplasmic tail of β-integrins are bound by adaptor proteins such as talin which in turn link integrins to the actin cytoskeleton. As previously mentioned, adherens junctions are comprised of VE-cadherin, a calcium dependent adhesion molecule, which is also tied to the actin cytoskeleton through cadherin tail interactions with the catenin complex (α/β-catenin) meaning these two spatially separate structures are interlinked through the cytoskeleton. Changes in cytoskeletal tension downstream of signaling at either adhesion is likely sensed at the other.

vesicular transport of molecules across endothelial cells, paracellular permeability is regulated by changes at AJs. More recently, the contributions of endothelial cell-matrix adhesions to pathological changes in barrier function have been of interest. As cell-cell and cell-matrix adhesions are interlinked through the actin cytoskeleton (Figure 1.6), several mechanisms which promote new vessel growth and barrier stabilization act through both types of adhesions. Of note, however, the integrin family of adhesion receptors have been well-studied in the context of postnatal angiogenesis, both physiological and pathological, but less is understood about their specific roles in vascular permeability. As barrier dysregulation is a common driving factor of a number of pathophysiologies, it is important to identify novel pathways that may regulate the barrier in diseased states. This section will serve to highlight major role players in cell-cell and cell-matrix adhesions as well as their known involvements in pathologies wherein barrier function or angiogenesis are co-opted to promote disease progression.

1.2.1 Dysregulation of EC Adhesion in Cancer

Angiogenesis plays a vital role in tumor progression by enabling rapid primary tumor growth and consequently driving disease pathology[23, 75]. In general, the early stages of tumorigenesis involve local proliferation and growth of transformed cells. As somatic mutations continue to accrue in transformed cells and the metabolic requirements for further proliferation increase, solid tumors will undergo an angiogenic switch whereby pro-angiogenic factors are secreted into the microenvironment by tumor and tumor-adjacent immune and stromal cells[76]. Indeed, these cues are sensed by neighboring quiescent endothelium and similar to physiological sprouting angiogenesis, tumor angiogenesis promotes the formation of new blood vessels from those neighboring the tumor[77]. These newly formed vessels not only provide the nutrient requirements to accommodate tumorigenesis, but they also serve as a gateway for individual cells to migrate away from the primary tumor to extravasate into circulation[78]. Although the processes which instigate new blood vessel growth overlap with those in physiological contexts such as wound healing, tumor angiogenesis promotes the formation of highly proliferative, leaky and unstable vessels[79, 80]. Some of the functional differences in vessels formed in the tumor environment can be derived from differences in EC adhesion and as well as extensive changes in the tumor microenvironment ECM[81]. One example of these changes can be seen in the differential integrin expression on the surface of “activated” ECs. Unlike the endothelium of quiescent vessels, tumor vasculature from a number of malignancies express high levels of the integrin heterodimers $\alpha v\beta 3$[57, 82] and $\alpha 5\beta 1$[83-85] (Figure 1.7). Inflammatory mediators such as TNF-α and growth factors like VEGF-A in the tumor microenvironment increases the expression of $\alpha v\beta 3$ which accommodates the increased migratory requirements of individual ECs during angiogenesis[82, 86]. In a similar manner, angiogenic endothelium also express higher levels of $\alpha 5\beta 1$ integrin likely to accomplish migration through the fibronectin-rich tumor microenvironment. As growth factors also promote increased expression of the collagen and laminin binding integrins $\alpha 2\beta 1$[87] and $\alpha 1\beta 1$[88], it is likely that these integrins may also play an important, but not yet fully understood role in pathological angiogenesis. The role of individual of integrin subunits and their differential requirements in pathological vs physiological integrins will be highlighted in a later chapter. Crucially, however, our current understanding of integrins in angiogenesis is incomplete but suggest a highly complex relationship between specific integrin subunits and their respective roles in regulating new vessel growth. This relationship is of significant importance given the

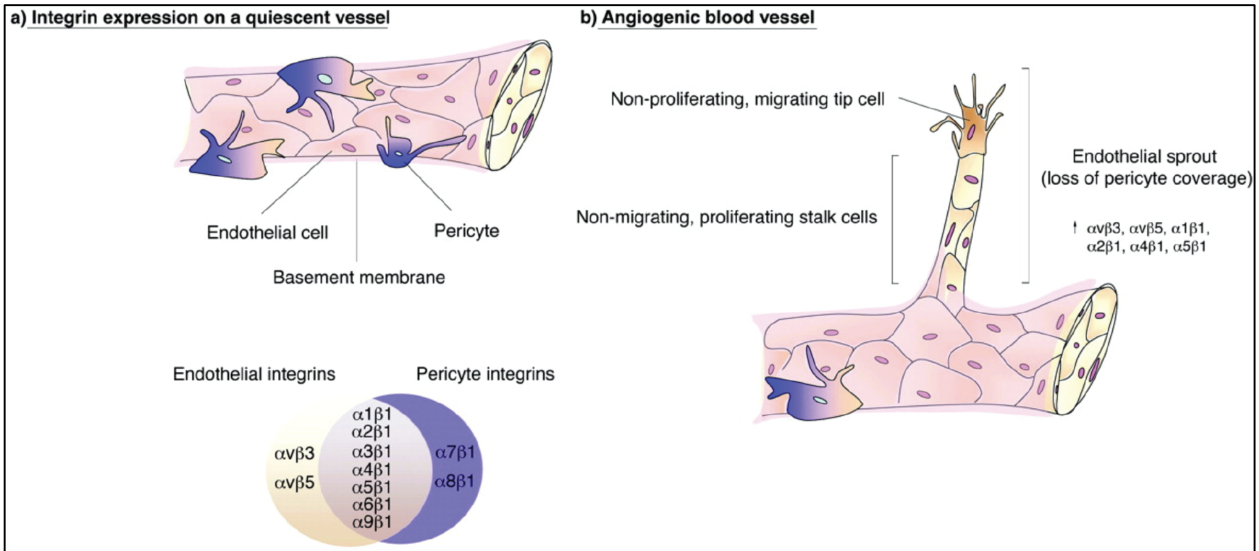

Figure 1.7. EC integrins in quiescent vs angiogenic states.

Adapted from Silva et al.[85] a) In quiescent vessels, ECs are closely packed with neighboring cells and are attached to the basement membrane through integrin-mediated interactions. A quiescent endothelium is also bound by mural cells such as pericytes which share a number of integrin heterodimer classes found in resting ECs. b) During angiogenesis, ECs sprout from preexisting vessels by detaching from the basement membrane and upregulate a number of integrin heterodimer classes to accommodate increased migration through the ECM. Of note, expression of EC integrins $\alpha5\beta1$, $\alpha4\beta1$, $\alpha2\beta1$, $\alpha1\beta1$, $\alpha v\beta5$ and $\alpha v\beta3$ is upregulated in angiogenic ECs.

degree of crosstalk between integrin signaling and growth factor signaling during tumor angiogenesis[89-91]. Concurrent with altered interactions between ECs and the ECM in the tumor microenvironment, the formation of leaky, immature vessels can also be attributed to altered EC-EC adhesion. The continual secretion of pro-angiogenic growth factors which drive excessive tumor angiogenesis precludes the formation of tight endothelial barrier likely by disrupting the balance of cell-cell junction mediated inhibition of EC proliferation[65] that act to negatively regulate new vessel growth. Constitutive secretion of VEGF as well as pro-inflammatory agonists within the tumor microenvironment disrupts the stability of cell-cell adhesions at AJs and result in a highly permeable vasculature. Tumor vessels exhibit reduced expression of VE-cad at cell junctions[92, 93]. Furthermore, the increased cytoskeletal contractility of angiogenic ECs results in disorganized linear junctions in favor of perpendicular AJ structures[71, 94] which retain some of their contacts to neighboring cells while permitting the leakiness associated with immature vasculature like that of the tumor vasculature. In general, the reports discussed above highlight the crucial contributions of dysregulated cell-cell and cell-matrix adhesions in tumor angiogenesis. Similarly, alterations in the organization, function and downstream signaling events of AJs and more recently, FAs, are implicated in other pathologies wherein blood vessel permeability is compromised.

1.2.2 Dysregulation of Cell-Cell Adhesion in Conditions of Hyperpermeability

Dysregulation of vascular permeability contributes to many common human pathological conditions including ischemia, cancer, diabetes and sepsis[18, 41, 95]. Here we will explore, in detail, the known organization and contribution of AJs in regulating barrier function. Homophilic interactions between VE-cad expressed on adjacent ECs maintain vascular permeability [38, 96]. VE-cad is stabilized at junctions through its interaction with p120 catenin (p120) and is tethered to the actin cytoskeleton through an interaction with the catenin complex[45, 46, 97, 98]. β-catenin, in complex with actin-bound α-catenin, directly binds the cytoplasmic tail of VE-cad[42, 43] conferring mechanosensitivity of AJs to cytoskeletal perturbations[40 99]. The catenin/actin linkage of VE-cad also acts as a local signaling hub for small GTPases which coordinate the stability of junctional cadherin complexes by regulating the stability of cortical actin stress fibers[94]. The requirement of VE-cad stabilization in adherens junctions was eloquently demonstrated *in vivo* by generating mice expressing a VE-cad/α-catenin fusion protein which is retained and resistant to endocytosis from junctions[100]. Mice expressing this VE-cad/α-catenin fusion protein were resistant to leukocyte extravasation in some tissues and agonist-induced models of hyperpermeability. In conditions that promote vascular permeability, AJs become destabilized, disassembled and VE-cad is endocytosed through a number of distinct mechanisms. In many of the aforementioned disease states, increased permeability is triggered by the secretion of soluble vascular endothelial growth factor (VEGF), fibroblast growth factor (FGF) and other pro-angiogenic factors. In a well-described process, VEGF binds to vascular endothelial growth factor 2 (VEGFR2) which leads to Src-dependent PAK-mediated phosphorylation of VE-cad at Ser665. VE-cad phosphorylation at Ser665 and Tyr685 is followed by β-arrestin2 binding which induces clathrin-dependent endocytosis of VE-cad[101, 102]. This pathway promotes cell migration, cytoskeletal rearrangement and AJ disassembly. Pro-inflammatory molecules present in conditions of chronic inflammation or sepsis such as TNF-α and LPS can also promote endothelial permeability. Treatment of ECs *in vitro* with TNF-α generates tensile structures termed focal adherens junctions (FAJs) due to increased cell contraction[71]. Secreted TNF-α is known to promote Fyn kinase-dependent phosphorylation of VE-cad cytoplasmic tail and VE-cad internalization which impairs pulmonary EC barrier function *in vitro*[103, 104]. Junctional disassembly induced by VEGF and TNF-α signal through independent pathways which converge at Src-family kinase-dependent VE-cad phosphorylation. Therefore, phosphatases like vascular endothelial protein tyrosine phosphatase (VE-PTP) play a critical role in maintaining junctional VE-cad[105] as its interaction with VE-cad stabilizes junctional cadherin pools in resting and inflammatory states[106, 107] . The disassembly of cell-cell junctions in both pro-angiogenic and inflammatory contexts are coupled with reorganization of the actin cytoskeleton. In resting states, a delicate tensional balance at cell-cell junctions permit the formation of linear AJs connected to circumferential actin that are regulated by small GTPases such as Ras-proximate protein 1 (Rap1), [108, 109] Rac[70, 101, 110] and Rho[111, 112]. Agonist-induced cell contraction increases tension at AJs and leads to the formation of zipper-like AJs. Collectively, these data highlight the importance VE-Cadherin stabilization at cell-cell contacts as well as the regulation of cell-cell tension in maintaining linear AJ organization in resting conditions. This section highlights the extensive knowledge of the critical function of AJs as canonical gatekeepers of vascular permeability. As suggested in an earlier section, recent developments have begun to implicate integrin-mediated adhesions as novel regulators of barrier function which is of significant interest as these two adhesive structures are interlinked through the actin cytoskeleton with considerable cross-talk[113]. While these recent findings are derived from early work by Lampugnani and others describing the localization of certain integrin heterodimers to the cell periphery, only until the last decade of research efforts utilizing inducible EC-specific mouse models have some of the underlying mechanisms of integrin signaling in barrier function been elucidated. Understanding how cell-matrix and cell-cell adhesions collectively coordinate the formation of new blood vessels and the stabilization of the vascular barrier is an essential endeavor that will likely inform novel strategies to target the vasculature in many pathophysiological contexts.

1.3 The Role of Integrins in Endothelial Cell Function

Integrins are transmembrane adhesion receptors expressed on the surface of most mammalian cell types. In addition to functioning as important adhesion receptors, integrins are bi-directional signaling hubs involved in numerous fundamental cellular processes including cell migration, survival and proliferation. Importantly, the regulation of integrin affinity for ligand is an essential step in all of the aforementioned cellular processes and will be discussed in detail in this and a later section. In this section, I will discuss how integrin function is regulated in ECs, how integrin signaling regulates angiogenesis and highlight the emerging role of these adhesion receptors in regulating vascular permeability in established vessels.

1.3.1 Integrin Adhesion and Signaling

Integrins are heterodimeric cell surface adhesion receptors consisting of one of 18 α- and one of 8 β-subunits which dictate ligand specificity[55]. The most well-studied integrin classes in ECs engage ECM components by binding directly to collagen (α1β1, α2β1), fibronectin (α5β1, α4β1, αvβ3), vitronectin (αvβ3, avβ5) and laminin (α3β1, α6β1)[114]. Integrins contain an extracellular domain that is able to become ligated to ECM components when integrins are an in an active conformation, a transmembrane domain and a cytoplasmic tail which interact with a number of cytoskeletal adaptor proteins. ECs rely on integrin-mediated adhesions at cell-matrix contacts to remain tethered to the sub-endothelial matrix and to interact dynamically with the ECM during cell migration. Although ECs express a repertoire of integrin subunits, it is of note that in ECs a subset of β-integrin subunits (β1, β3 and β5) makeup the majority of the β-subunit pairings in all EC integrin heterodimers highlighting the importance of these subunits in EC function. In general, integrin affinity for ECM ligands is regulated in two distinct methods with major differences across the heterodimeric pairings expressed in ECs arising from their downstream signaling effectors as well as crosstalk with other signaling pathways. On one hand, integrin affinity for ECM ligand is regulated through so called “inside-out” integrin signaling (integrin activation) [115] whereby extracellular signals are transduced into the cell through cell-surface receptors (e.g. receptor tyrosine kinases, G-protein coupled receptors) that in turn ultimately lead to the binding of cytoplasmic, integrin activating proteins such as talin [116-118] and kindlin[119] to the β-integrin cytoplasmic tail. On the other hand, integrin “outside-in” signaling can occur in response to integrin binding extracellular ligands and subsequent activation of cytoplasmic signaling pathways [55]. Furthermore, integrins lack intrinsic enzymatic activity but tyrosine phosphorylation of the β integrin cytoplasmic tail regulates the binding of adaptor proteins that in turn recruit non-receptor tyrosine kinases. In this way, integrins serve as a hub for signaling pathways essential to diverse and fundamental cellular functions including phosphatidylinositol-3 kinase (PI3K) and mitogen-activated protein kinase (MAPK)[55]. In addition, integrins can activate Ras and Rho family small GTPases that profoundly impact cytoskeletal organization and dynamics[81] (Figure 1.8). Cytoskeletal reorganization requires the disassembly and reassembly of integrin adhesion complexes, processes that are regulated

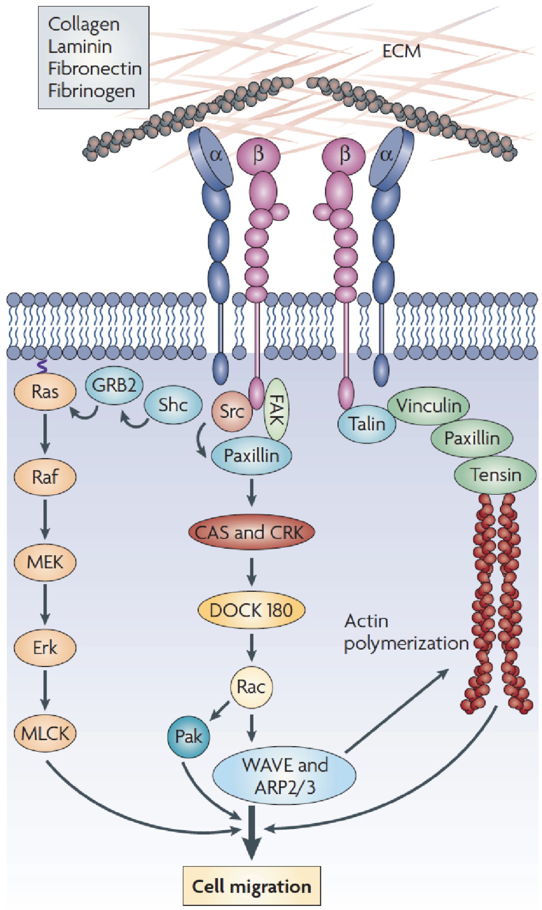

Figure 1.8. Integrin-mediated regulation of cell migration and cytoskeletal dynamics

Adapted from Avraamides et al.[81] To integrate signals and activate intracellular signalling pathways, integrins co-cluster with serine, threonine and tyrosine kinases, phosphatases and adaptor proteins in focal adhesions. Focal adhesion complexes are composed of integrins, protein kinases such as focal adhesion kinase (FAK), Src and many other kinases, adaptor proteins such as Shc, signalling intermediates such as phosphatidylinositol-3 kinase, Rho and Rac GTPases and actin-binding cytoskeletal proteins such as talin, α-actinin, paxillin, tensin and vinculin. Integrin signalling promotes cell migration by providing traction along the ECM and by promoting actin remodelling through the Rho family small GTPases.

spatially and temporally by complex and context-dependent signaling events[120, 121]. Regulation of cytoskeletal organization and dynamics highlights a key intertwined relationship between integrin-mediated adhesions and AJs and this relationship will be a central focus of my dissertation goals which will be discussed in a later chapter.

1.3.2 Integrin Signaling and Function in Angiogenesis

The role of EC integrins in developmental and postnatal angiogenesis has been extensively studied. In this section, I will cover the roles of the major endothelial integrin classes as they function in the contexts of developmental and pathological angiogenesis. Generally, in the context of angiogenesis, EC integrins regulate cell growth, migration and survival (Figure 1.8). Early *in vivo* and *in vitro* studies pointed to distinct roles for the major integrin classes expressed in the endothelium. These early global knockout models of specific integrin subunits are summarized in Avraamides et al. More cogent to the specific role of integrins within the endothelium, the development of endothelial-specific transgenic knockout mouse models have been extremely informative in discerning some of the specific contributions of individual subunits and are reviewed in detail in Payne and colleagues [122]. An elegant study by Van de Flier et al tested the specific role of the fibronectin receptor α5 and αv-integrins and determined that loss of either subunit in ECs during development resulted in viable mice with no visible defects in the developing vasculature[123]. Curiously, deletion of both α5 and αv-integrins in ECs resulted in embryonic lethality by E14.5 likely due to defective vessel remodeling and gross defects in aortic development. The lack of a vascular phenotype in the individual EC-α5/αv knockout mice suggest a likely compensatory response by either subunit in the absence of the other. It is important to note that the double-knockout mice undergo embryonic vasculogenesis and angiogenesis normally up to E14.5 suggesting that the lethality observed in these mice may be in part due to defective vascular remodeling that takes place during late embryogenesis. Interestingly, constitutive deletion of EC-β1, which pairs with α5-integrin to bind fibronectin, integrin results in earlier embryonic lethality by E10 with extensive defects in lumen formation and incomplete vascular patterning[124, 125]. Defective lumen formation was determined to be in part due to the downregulation of Par3, an essential regulator of endothelial polarity which resulted vessel occlusion and incomplete vessel formation. These studies, though essential and informative highlight the complicated nature of studying the function of EC integrins in angiogenesis as they point to a complicated temporal and contextual involvement of integrin signaling during developmental angiogenesis. A few considerations that remain unaddressed include whether the collagen binding integrins which partner with β1 integrin are indispensable for pathological angiogenesis given their dispensable roles during development. A recent report from Ghatak and colleagues report modest defects in wound healing and tumor angiogenesis in global α1/α2-integrin double knockout mice[126], although it would be prudent to investigate the EC-specific contributions of these defects using a cell-type specific cre-system. The complicated nature of subunit-specific knockout models can also be seen in the extensive studies that have attempted to address the curious role of EC-β3 integrin during developmental but also pathological angiogenesis. The interest in understanding the role of β3 integrin angiogenic contexts was of high initial priority as tumor vessels appear to have increased expression of the αvβ3 receptor relative to very low levels of expression on quiescent vasculature[82, 86]. Global deletion β3[127] or its partner αv-integrin[128] result in 50% embryonic lethality and 80% embryonic/postnatal lethality, respectively. Mice which did survive β3 deletion during development were further assessed in a follow up study looking at the role of β3/β5 integrin knockout on tumor angiogenesis. Intriguingly, these mice exhibited increased tumor neovascularization relative to wildtype due to enhanced VEGFR2 expression and downstream signaling which drove this enhanced vascularization [129]. Furthermore, the generation of mice expressing a β3-integrin with mutated cytoplasmic residues Y747/Y759F (DiYF) which are critical for downstream integrin signaling are viable with no observed developmental vascular defects[130]. While developmental angiogenesis was unaffected in DiYF, DiYF mice exhibited significantly decreased tumor vascularization using the B16F0 and RM-1 murine models of melanoma and prostate cancer, respectively. This striking observation differed with the Reynolds et Al report stating the absence of β3 integrin enhanced pathological angiogenesis through VEGF-mediated compensation. A final report looking to explains the disparity in these two reports utilized multiple EC-β3 integrin knockout mouse models, an inducible EC-specific and constitutive EC-specific line to come to a critical conclusion: induced, acute depletion of EC-β3 integrin during tumor growth transiently impairs neovascularization and reduces tumor growth while constitutive deletion resulted in the enhanced neovascularization phenotype observed in Reynolds et al[131]. These findings again highlight the complex contributions of individual integrin subunits in the context of new vessel growth specifically that factors such as temporal length of deletion and Cre-Recombinase mouse models may result in differing interpretations. With the onset of inducible EC-specific mouse models, some of these disparities across mouse lines used are beginning to be elucidated. Additionally, the inducible systems accommodate the investigation of integrin function in already established vessels wherein integrins appear to play crucial roles in the maintenance of quiescent vasculature. Interestingly, the many cues which instigate new blood vessel growth play an equally important role in the maintenance of the vascular barrier in mature vessels.

1.3.3 Integrin Signaling and Function in Vascular Permeability

Here, I will discuss what is currently known about the contribution of integrins in the maintenance of the vascular barrier in both resting conditions as well as in the context of agonist-induced hyperpermeability. Early evidence indicated that deletion of β3 in mice resulted in increased VEGF and lipopolysaccharide (LPS)-induced Evan's Blue leakage in dermal and lung/intestinal vessels, respectively[132], whereas baseline permeability appeared similar relative to control littermates. Eloquent studies by Su et al.[133] showed that the permeability-inducing effects of VEGF, TGF-β and thrombin on pulmonary ECs were exacerbated by pre-treatment with αvβ3 blocking antibodies consistent with the notion that β3 integrin promotes EC barrier. Furthermore, treating human umbilical vein endothelial cells (HUVECs) with the barrier-enhancing agent sphingosine 1-phosphate promoted αvβ3 localization to cell-cell contacts and sites of cortical actin and this was inhibited by pre-treatment with an αvβ3 function blocking antibody. Interestingly, activation of αvβ3 with low doses of the cyclic RGD peptide, cilengitide, reduced HUVEC monolayer permeability likely by promoting Src kinase-mediated phosphorylation of VE-cad at Y731 and Y658 thereby promoting the internalization of VE-cad[134]. The mechanism(s) underlying these observed effects of cilengitide on HUVEC barrier function are unclear but could include indirectly inhibiting β1 integrin through trans-dominant inhibition[134, 135]. Interestingly, the role of αvβ5 in response to sepsis-induced leak contrasts with the barrier-protective role of αvβ3 in LPS-induced leak. Antibody blockade of HUVEC αvβ5 attenuated

LPS-induced barrier dysfunction *in vitro* while β5 knockout mice exhibit increased survival in a cecal ligation model of sepsis relative to WT mice[136]. It was proposed that blockade of β5 integrin mitigates the induction of cytoskeletal contraction in these contexts thereby stabilizing cell-cell junctions. As β5 integrin was deleted globally in the mice used in this study, the relative contributions of β5 integrin in ECs versus other cell types remains an open question.

Yet another recent indication of the importance of integrin function in regulating vascular permeability can be seen in studies whereby β1 integrin was deleted during postnatal angiogenesis and in a separate report in established vessels. A role of β1 integrins in endothelial barrier function was first discovered when antibodies specific to α5β1 integrin revealed a localization pattern of this receptor at cell-cell junctions in addition to its well-described localization to FAs[137]. In contrast, cell-cell junction localization of αvβ3 integrin was not observed. Furthermore, antibody blockade of α5β1, but not αvβ3, impaired monolayer permeability *in vitro*. A recent study by Yamamoto et al. demonstrated that EC-specific deletion of β1 integrin during postnatal development promoted VE-cadherin internalization and cell-cell junction disassembly[138]. These investigators convincingly demonstrated that junctional disassembly in β1 integrin-deficient ECs was due to reduced Rap1/MRCK and Rho/Rho-kinase activity that impaired VE-cad trafficking to cell-cell junctions. Intriguingly, work by Hakanpaa et al. showed that deletion of a single β1 integrin allele in ECs of established blood vessels did not alter basal permeability but rather protected β1 EC heterozygous mice from LPS-induced hyperpermeability compared to wild type littermates[139]. Pharmacological inhibition of β1 integrin also mitigated LPS-induced tracheal permeability relative to mice pre-treated with non-immune IgG. It was therefore proposed that in quiescent endothelium β1 integrin predominantly localizes to FAs whereas inflammatory molecules acting in an angiopoietin-2-dependent manner induce β1 integrin association with tensin at fibrillar adhesions. β1 integrin-positive fibrillar adhesions in turn promote cytoskeletal tension that alters cell-cell junctions and increases vascular permeability. Together, the data presented in this section serves to highlight the essential role that integrins play in the regulation of vascular permeability. While these collective studies implicate specific integrin subunits with regards to their contributions in regulating vascular permeability in specific vascular beds, a critical open question that remains whether the modulation of integrin affinity through cytoskeletal adaptors such as talin contribute in the aforementioned contexts. As all integrins are activated through a fairly conserved mechanism whereby the cytoskeletal adaptor protein talin binds to the β-integrin cytoplasmic tail to promote the active conformation of integrin receptors during inside-out activation, it is therefore important to understand how modulation of integrin affinity for ligands occurs and its potential role in pathologies that implicate integrin function in ECs.

1.4 Talin: Master Regulator of Integrin Activation

Essential to the adhesive and signaling properties of integrins across all cell types, talin is a cytoskeletal adaptor protein which binds β-integrin cytoplasmic tails inducing a conformational switch in the integrin associated with increased integrin ligand affinity. Talin was first discovered as a component of focal adhesions in cultured cells [140]and extensive *in vitro* studies revealed its integral function in cell spreading and focal adhesion formation[141-144]. Binding of talin to the β-integrin cytoplasmic tail is a key final step in the modulatory process of integrin confirmation termed 'inside-out' activation[115, 145]. The N-terminal talin head contains an atypical FERM domain which is linked through a flexible linker to the carboxy-terminal talin rod which

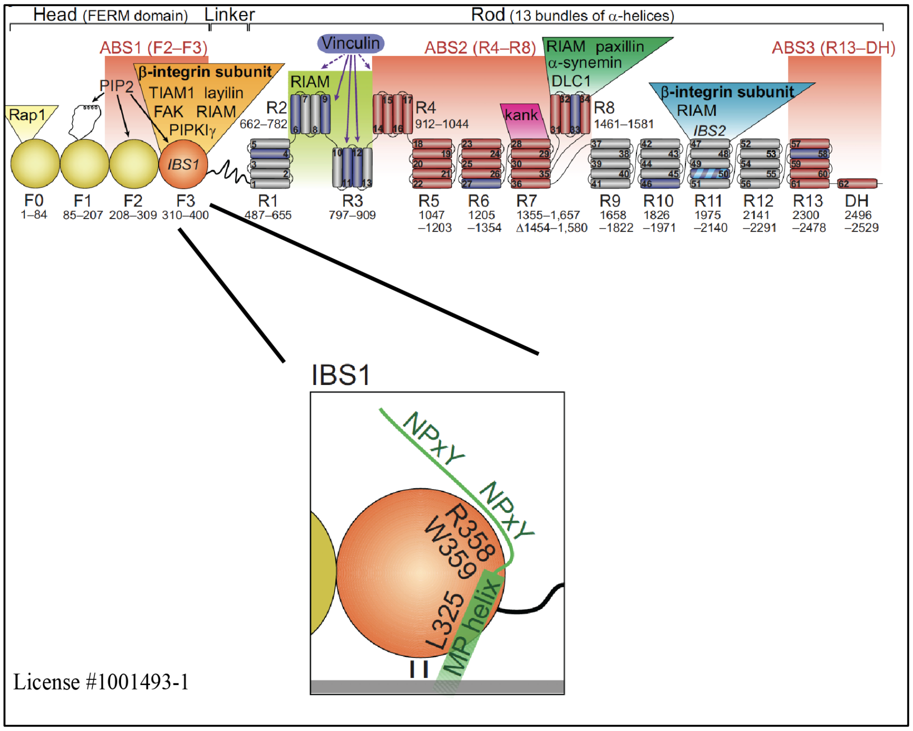

Figure 1.9. Structure and domains of talin

Adapted from Klapholz et al.[146] The talin 'head' is an atypical FERM domain with four subdomains (F0–F3, in yellow and orange), followed by an ~80 amino acids 'linker' that connects to the 'rod'. The talin rod is composed of 61 α-helices that fold into 13 bundles (R1–R13). Binding sites for interacting proteins are indicated: the integrin-binding site 1 (IBS1) is in orange, actin-binding sites of the rod are in red, and α-helices that are vinculin-binding sites (VBSs) are in purple. The inset is a simplified representation of IBS1 bound to integrin. Different residues of F3 mediate interactions with the membrane proximal α-helix (e.g. L325 of F3) and the membrane-proximal NPxY motif (e.g. R358, W359 of F3) of the cytoplasmic region of integrin β-subunit (green). Mutagenesis disrupting talin binding to the membrane proximal region of β integrin impairs integrin activation, whereas disrupting talin binding to the membrane distal region of β integrin impairs all talin-integrin interactions and thus, integrin activation. The two vertical lines indicate membrane binding.

contains binding sites for a number of associated cytoskeletal adaptors as well as several distinct actin binding sites[146] (Figure 1.9). As a result of these interactions, when talin is bound to the β-integrin tail it serves as a mechanical linkage between the ECM and the actin cytoskeleton.

1.4.1 Mechanism of Talin-Mediated Integrin Activation

Integrin activation occurs in response to extracellular cues sensed by cell-surface receptors which induce the recruitment of talin, through a partially understood mechanism, to the plasma membrane where it binds the β-integrin tail at two distinct sites: a membrane proximal (MP) and membrane distal (MD) site[116-118]. In the well-studied platelet αIIbβ3 integrin model, this binding event disrupts the transmembrane interactions between the transmembrane domains of the α and β subunits to accommodate the conformational change to the extended open conformation of the receptor[118]. To understand this key modulatory step that is essential in the integrin activation cascade, it is important to understand the structural and conformational makeup of talin in steady state and induced conditions. Talin contains an atypical FERM (4.1 protein, ezrin, radixin and moesin) domain, a module involved in the localization of cytosolic proteins to the plasma membrane, and an extensive rod domain comprised of 13 helical bundles of 4-5 helices each (R1-R13). The FERM domain is considered atypical as it contains a F0 subdomain (as opposed to the canonical F1-F3 subdomains) and because these subdomains adopt a linear arrangement rather than the cloverleaf-like structure noted in other FERM domain containing proteins[147]. Prior to recruitment to the plasma membrane, several reports indicate that talin exists in an auto-inhibitory conformation whereby the integrin binding site 1 (IBS1) within the F3 sub-domain of the talin head is shielded by the talin rod sub-domains R9-R12[148-150]. The autoinhibitory state is a crucial regulatory step in retaining talin in an off state as certain cellular environments contain concentrations of talin as high as 50 μM[151, 152]. Elegant studies using exogenous expression of αIIbβ3 integrin and talin in Chinese hamster ovary revealed that extracellular cues induce an interaction between the small GTPase RAP1 and the talin F1 subdomain that is essential for the recruitment of talin to the plasma membrane, where it can interact with β-integrin tails[152-154] (Fig 1.10). Recruitment to the membrane is essential in this process as the talin head must also interact with PtdInsP kinase Iγ (PIPKγ) which locally synthesizes PIP_2 that then binds the talin head to orient talin in a manner which accommodates its interaction with β-integrin[155-157]. Once bound to the integrin tail and the integrin binds extracellular ligand, mechanical forces transmitted through the integrin-talin-actin linkage induce unfolding of talin R1-R13 to facilitate interactions with other mechanosensitive proteins such as vinculin[158-160]. Unfolded talin rod stretches the depth of the focal adhesion signaling complex layers[161, 162] and structurally acts as a key component of the focal adhesion signaling hub driving critical cellular processes tied to cell survival, proliferation and migration. *In vivo*, global deletion of talin1 results in embryonic lethality by E9.5 due to defects in gastrulation[163]. Generation of cell-type specific talin1 knockout and mutant talin1 knock-in mouse models have been essential in understanding the context-specific requirement of inside-out integrin activation in resting conditions and pathological settings and will be discussed in the following sections. Recently, important mechanisms underlying talin-dependent integrin activation have been elucidated in several types of hematopoietic cells which will be discussed in the following section.

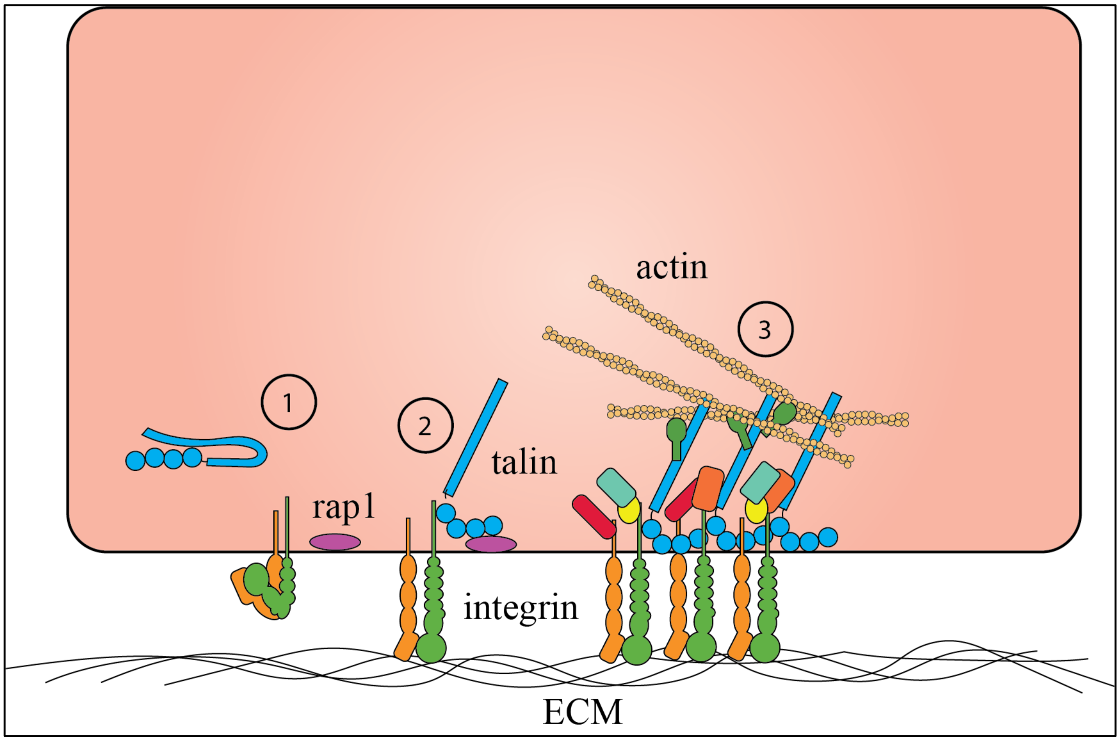

Figure 1.10. Talin-dependent integrin activation and focal adhesion maturation.

Adapted from Pulous et al.[69] (1) Prior to localization to the plasma membrane, talin adopts an auto-inhibitory conformation. In response to extracellular cues that are sensed by receptor tyrosine kinases and other cell-surface receptors, the autoinhibitory conformation of talin is relieved and in an incompletely understood process is recruited it to the plasma membrane[150]. (2) The talin-head is bound by membrane lipids and the small GTPase rap1 in a manner which accommodates F3 sub-domain interactions with the β-integrin tail at two distinct sites which in turn induces a tilt of the β-integrin transmembrane helix. This tilt results in separation of the α- and β-subunit transmembrane domains thus accommodating the extended open confirmation of integrins and eventual ligation to the ECM. (3) Ligated integrins cluster and promote the recruitment of adapter, signaling, and actin binding proteins crucial for cellular processes like migration, proliferation and survival.

1.4.2 The Role of Talin in Blood Cells

Extensive effort has been put forth to understand the role and requirement of talin-mediated integrin activation in blood cells by a number of different groups. In general, integrins in blood cells have low affinity for extracellular ligands and require activation through the recruitment and binding of talin to the β-integrin cytoplasmic tail including β1[115, 117], β2[164], β3[165-168] and β7[169] integrins. The importance of inside-out integrin activation is illustrated in the tightly regulated processes which drive platelet adhesion and aggregation in hemostasis and thrombosis. Of note, platelets express multiple integrin classes with the highest expressed heterodimer being αIIbβ3 which is capable of binding fibrinogen, von Willebrand factor and fibronectin while α2β1 regulates binding to collagen. Integrins of circulating quiescent platelets reside in a low-affinity state. Upon exposure to soluble agonists like adenosine diphosphate or thrombin, platelet integrins are activated through inside-out signaling that promotes αIIbβ3 binding to soluble fibrinogen whereas β1 integrin binds subendothelial collagen that is exposed to blood in injured blood vessels. Induced deletion of talin1 in platelet-specific manner impairs both β1 and β3 integrin activation as evidenced by increased tail bleeding time relative to control mice as well as impaired clot formation in a carotid artery injury model[165]. Following this study, two reports carefully examined the specific contributions of the talin-integrin interaction and talin-actin interactions in the context of clot formation. Structural studies by Wegener et al described a model whereby talin activates integrin by sequentially interacting with two distinct sites in the β integrin tail. Initially, the talin MD-β tail interaction provides the majority of talin-integrin binding energy. This interaction enables interaction of talin with a second, membrane proximal (MP), site in the β tail. Despite providing a negligible fraction of the binding energy, this talin-integrin MP contact is essential for talin-mediated integrin activation[116-118]. Importantly, structural and biochemical studies identified mutations in talin that selectively disrupt the MD (talin(W359A)) and MP (talin(L325R)) interactions with integrin thereby enabling testing of this two-step model *in vivo* (Fig 1.9). The model predicts that, in contrast to talin1(W359A), which is predicted to disrupt both MP and MD interactions, talin1(L325R) should selectively disrupt the MP interaction, thereby retaining the capacity of talin to mechanically link integrin to the actin cytoskeleton. Genetically modified mice expressing either talin1(W359A) or talin1(L325R) in platelets have revealed important insights into the functions of these distinct talin-integrin interactions in the context of hemostasis and thrombosis [168, 170]. Platelets expressing talin1 L325R exhibited marked reductions in β3 integrin activation as measured by binding of soluble fibrinogen and binding of an active conformation-specific integrin antibody which phenocopied talin1-depleted platelets[170]. In contrast, Tln1 W359A platelets exhibited delayed β3 integrin activation that was reduced by 50% relative to wildtype platelets. Both talin1(L325R) and talin1(W359A) platelet mice were protected from chemical injury-induced carotid artery thrombosis. Interestingly, talin1(W359A) mice exhibited only mild defects in hemostasis whereas talin1 L325R mice exhibited profound hemostatic dysfunction similar to mice with talin-deficient platelets. The differences in the platelet and hemostatic phenotypes of talin1 L325R and talin W359A is likely attributable to how effective the mutations are in inhibiting particular talin-integrin interactions. Indeed, the talin1(W359A) mutation reduces talin affinity for integrin (~3.5 fold) but does not completely abolish binding. Together, these data indicated that manipulation of specific talin-integrin interactions may be a potentially useful strategy for the design of new anti-thrombotic therapeutics that may better preserve hemostasis compared to current approaches like aspirin and ADP receptor blockade. Additionally, the reports that lead to these intriguing discoveries highlight that a better understanding of how the contributions of talin-mediated integrin affinity modulation in disease states and across cell-types, including endothelial cells, may result in clinically translatable insights.

1.4.3 The Role of Talin Function in ECs

All vertebrate genomes encode two highly homologous but functionally distinct talin isoforms, talin1 and talin2 which share 74% amino acid identity and 86% similarity[171, 172]. Talin1 is ubiquitously expressed whereas talin2 is most highly expressed in striated muscle and neurons[171, 173]. Importantly, work by Kopp et al suggest that ECs express only talin1[174]. From early transgenic knockout mouse models of talin1[163] or talin2[175] it became evident that there are distinct differences in the requirement and function of talin isoforms. Strikingly, deletion of talin1 in mice results in embryonic lethality due to defects in gastrulation with embryos not developing past E8.5 which is in stark contrast talin2-null embryos which develop normally. Kopp and colleagues generated an inducible talin1 knockout mouse model in order isolate multiple cell types for *in vitro* analyses. Interestingly, induction of talin1 deletion in mouse embryonic fibroblasts (MEFs) isolated from these mice resulted in upregulation of talin2[174]. However, deletion of talin1 in HUVECs by small interfering RNA (siRNA) did not phenocopy the observed upregulation of talin2 in MEFs suggesting that ECs were an ideal model system to study the function of talin1. siTln1-HUVECs were able to initially adhere to fibronectin coated cover slips but were incapable of normal cell spreading. Furthermore, while initial adhesion was observed in tln1-depleted HUVECs, adhesion over longer time courses was lost. Reconstitution of tln1-depleted HUVECs with green fluorescent protein (GFP)-Tln1 were able to rescue defects in cell spreading and prolonged adhesion whereas reconstitution with GFP-Tln1-L325R were insufficient to rescue these defects. The GFP-Tln1-L325R data points to the specific requirement of talin in activating integrins in ECs as being integral to EC function as this mutant is able to interact with actin normally[174]. In a subsequent elegant study, Monkley and colleagues generated an EC-specific talin1 knockout mouse using the Tie2-Cre recombinase system to study the specific contributions of endothelial talin1 during embryonic angiogenesis[176]. Tie2-Cre+ embryos lacking talin1 exhibited gross vascular hemorrhaging and early lethality by E.8.5 relative to Tie2-Cre- littermate controls. Whereas established vessels in the embryo appear intact in Tie2-Cre+ mice, angiogenic vessel ECs appear flattened and unable to spread completely indicating a possible specificity of the requirement of talin1 in newly developing vessels. Furthermore, the timing of the embryonic lethality in Tie2-Cre+ mice resembles that of the global talin1 knockouts suggesting that defects in embryogenesis was likely due to the absence of EC talin1 in both models. The phenotype of talin1 deletion in embryonic angiogenesis is also reminiscent of the report of incomplete lumen formation from Zovein et al wherein β1-integrin was deleted in ECs during embryogenesis[124]. Together, these data indicate an intriguing potential requirement for talin-mediated β1 integrin activation in the context of angiogenesis. However, the mechanism underlying these changes are not completely understood and warrant further study. Additionally, whether talin is required during postnatal angiogenesis or in mature established vessels of adult mice, as it is for embryonic angiogenesis, remains unclear.

1.5 Dissertation Goals

Given the incomplete knowledge concerning the role of endothelial cell talin-mediated integrin activation in the contexts of postnatal angiogenesis and endothelial barrier function, my dissertation goals will be to test the requirements of talin1 in these contexts utilizing both *in vivo* and *in vitro* approaches. The second chapter of my dissertation examines the contributions of EC-talin1 during postnatal angiogenesis, both in physiological and pathological contexts of new blood vessel growth. Additionally, utilization of the EC-talin1 knockout and EC-talin1 L325R mouse model allows us to discern between integrin activation-dependent and independent roles of talin during postnatal angiogenesis. The third chapter of my dissertation presents data using the EC-talin1 knockout model to test whether EC-talin1 is required for endothelial barrier function in established vessels. I propose an intriguing role for talin-mediated β1 integrin activation in regulating the intestinal vascular barrier by disrupting VE-cadherin stability at cell-cell junctions. This report adds another layer of complexity to the cross-talk between cell-cell and cell-matrix adhesions in EC function and opens up new areas of research to further explore how integrin activation may be targeted in diseases driven by hyperpermeability. In Chapter 4, I present new methods that I have developed to identify novel talin interacting proteins in ECs that may generate new hypotheses regarding the mechanisms of talin function in EC barrier function. To understand the spectrum of potential contributions whereby talin regulates EC barrier function, we have undertaken an unbiased proximity-dependent biotin labeling approach to identify novel talin interacting proteins that cooperate to regulate EC barrier function in resting and leaky states. Finally, I will conclude by discussing the sum of the findings presented in my research efforts in the context of the current state of the field and speculate on how the data presented may be utilized in future research.

Chapter 2. Endothelial Cell Talin-Dependent Integrin Activation is Required for Postnatal Angiogenesis

Fadi E. Pulous BA, Jamie C. Carnevale, Brian G. Petrich PhD

From the Department of Pediatrics, Aflac Cancer and Blood Disorders Center (FEP, BGP), Cancer Biology Graduate Program (FEP), Emory University School of Medicine, Atlanta, GA 30322, USA.

2.1 Abstract

Talin-mediated integrin activation plays a critical role in a number of blood and immune cell processes but the role of EC integrin activation during postnatal angiogenesis has not been explored. Here, I utilized an inducible EC-specific talin1 KO mouse (Tln1 EC-KO) and an inducible, EC-specific talin1 L325R mouse mutant, in which the capacity of talin to activate integrins is inhibited whereas the talin binding to the β-integrin tail is retained, to determine the requirement of inside-out integrin activation during angiogenesis. Deletion of talin1 during postnatal days 1-3 (P1-P3) resulted in lethality by P8 of Tln1 EC-KO pups with extensive defects in retinal angiogenesis and hemorrhaging in brain, gut and retinal tissues, which were not observed in Tln1 CTRL littermates. Defects in retinal angiogenesis in Tln1 EC-KO mice included reduced retinal vascular area, impaired EC sprouting and reduced EC proliferation relative to Tln1 CTRL. Curiously, induction of talin1 L325R expression during P1-P3 in Tln1 L325R mice resulted in more modest defects in retinal angiogenesis with mice surviving to adulthood but being significantly smaller relative to control littermates. Strikingly, B16-F0 tumors grown in Tln1 L325R adult mice were 55% smaller than tumors in Tln1 L325R mice relative to Tln1 Het Controls and significantly less vascularized. These data point to the

requirement of EC-talin1 during postnatal angiogenesis. Specifically, my results suggest that talin-dependent integrin activation is indispensable for tumor angiogenesis whereas integrin activation-independent functions of talin in ECs may be more important during development.

2.2 Introduction

Endothelial cells (ECs) form a tight, continuous monolayer of cells to form the luminal surface of blood vessels. ECs form adhesive contacts with the basement membrane at cell-matrix adhesions and are connected to neighboring cells at cell-cell contacts. In physiological contexts such as retinal angiogenesis but also in pathological contexts like tumor angiogenesis, ECs in pre-existing vessels facilitate new blood vessel growth by sensing and migrating towards soluble pro-angiogenic growth factors in their local microenvironment in a process broadly termed sprouting angiogenesis[177]. An essential activity during the early stages of sprouting angiogenesis necessitates the tight regulation of EC adhesive interactions with the extracellular matrix (ECM) as sprouting tip ECs navigate through the matrix[23, 75]. ECs engage ECM components such as fibronectin, collagen and laminin through the integrin family of cell-surface adhesion receptors [55, 72].

Integrins are heterodimeric, transmembrane receptors comprised of one of 18 α- and one of 8 β-subunits which in-turn dictate specificity for ligand. ECs express a diverse repertoire of integrin receptors with the best-studied receptors binding directly to collagen (α1β1, α2β1), fibronectin (α5β1, α4β1, αvβ3), vitronectin (αvβ3, avβ5) and laminin (α3β1, α6β1)[114, 178]. Integrin receptors operate as bi-directional signaling hubs which transmit signals in both directions across the plasma membrane. Ligation of integrins to ECM ligands initiate intracellular signaling through so-called outside-in signaling which includes integrin clustering, recruitment of adapter proteins, kinases, phosphatases and reinforcement of integrin linkage to the actin cytoskeleton[179, 180]. On the hand the affinity of integrins for extracellular ligands can be dynamically regulated by so-called inside-out signaling, or integrin activation, when intracellular signals, often downstream of growth factor receptor activation, initiate a signaling pathway that ultimately results conformational changes in the integrin extracellular domain associated with high ligand affinity. This bi-directional signaling drives a host of critical cell processes including migration, proliferation and survival[55, 72].

Activation of integrin receptors into a high ligand affinity confirmation requires the binding of the cytoskeletal adaptor protein, talin, to the cytoplasmic tail of β-integrin [115-117]. An example of this conserved regulatory mechanism is observed in platelet adhesion during clot formation wherein soluble cues such as thrombin or adenosine diphosphate induce downstream signaling events which recruit talin to the plasma membrane allowing talin to activate the platelet receptors αIIbβ3 and α2β1[165, 166]. Following these studies, several reports determined that ablation of talin1 in platelets impairs platelet adhesion during hemostatic and thrombotic contexts while expression of a talin1 mutant which abrogates the MP binding interaction required for inside-out activation phenocopied the loss of talin[168, 170]. While these studies have greatly informed therapeutic interventions for patients with defective platelet integrin signaling, the role of integrin affinity modulation in ECs has been relatively understudied.

The roles of specific integrin subunits in ECs during developmental and postnatal angiogenesis have been investigated and are reviewed concisely in other literature [81]. Indeed, studies utilizing individual integrin subunit deletion *in vivo* have been informative yet given the complex subunit-specific contributions as well as the context-dependent nature of these contributions much remains to be understood; specifically, in regards to whether inside-out integrin activation is essential for EC function in postnatal life. Early work determined the essential requirement of EC talin1 during embryonic angiogenesis as its deletion results in embryonic lethality by E10.5 due to extensive vascular defects[176] while inducible deletion of talin1 in established embryonic vessels results in early lethality due to defects in vascular permeability[181]. However, whether talin-mediated integrin activation is required for either pathological or physiological angiogenesis remains largely unanswered.

Here, we provide evidence to support the notion that talin and its role in activating integrins from the inside-out are indispensable for postnatal angiogenesis. Specifically, inducible deletion of EC talin1 during early postnatal development results in extensive defects in retinal angiogenesis, EC proliferation relative to littermate controls and early lethality of Tln1 EC-KO pups by P8. Deletion studies were complemented by an inducible, EC-specific talin1 L325R knock-in model to discern between integrin activation-dependent and independent talin functions in angiogenesis. Interestingly, whereas Tln1 L325R mice exhibited defects in retinal and tumor angiogenesis relative to littermate controls, induced expression of the mutant allele during postnatal development was not lethal, as was observed with Tln1 EC-KO mice, but resulted in significantly smaller mice that survive into adulthood. Our data point to an essential role for talin1 in postnatal angiogenesis although the specific contributions of integrin activation-dependent functions of talin require further investigation.

2.3 Methods

Mice

We generated EC-specific talin1 knock-out mice using *Tln1* floxed mice[165, 166]expressing a tamoxifen-inducible Cre driven by the cadherin 5 (*Cdh5*) promoter[182]. Our breeding scheme generated *Tln1*$^{f/f}$;Cdh5-CreERT2$^{-/-}$ (referred to as Tln1 CTRL) and *Tln1*$^{f/f}$;Cdh5-CreERT2$^{+/-}$ (Tln1 EC-KO) mice. For postnatal angiogenesis and developmental studies, mice were intragastrically administered 50µg of tamoxifen (Cayman Chemicals) dissolved in corn oil (Sigma) daily on P1-P3. For tumor studies in adult Tln1 Het/L325R mice, 8-10 week old mice were administered 2.5 mg of tamoxifen once daily for 3 days to induce L325R expression. Tln1 Het (*Tln1*$^{f/wt}$; Cdh5-CreERT2$^{+/-}$) and Tln1 L325R (*Tln1*$^{f/L325R}$; Cdh5-CreERT2$^{+/-}$) mice[168] were made by breeding *Tln1*$^{f/L325R}$[168] with the EC-specific Cdh5-CreERT2 mouse line [182, 183]. Studies using the tdTomato reporter were done by comparing mice with genotype *Tln1*$^{f/wt}$;Cdh5-CreERT2$^{+/-}$;Rosa26-tdTomato$^{+/-}$ with *Tln1*$^{f/L325R}$;Cdh5-CreERT2$^{+/-}$;Rosa26-tdTomato$^{+/-}$ mice. Similar ratios of males and female mice were used for experiments and experimenters were blinded to the genotypes of mice until all data was collected. In control experiments to test the effects of tamoxifen versus corn oil on survival, mice were randomly assigned to treatment groups. Experimental procedures were approved by the Emory University Institutional Animal Care and Use Committee (IACUC).

Retinal Angiogenesis Model and Staining

Retinal mounts and immunofluorescence were performed as previously described[184]. Briefly, retinas were dissected out of mice at specified times after tamoxifen treatment, fixed in 4% PFA for either 2hrs at Room Temperature or overnight at 4° C. Whole mount retinas were then subject to antibody staining of FITC-lectin staining as previously described[181]. Tissue was mounted using Fluoromount (Life Technologies) and imaging was performed on an Olympus FV1000 inverted confocal microscope. For staining of whole retinal mounts, the vasculature was visualized with FITC-conjugated Isolectin (Vector Labs: FL-1101-5). Where noted, tdTomato was visualized to analyze recombination efficiency across whole retinal mounts. Primary antibodies used for staining were rat anti-mouse CD31 at 1:100 (BD Pharm: 553370), rabbit anti-mouse talin at 1:100 (Santa Cruz: sc-15336) and rabbit anti-mouse collagen IV at 1:100 (Bio-Rad: 21501470). Species specific secondary donkey antibodies conjugated with Alexa-488/568/647 fluorophores at 1:400 (Life Technologies) antibodies were used for primary antibody detection.

Tumor Studies

Both LLC and B16-F0 murine tumor models were performed on 8-10 week-old adult Tln1 Het and Tln1 L325R mice which were administered tamoxifen as described above prior to subcutaneous implantation. For B16-F0 experiments, mice were anesthetized by isoflurane in a procedure approved by Emory IACUC two weeks after the last dose of tamoxifen and injected subcutaneously with 5.0×10^5 B16-F0 cells. Animal health and tumor growth were monitored for 14 days prior to sacrifice and tumor volume was measured using calipers. After 14 days, tumors were excised and weighed for relative analysis. 1.0×10^6 LLC cells were subcutaneously injected into the right or left flank and tumor growth monitored for 14 days after which tumors were excised and weighed. Where noted for frozen sectioning experiments, tumors were perfusion fixed with 4% PFA, excised, further fixed overnight at 4°C in 4% PFA and embedded in O.C.T Compound (TissueTek). 10μm sections were cut from processed tissue every 50um for blood vessel immunostaining experiments.

Immunofluorescence and Tissue Staining

Tissue sections prepared as described above were subjected to overnight permeabilization and blocking in PBS with 1% BSA and 0.3% Triton-x (PB Buffer) at 4° C. Primary antibody labeling with rat anti-mouse CD31 at 1:100 (BD Pharm: 553370) and goat anti-mouse podocalyxin at 1:100 (R and D Systems: AF1556) were performed in PB Buffer overnight at 4° C followed by PBS+ washes and secondary antibody staining with species specific donkey IgG conjugated with Alexa-488/647 fluorophores at 1:400 (Life Technologies). Imaging was performed on an Olympus FV1000 Confocal Microscope. For edu analysis in neonatal Tln1 CTRL and EC-KO pup retinas, mice were administered 100ug edu 30' prior to sacrifice, retinal tissue processed as previously described[184] followed by Click-iT detection per manufacturers recommended protocol (Thermo-Fisher: C10340). Retinas were co-stained with FITC-lectin and the # of edu+/FITC-lectin+ cells counted per field of view.

Image Analysis

For vascular area measurements, stitched images were acquired of the entire retinal tissue. The retinal area was measured and the vascular area is representation of FITC-lectin positive areas within the greater retinal area using FIJI analysis. Junctional Density was measured using AngioTool[185] by masking the FITC-lectin positive area within each field of view and then algorithmic fitting of branching points within the thresholded vascular area to determine junctional density per area. This analysis was performed on 4-6 images per retina analyzed with the n>4 for all groups. For sprout and filopodia quantitation, high magnification (60x,100x) images of overnight 4% PFA-fixed whole-mount retinas were analyzed by counting the number of either structure across the length of the angiogenic front from 4-6 images per retina. 4-6 retinas were analyzed per group as noted in the figure legends. Collagen IV+/lectin- sleeves were measured by taking 3-5 images from 3-4 retina per group. Collagen IV+/lectin- were identified using Image J and normalized to the vascular area within each field of view. For tdTomato tumor blood vessel quantitation, 3 frozen sections from 8-9 tumors were analyzed. 3-4 20x images from each frozen section was thresholded using FIJI binary thresholding and values representing %tdTomato+ area per field of view analyzed. To analyze Pod+/Tom+ blood vessels in B16-F0 tumor sections, 4-6 fields of view from 2 individual frozen sections of 5-6 tumors per group were analyzed. Images were thresholded using pre-set FIJI settings across all acquired images and % area of each channel was then measured using FIJI. Ratios represent the % areas of either Pod+ or Tom+ vessels across identical fields of view.

Statistical Analysis

All statistical tests were performed and survival curves generated using Prism Software 8.0. The specific test that was used. to analyze individual experiments is noted in the figure legends but briefly for comparison of parametric data from two groups, an unpaired t-test was used. Data sets analyzed with parametric statistical tests were tested for a normal distribution using a Shapiro-Wilk test.

2.4 Results

Endothelial Cell Talin1 is Indispensable for Postnatal Development

To test the role of EC talin1 during postnatal angiogenesis, we generated EC-specific talin1 knock-out mice using *Tln1* floxed mice[165, 166] expressing a tamoxifen-inducible Cre driven by the cadherin 5 (*Cdh5*) promoter[182]. Our breeding scheme generated *Tln1*$^{f/f}$;Cdh5-CreERT2$^{-/-}$ (referred to as Tln1 CTRL) and *Tln1*$^{f/f}$;Cdh5-CreERT2$^{+/-}$ (Tln1 EC-KO) neonates which were

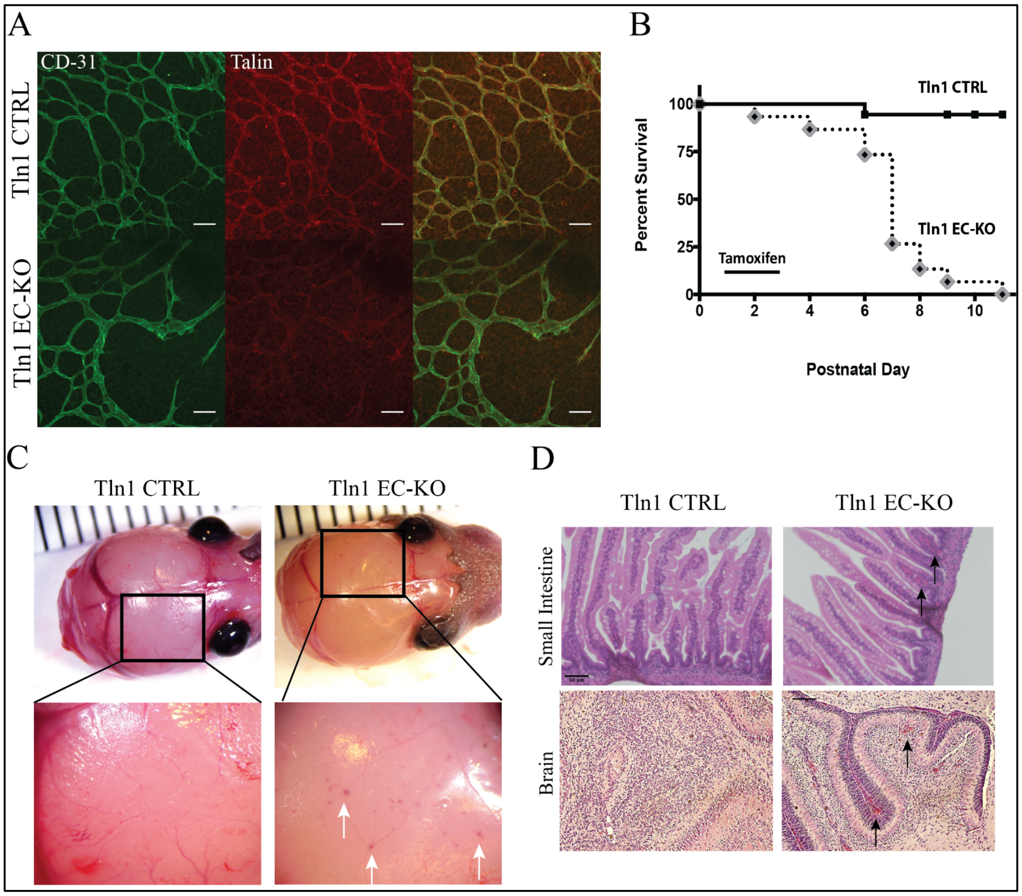

Figure 2.1. EC-specific deletion of talin1 during postnatal development causes vascular hemorrhage and death

Tln1 (talin1) EC-KO (knockout; Tln1fl/fl;Cdh5creERT2+/−) and Tln1 CTRL (control; Tln1fl/fl;Cdh5creERT2−/−) neonates were administered tamoxifen P1-P3 and analyzed at P5 where indicated. **(A)** Immunostaining of whole-mounted retinas from Tln1 CTRL and Tln1 EC-KO mice. Talin protein is markedly reduced in Tln1 EC-KO CD-31+ ECs. (n=3; scale= 50 μm) **(B)** Survival of Tln1 EC-KO and Tln1 CTRL mice following tamoxifen treatment. Tln1 EC(n=15, Tln1 CTRL and n=18, Tln1 EC-KO). **(C)** Light microscopy of whole brains from Tln1 CTRL and Tln1 EC-KO mice. Inset zoom highlight focal hemorraghing (arrows) in brain microvasculature of Tln1 EC-KO pups not observed in Tln1 CTRL mice. **(D)** H and E sections of Tln1 CTRL and EC-KO small intestine and brain from P7 pups. Red blood cell accumulation is observed in Tln1 EC-KO intestinal villi and brain microvessels (arrows) that is not observed in Tln1 CTRL sections (n=3-4 per group, scale = 50 μm).

administered tamoxifen intragastrically on postnatal days 1-3 to induce Cre-mediated deletion of talin1. To examine talin1 protein levels in Tln1 CTRL and Tln1 EC-KO pups, retinas were excised at P5 and the retinal endothelium immunostained for talin (Figure 2.1A). Tln1 EC-KO retinal ECs exhibited a marked reduction in talin1 protein signal relative to Tln1 CTRL. This finding is consistent with our recently published data showing that lung ECs isolated from adult Tln1 EC-KO mice had significantly reduced levels of talin protein and transcript levels relative Tln1 CTRL lung ECs[181]. Induction of talin deletion during P1-P3 resulted in early lethality of Tln1 EC-KO mice by P8 whereas Tln1 CTRL littermates survive normally (Figure 2.1B). To understand the lethality observed in Tln1 EC-KO mice, tamoxifen-injected pups were sacrificed at P5 and whole organs analyzed after sacrifice. Tln1 EC-KO mice exhibited cranial hemorrhaging which were not present in brains excised from Tln1 CTRL mice (Figure 2.1C). Additionally, histological sections of small intestine tissue excised from Tln1 EC-KO mice displayed extensive extravascular red blood cell accumulation in the intestinal villi while the intestinal villi of Tln1 CTRL mice appeared intact and normal (Figure 2.1D). This phenotype was also observed in H and E sections of Tln1 EC-KO brains whereas Tln1 CTRL brain sections appeared normal. Collectively, these data point to the indispensable function of EC talin1 during postnatal development across a number of vascular beds.

EC Talin1 is required for retinal angiogenesis and EC Proliferation

Previous studies have established the requirement of EC talin1 during embryonic angiogenesis though little is known about the contributions of talin during postnatal angiogenesis. As the retinal vasculature develops postnatally, we utilized the retinal angiogenesis model to test the

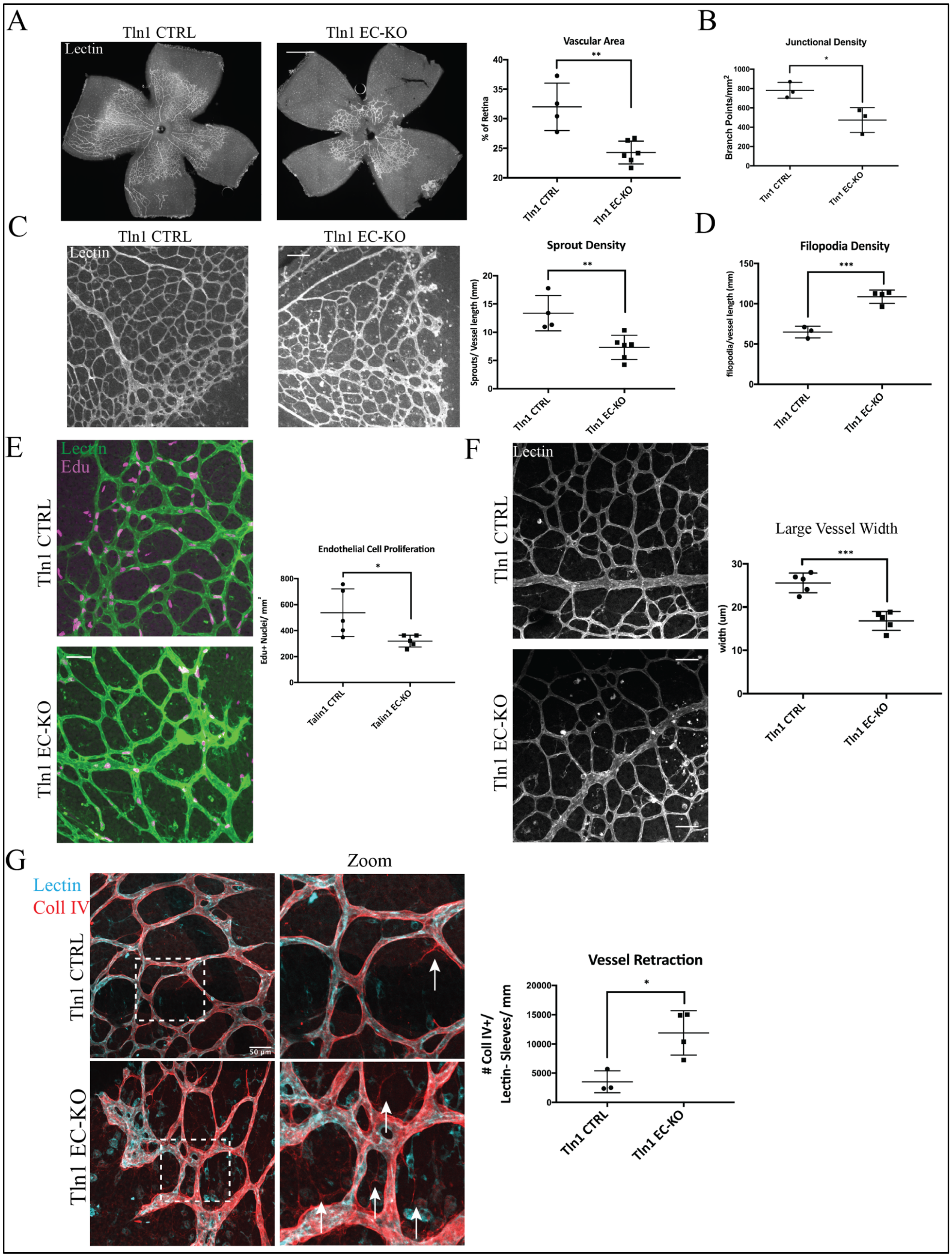
A
Tln1 CTRL
Tln1 EC-KO
Lectin
Vascular Area
% of Retina
Tln1 CTRL
Tln1 EC-KO
B
Junctional Density
Branch Points/mm2
C
Sprout Density
Sprouts/ Vessel length (mm)
D
Filopodia Density
filopodia/vessel length (mm)
E
Lectin
Edu
Endothelial Cell Proliferation
Edu+ Nuclei/ mm2
Talin1 CTRL
Talin1 EC-KO
F
Large Vessel Width
width (um)
G
Zoom
Lectin
Coll IV
50 μm
Vessel Retraction
Coll IV+/ Lectin- Sleeves/ mm

Figure 2.2. EC talin1 is required for retinal angiogenesis and EC proliferation

(A) FITC-lectin staining of whole-mount Tln1 CTRL and EC-KO retinas. FITC-lectin+ area was measured as a % of the total retinal area. (n=4-6; scale = 1 mm; ***P*=.0033) **(B)** Junctional density of Tln1 CTRL and EC-KO retinal vessels visualized by FITC-lectin staining. Retinal vessel area and junction counts were measured using Angiotool and revealed a reduction of vessel junctions in Tln1 EC-KO retinas relative to CTRL (n=3; **P*= .025) **(C)** Sprout density of Tln1 CTRL and Tln1 EC-KO whole-mount retinas stained with FITC-lectin. The number of sprouts across the length of the angiogenic front were reduced in Tln1 EC-KO retinas relative to Tln1 CTRL (n=4-6, scale = 100 µm; ***P*=.0063) **(D)** Filopodia density of Tln1 CTRL and Tln1 EC-KO retinal vessels which were stained with FITC-lectin. The number of filopodia across the length of the angiogenic front were increased in Tln1 EC-KO retinas relative to Tln1 CTRL (n=3-4; ****P*=.0007) **(E)** EC proliferation in Tln1 CTRL and Tln1 EC-KO retinal vessels was measured by quantitating edu+/lectin+ events. EC proliferation is reduced in Tln1 EC-KO retinas relative to control littermates (n=4; scale = 50 µm ; **P*=.045) **(F)** Large vessel widths measured in Tln1 CTRL and Tln1 EC-KO retinas stained with FITC-lectin. Large vessel width is reduced in Tln1 EC-KO retinal vasculature relative to Tln1 CTRL (n=5; scale = 50; ****P*=.0003) **(G)** Vessel retraction in Tln1 CTRL and Tln1 EC-KO retinal vessels measured by staining for basement membrane component Collagen IV (red) in conjunction with FITC-lectin. Retracted vessels are marked by white arrows representing coll IV deposition lacking a new vessel sprout. Vessel retraction is increased in Tln1 EC-KO retinas relative to Tln1 CTRL (n=3-4; scale = 50 µm; **P*=.018) (*P*-values listed for individual experiments were generated using a 2-tailed unpaired t-test).

contributions of EC talin1 during postnatal angiogenesis[184]. Retinas were dissected from Tln1 CTRL and Tln1 EC-KO pups at P5 and the endothelium visualized by FITC-lectin staining. The total FITC-lectin+ vascular areas of Tln1 EC-KO retinas were reduced by 30% relative to Tln1 CTRL littermates (Figure 2.2A). Furthermore, Tln1 EC-KO vascular networks appeared underdeveloped as measured by a reduction in the junctional density of the vascularized areas relative to Tln1 CTRL retinas (Figure 2.2B). Analysis of the angiogenic front where individual ECs sprout from pre-existing vessels to form a new vessel revealed an approximately 50% reduction in EC sprouts in Tln1 EC-KO retinas relative to littermate controls (Figure 2.2C). Although Tln1 EC-KO retinas had fewer sprouts across the angiogenic front, these sprouts exhibited a higher number of filopodia across this vascular front suggesting that ECs are able to extend filopodial protrusions, but that ECs are then unable to migrate through the ECM (Figure 2.2D). We hypothesized that reduced sprout formation and a reduced vascular area throughout the retina in Tln1 EC-KO mice may be suggestive of altered EC proliferation rates in retinal ECs from Tln1 EC-KO retinas relative to control littermates. To measure EC proliferation, pups were first administered tamoxifen intragastrically from P1-P3 to induce talin deletion. However, prior to being sacrificed, mice were injected with a tagged nucleoside analog, edu which is actively incorporated into dividing cells and detected using a Click-iT chemistry approach. To selectively analyze proliferating ECs, retinas were subject to FITC-lectin staining to visualize only the endothelium. Indeed, the number of lectin+/edu+ cells were significantly reduced in Tln1 EC-KO retinas relative to retinas from Tln1 CTRL pups (Figure 2.2E). The reduction in EC proliferation was noted throughout the vascular network at both the angiogenic front as well as in already established vessels within the central plexus of the network. Interestingly, mature vessels of Tln1 EC-KO retinas were significantly smaller than those of Tln1 CTRL retinal veins possibly due to reduced rates of EC proliferation (Figure 2.2F). To measure the vascular stability of the retinal vessels, we stained for the basement membrane component collagen IV (coll IV) in conjunction with FITC-lectin staining to measure the number of collagen IV+/lectin- sleeves. The presence of basement membrane without a lectin+ vessel is indicative of vessel retraction which was increased approximately three-fold in Tln1 EC-KO retinas compared to the Tln1 CTRL retinas (Figure 2.2G). The observed reductions in EC proliferation, retinal vascularization, EC sprouting and increased instability of Tln1 EC-KO vessels highlight the essential function of EC talin1 during retinal angiogenesis.

Expression of an integrin activation-deficient talin1 L325R mutant in ECs impairs postnatal angiogenesis

Talin activates integrins by binding to the β-integrin cytoplasmic tail at two distinct sites to induce the active conformation of the integrin receptor [116-118, 186]. We and others have reported a single amino acid mutation in the talin head (talin1 L325R) which inhibits the membrane proximal interaction required for talin to activate integrin yet retains binding to the membrane-distal site that mechanically links integrins to actin[168, 174]. Induced expression of this mutant in mouse platelets inhibited platelet integrin activation and resulted in impaired platelet function during hemostasis and thrombosis[170]. We hypothesized that expression of talin1 L325R in ECs would allow us to discern the specific requirement of talin-mediated integrin activation from its integrin-independent functions and allow us to specifically test the requirement of inside-out integrin activation during angiogenesis. We generated *Tln1*$^{f/wt}$; Cdh5-CreERT2$^{+/-}$ (referred to as Tln1 Het) and *Tln1*$^{f/L325R}$; Cdh5-CreERT2$^{+/-}$ (Tln1 L325R) mice by crossing previously described *Tln1*$^{f/L325R}$ mice with an inducible EC-specific Cre-recombinase mouse line. As a single allele of *Tln1* is sufficient for normal development and for platelet integrin activation[170], control mice in the experiments done in comparison to Tln1 L325R mice are heterozygous for the *Tln1* allele in order to accommodate breeding in of a tdTomato reporter allele to keep track of genetic recombination. Recombination efficiency of Cre-mediated talin deletion was measured by qualitative analysis of tdTomato reporter expression in retinal vessels and in later experiments, frozen tumor sections (Fig S2.1 and 2.2). Tln1 Het and Tln1 L325R neonates were intragastrically administered tamoxifen once per day to induce Cre activity from P1 to P3. Intriguingly, Tln1 Het and Tln1 L325R mice both reach weaning age and adulthood, but Tln1 L325R exhibited a marked reduction in body weight and development that was maintained into adulthood (Figure 2.3A and 2.3B). The Tln1 L325R phenotype differed from the early lethality observed in Tln1 EC-KO mice. Curiously, Tln1 L325R retinas examined at P5 exhibited defects in retinal angiogenesis as measured by vascular area and vascular density relative to Tln1 Het control mice (Figure 2.3C and 3D). These data indicate a requirement of talin-mediated EC integrin activation during retinal angiogenesis but also point to other possible talin-dependent functions that may be required for postnatal development given the severity of the phenotype observed in Tln1 EC-KO mice. In light of the defective postnatal angiogenesis exhibited in Tln1 L325R pups, we wondered whether talin-dependent integrin activation played a similar role in pathological contexts of angiogenesis. To answer this question, 2 weeks after tamoxifen administration to adult Tln1 Het and Tln1 L325R mice, we subcutaneously injected B16-F0 murine melanoma cells and analyzed the growth of primary tumors as well as the vascularization of the tumors. Strikingly, tumors injected in Tln1 L325R mice grew slower than Tln1 Het tumors and were 55% smaller by weight at removal 14 days post-implantation (Figure 2.3E). These tumors were excised, processed for frozen sectioning and blood vessel density of tumors

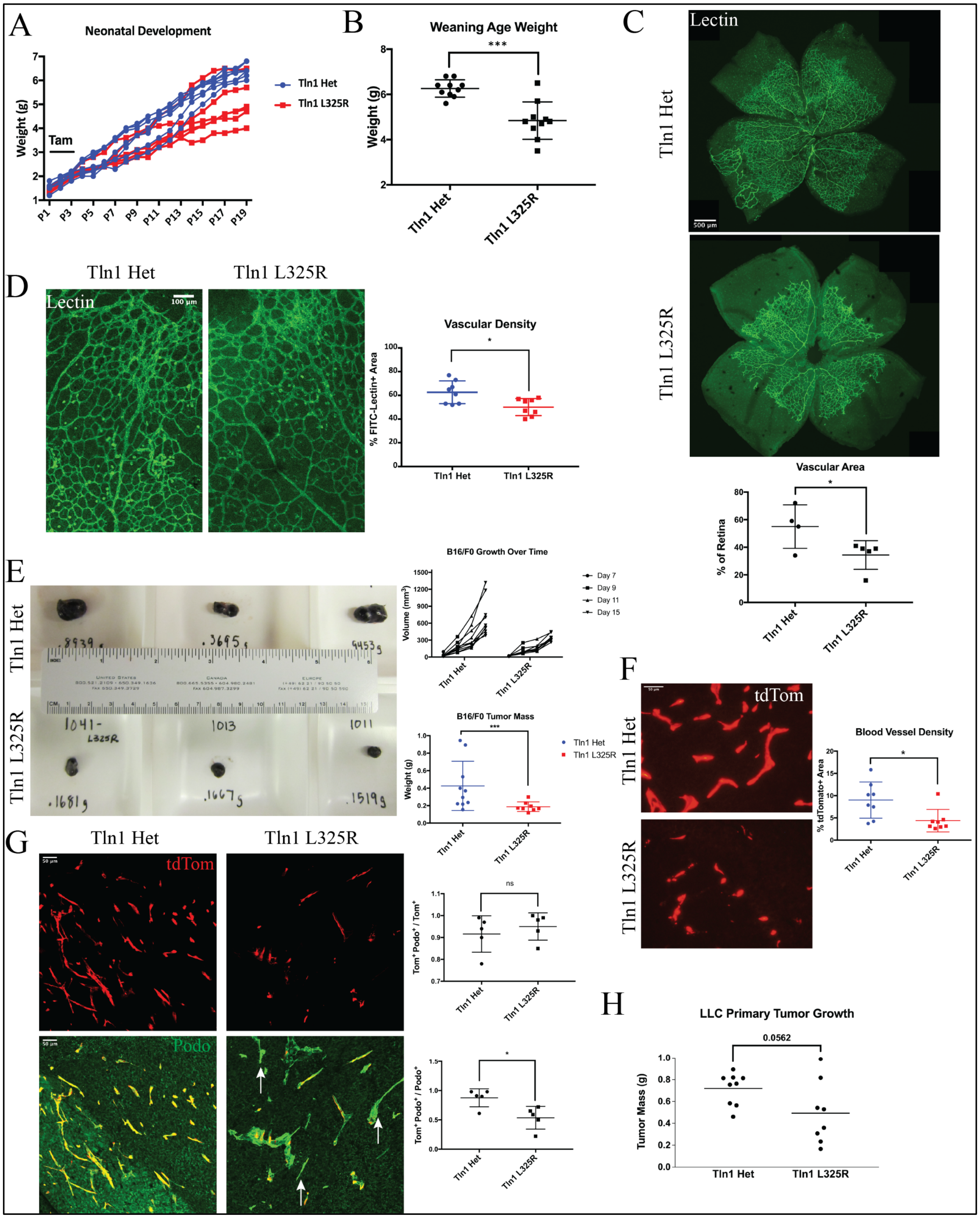
A
Neonatal Development
Weight (g)
Tam
Tln1 Het
Tln1 L325R
B
Weaning Age Weight
C
Lectin
D
Tln1 Het
Tln1 L325R
Vascular Density
% FITC-Lectin+ Area
Vascular Area
% of Retina
E
B16/F0 Growth Over Time
Volume (mm3)
Day 7
Day 9
Day 11
Day 15
B16/F0 Tumor Mass
F
tdTom
Blood Vessel Density
% tdTomato+ Area
G
Podo
Tom+ Podo+ / Tom+
Tom+ Podo+ / Podo+
H
LLC Primary Tumor Growth
0.0562
Tumor Mass (g)

Figure 2.3. Expression of mutant talin1 L325R incapable of activating integrins inhibits retinal angiogenesis, primary tumor growth and tumor angiogenesis

(A) Tln1 Het and Tln1 L325R neonates were weighed daily from P1-P19 prior to weaning. Tln1 L325R pups were undersized relative to littermate control Tln1 Het pups. (n= 7 Tln1 Het and 6 Tln1 L325R) **(B)** Tln1 Het and Tln1 L325R pups were weighed at P24 to determine weaning age weights. Tln1 L325R were 23% smaller than littermate controls. (n=10 per group; **P*=.0001) **(C)** Vascular area as % of total retinal area was measured on retinas from P5 Tln1 Het and Tln1 L325R pups stained for FITC-lectin. Total vascularized area was reduced in Tln1 L325R retinas relative to Tln1 Het mice. (n=4-5, scale = 500 µm ; **P*=.0498) **(D)** Vascular density in P7 Tln1 Het and L325R retinas was measured by staining for FITC-lectin. Tln1 L325R retinas exhibit a less dense vascular network relative to Tln1 Het littermate controls. (n=8; scale = 100 µm; **P*=.0105) **(E)** B16-F0 tumors were subcutaneously implanted in Tln1 Het and Tln1 L325R adult mice. Tumors were allowed to grow for 14 days with volume measured over time and mass of primary tumor taken on the final day. Tumors grown in Tln1 L325R mice grew slower and were smaller at the final time point relative to Tln1 CTRL mice (n=10 Tln1 Het, n=8 Tln1 L325R; ****P*=.0003) **(F)** Blood vessel density measured by tdTomato+ area in B16-F0 tumor sections from tumors grown in Tln1 L325R and Tln1 Het mice revealed reduced blood vessel density in Tln1 L325R tumor sections. (n=8; scale = 50 µm; **P*=.0163) **(G)** B16-F0 tumor sections visualized for tdTomato and stained for Podocalyxin (green) and analyzed for Tom+/Pod+ area relative to either total Tom+ area or total Pod+ area from Tln1 L325R and Tln1 Het mice. Although the ratio of Tom+/Pod / Tom+ areas is comparable, Tln1 L325R tumors have a reduced Tom+/Pod+/Pod+ areas relative to Tln1 CTRL indicating that most lumenized vessels in Tln1 L325R tumors are non-recombined. (n=5; scale = 50 µm ; *ns*=not signficiant, **P*=.0153) **(H)** Subcutaneously implanted Lewis Lung Carcinoma (LLC) tumors grown for 14 days in Tln1 L325R and Tln1 Het mice phenocopy reductions in primary tumor growth observed in the B16-F0 model. (n=9 Tln1 Het, n=8 Tln1 L325R; *P*=.0562) (*P*-values listed for individual experiments were generated using a 2-tailed unpaired t-test).

in both groups analyzed. Tln1 L325R frozen sections had an approximately 50% reduction in tdTomato+ area relative to Tln1 Het tumor sections (Figure 2.3F). Given the significant reduction in blood vessel density in Tln1 L325R tumors and the well-established paradigm that tumor vessels are immature, we wondered whether the vessels in the respective tumor groups differed in the extent of their lumenization as measured by the luminal marker Podocalyxin (Pod). To test this question, we stained Tln1 Het and L325R B16-F0 tumor sections and quantitated the coverage of Pod+Tom+/Pod+ and Pod+Tom+/Tom+ events. The first metric represents the proportion of lumenized, recombined vessels to all lumenized vessels in the section while the second metric represents the ratio of lumenized, recombined vessels to all recombined vessels. Tln1 Het and L325R tumors contained a similar number of Pod+Tom+/Tom+ vessels whereas Tln1 L325R contained fewer Pod+Tom+/Pod+ structures meaning a significant number of the vessels in L325R tumors were likely unrecombined, lumenized structures and thus wildtype talin1 containing vessels (Figure 2.3G). We used an independent syngeneic lung cancer cell line, Lewis Lung Carcinoma (LLC), to test whether the defects in tumor growth observed with B16-F0 were applicable to other primary tumor models. LLC tumors grown in Tln1 L325R mice were 31% smaller by mass relative to those grown Tln1 Het mice although this data did not reach statistical significance (p-value = 0.0562) (Figure 2.3H). Together, these data indicate that expression of talin1 L325R strongly inhibits tumor angiogenesis in a cell-autonomous fashion suggesting that EC integrin activation is essential for pathological blood vessel growth.

2.5 Discussion

Our results provide the first evidence that endothelial cell integrin activation is requisite for retinal and pathological angiogenesis. To test the requirement of integrin activation in these contexts, we utilized two novel mouse models: 1) an inducible, EC-specific talin1 knockout model 2) an inducible, EC-specific talin1 L325R model in which talin can bind to, but not activate, integrins. Induced deletion of EC-talin1 in neonates resulted in early lethality of Tln1 EC-KO pups by P8. Tln1 EC-KO mice exhibited impaired retinal angiogenesis, cranial and gastrointestinal hemorrhaging none of which were observed in control littermates. Deletion of talin in the retinal endothelium resulted in reduced vascularized area, reduced EC sprouting and reduced EC proliferation relative to retinal vessels of Tln1 CTRL mice. Induction of talin1 L325R expression during early postnatal development resulted in smaller mice at weaning age relative to control littermates and these lower body weights persisted into adulthood. Notably, we did not observe reduced survival in Tln1 L325R as we observed in Tln1 EC-KO pups. Tln1 L325R neonates exhibited impaired retinal angiogenesis as measured by vascular area and vascular density relative to their Tln1 Het littermates. Strikingly, Tln1 L325R adult mice subcutaneously implanted with either B16-F0 murine melanoma or Lewis Lung Carcinoma grew smaller tumors than their control counterparts with defects in tumor vascularization. Together these data indicate that talin-mediated integrin activation is required during postnatal angiogenesis and also highlight the intriguing finding that integrin-independent functions of talin may play a critical, not yet fully understood role in new blood vessel growth.

An important consideration in light of the observed differences between the Tln1 EC-KO and Tln1 L325R neonates is that ablation of talin eliminates an important adaptor protein that mechanically links integrin to the actin cytoskeleton[187, 188]. Presumably, Talin1 L325R retains this actin cytoskeleton linkage capacity in ECs. Indeed, the importance of the linkage to the actin cytoskeleton is highlighted in the different phenotypes observed in talin1 L325R and talin1-null platelets during clot retraction[168]. Whereas both talin1 L325R and talin1-null platelets exhibit defects in clot retraction, a process which requires integrin to be linked to the actin cytoskeleton, defects in talin1 L325R platelet clot retraction could be rescued by exogenously activating integrins with manganese but were lost when actin polymerization was inhibited by cytochalasin D[170]. Importantly, reports from Stefanini and colleagues as well as Haling and colleagues both report indicate that there is no difference in binding affinity of the L325R mutant relative to wildtype talin1[168, 170]. This observation indicates that the integrin-talin(L325R)-actin cytoskeleton linkage remains functionally intact. Therefore, it is reasonable to extrapolate that differences in Tln1 EC-KO and Tln1 L325R pup development may be due to retention of the talin rod interactions with the actin cytoskeleton in L325R pups. Additionally, the absence of the talin rod disrupts mechanosensitive interactions of the talin with the actin binding protein vinculin which binds cryptic sites in the talin rod that are exposed in tension-dependent manner [160, 187]. Specific vinculin-talin interactions promote binding of talin to actin cytoskeleton and are indispensable for focal adhesion stability[189]. Therefore, it is possible that talin engagement with the acto-myosin machinery may be of importance in other vascular beds other than the retina such as the small intestine and the brain where hemorrhaging was observed in Tln1 EC-KO pups (Figure 2.1C and 2.1D) but absent in Tln1 L325R pups. It is plausible that ECs in these vascular beds are subject to increased mechanical forces which in the absence of talin result in vascular instability but are mitigated in the presence of talin1 L325R.

As deletion of EC talin1 in established vessels is lethal due to defects in vascular permeability that are in part regulated by β1 integrin activation[181], it is remarkable that induction of talin1 L325R in already established vessels does not result in a similar effect on quiescent vessels. The aforementioned talin rod-mediated interactions with the actin-cytoskeleton may also explain the disparity in these two models meaning there are likely other important functions of talin outside of its role in activating integrins that may be of note in mature vasculature. However, while mature vessels in quiescent states appear unaffected by talin1 L325R induction (data not shown), Tln1 L325R mice display extensive defects in tumor growth and angiogenesis relative to their littermate controls suggesting that the defects observed in tumor angiogenesis in Tln1 L325R mice are in part due to defective integrin activation. Furthermore, my observation that the number of unrecombined, lumenized vessels were increased 39% in Tln1 L325R B16-F0 tumors indicates that Tln1 L325R may be critical in the process by which immature vessels, stabilize and form lumens. This result is suggestive of integrin-activation-independent interactions of talin with other proteins that may be critical for lumen formation. This observation is reminiscent of a report from Zovein and colleagues wherein deletion of β1 integrin in ECs during development resulted in occluded, unlumenized vessels[124] due to deficient Par3-mediated EC polarization during developmental angiogenesis. It may therefore be prudent to investigate the contributions of talin1 to EC polarity and whether talin1-null ECs exhibit altered Par3 signaling. Additionally, are defects observed in vessel growth and lumen formation in Tln1 L325R tumors driven by defects in integrin signaling of a specific heterodimer or subunit? Can the observed differences be “rescued” through exogenous activation of integrins?

Collectively, our studies point to a role for EC talin1 during postnatal angiogenesis at least in part through its integrin activating function. Future investigation into the molecular mechanisms underlying our observed defects in postnatal and tumor angiogenesis in Tln1 L325R mice should be enlightening.

2.5 Supplement

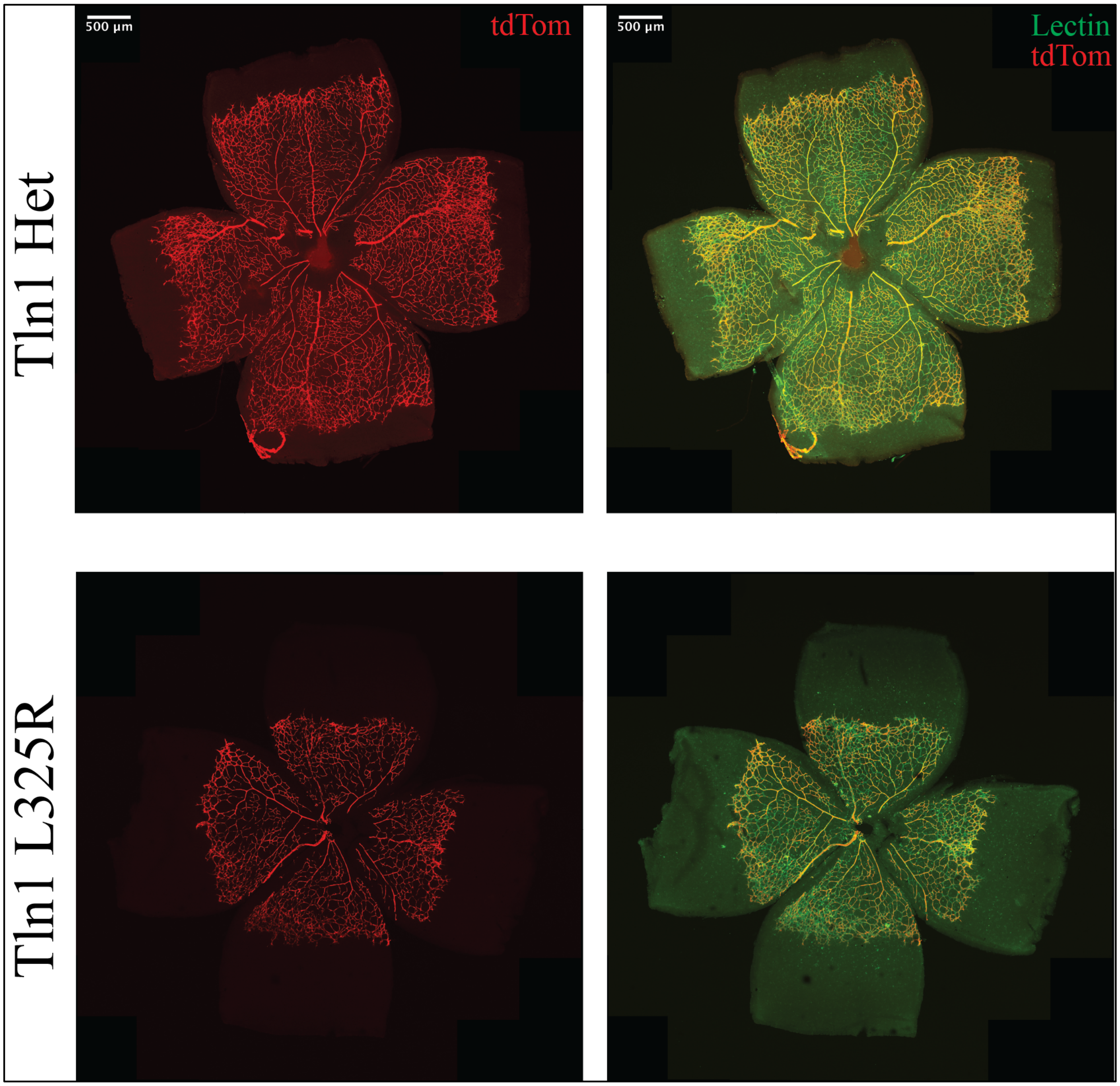

Figure S2.1. Recombination efficiency in Tln1 Het and Tln1 L325R ECs
Tln1 Het and Tln1 L325R retinas were excised from pups at P5 following tamoxifen injections from P1-P3. tdTomato+ reporter fluorescent protein is expressed in a majority of ECs that are co-stained with FITC-lectin indicating efficient cre-mediated recombination throughout the endothelium.

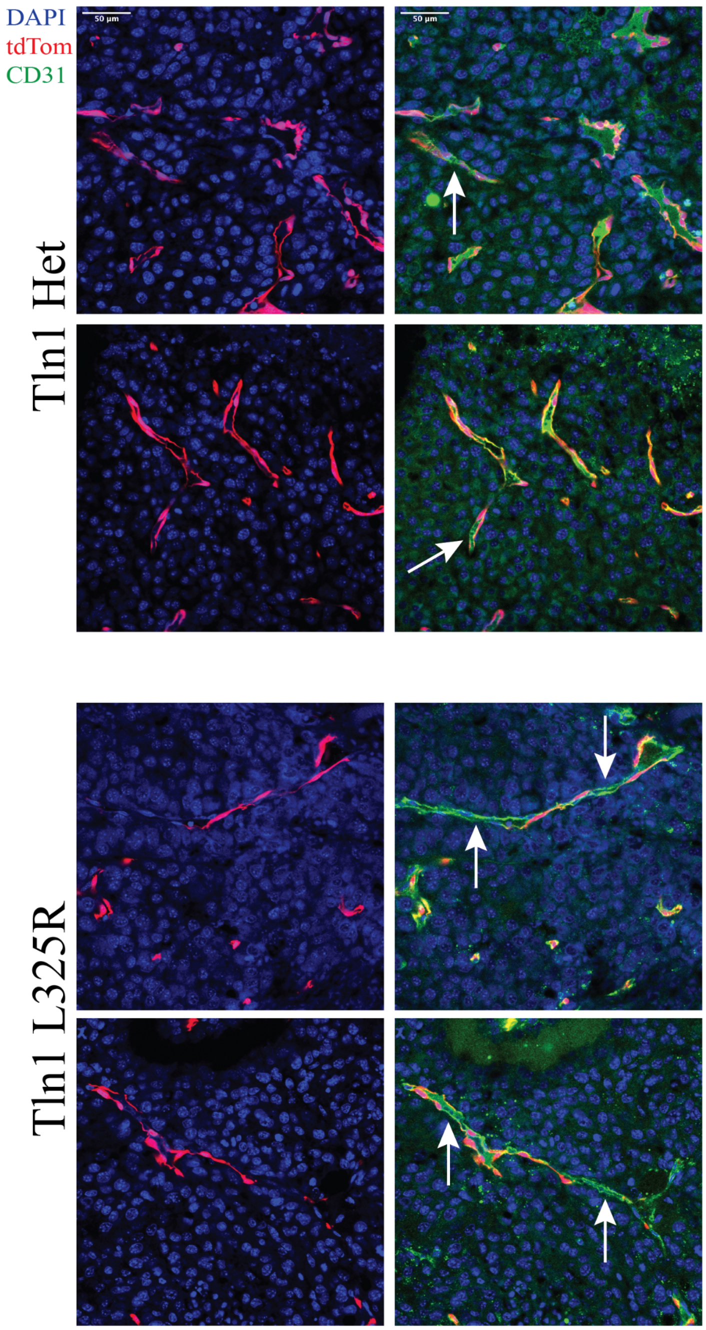

Figure S2.2. Tln1 Het and Tln1 L325R tumor vessels are recombined

B16-F0 tumor sections from tumors grown in Tln1 L325R and Tln1 Het mice were stained for CD31 to qualitatively analyze recombination efficiency. Most ECs in Tln1 Het sections were recombined while Tln1 L325R tumor sections had a greater number of unrecombined ECs.

Chapter 3. Talin-Dependent Integrin Activations Regulates VE-cadherin Localization and Endothelial Cell Barrier Function

Fadi E. Pulous BA, Cynthia M. Grimsley-Myers PhD, Shevali Kansal PhD, Andrew P. Kowalczyk PhD, Brian G. Petrich PhD

From the Department of Pediatrics, Aflac Cancer and Blood Disorders Center (FEP, SK, BGP), Cancer Biology Graduate Program (FEP), Department of Cell Biology (CMG, APK), Winship Cancer Institute and Department of Dermatology (APK), Emory University School of Medicine, Atlanta, GA 30322, USA.

This work was adapted from work published in *Circulation Research*:

Pulous FE, Grimsley-Myers CM, Kansal S, Kowalczyk AP, Petrich BG. Talin-dependent integrin activation regulates VE-cadherin localization and endothelial cell barrier function. Circ Res. 2019;124:891–903.

3.1 Abstract

Rationale: Endothelial barrier function depends on the proper localization and function of the adherens junction protein VE-cadherin. Previous studies have suggested a functional relationship between integrin-mediated adhesion complexes and VE-cadherin yet the underlying molecular links are unclear. Binding of the cytoskeletal adaptor protein talin to the β integrin cytoplasmic domain is a key final step in regulating the affinity of integrins for extracellular ligands (activation) but the role of integrin activation in VE-cadherin mediated endothelial barrier function is unknown.

Objective: To test the requirement of talin-dependent activation of β1 integrin in VE-cadherin organization and endothelial cell barrier function.

Methods and Results: Endothelial cell-specific deletion of talin in adult mice resulted in impaired stability of intestinal microvascular blood vessels, hemorrhage and death. Talin-deficient endothelium showed altered VE-cadherin organization at endothelial cell-cell junctions *in vivo*. shRNA (short hairpin RNA)-mediated knockdown of talin1 expression in cultured endothelial cells led to increased radial actin stress fibers, increased adherens junction width and increased endothelial monolayer permeability measured by electrical cell-substrate impedance sensing. Restoring β1 integrin activation in talin-deficient cells with a β1 integrin activating antibody normalized both VE-cadherin organization and endothelial cell barrier function. In addition, VE-cadherin organization was normalized by re-expression of talin or integrin activating talin head domain but not a talin head domain mutant that is selectively deficient in activating integrins.

Conclusions: Talin-dependent activation of endothelial cell β1 integrin stabilizes VE-cadherin at endothelial junctions and promotes endothelial barrier function.

3.2 Introduction

Endothelial cells line the luminal blood vessel surface forming a barrier that separates the blood from surrounding tissues. EC barrier function is tightly regulated, dynamic and plays a central role in human health and disease. The EC barrier is maintained in part by adherens junctions , comprised of VE-cadherin and associated cytoplasmic interacting proteins[18, 37, 190]. In response to permeability inducing hormones and autocoids such as vascular endothelial growth factor and thrombin, AJs remodel and the endothelium becomes more permeable. These changes in vascular permeability play an important role in leukocyte transmigration and tissue fluid homeostasis[191-193].

The plasticity of AJs in response to extracellular cues depends upon connections to the actin cytoskeleton. VE-cadherin is linked indirectly to actin through its interaction with the β-catenin and α-catenin complex. [194] Mice expressing a VE-cadherin-α-catenin fusion which is retained at AJs were protected from VEGF-induced permeability clearly demonstrating the functional significance of VE-cadherin junctional stability in vivo. [100] Actomyosin-dependent contraction of ECs regulates the endothelial barrier and the reorganization of junctional VE-cadherin pools in response to the altered actin cytoskeleton tension induces the appearance of tensile AJs referred to as focal adherens junctions (FAJs). [71, 94] Like AJs, integrin containing adhesion complexes are linked indirectly to the actin cytoskeleton through interactions with cytoskeleton adaptor proteins[59] . Indeed, a functional relationship been AJs and integrins is well-established but the underlying molecular mechanisms are yet unclear[113].

Integrins are heterodimeric adhesion receptors comprised of α and β-subunits which bind, among other ligands, extracellular matrix components important in mediated cell adhesion to the basement membrane.[195] Quiescent endothelium expresses at least seven classes of integrin with β1 integrin, one of the best studied in endothelium, dictating specificity for fibronectin (α5β1), collagen (α1β1, α2β1) and laminin (α3β1, α6β1). [114] Concomitant endothelial-specific deletion of α5 and αv leads to cardiovascular defects and embryonic lethality by E14.5.[123] EC-specific deletion of β1 integrin during development resulted in embryonic lethality between E9.5-E.10.5 characterized by vascular patterning defects and vessel malformations[196] whereas inducible genetic deletion of β1 integrin in ECs or postnatal pharmacological blockade of β1 integrin resulted in impaired lumen formation and defects in EC apical-basal polarity during new vessel growth.[197] More recently, EC-specific genetic deletion of β1 integrin in mice supported a role for β1 integrin expression in stabilizing VE-cadherin at cell-cell junctions.[138] Collectively, these data indicate that the expression of β1 integrin in ECs is critical for normal vascular development and blood vessel stability.

An important property of integrins is the modulation of affinity for extracellular ligands, a process termed integrin activation or "inside-out integrin signaling". A key final step in activating integrins is binding of the N-terminal head domain of the cytoskeletal protein talin to the β integrin cytoplasmic domain. [116-118, 198] Whereas many of the molecular and structural details of how talin binding activates integrins[118] and the biological significance of talin-dependent integrin activation have been clearly demonstrated in hematopoietic cells[165, 166, 170, 199, 200], the requirement for talin-dependent integrin activation in established blood vessels has not been tested. EC-specific deletion of *Tln1* in mice causes embryonic lethality due to defects in angiogenesis resulting in extensive vascular hemorrhaging and lethality by E9.5 [201] supporting a clear role of talin in embryonic developmental angiogenesis.

Here, we analyzed mice in which we have genetically deleted *Tln1* selectively in the endothelium of established blood vessels of adult mice using an inducible conditional Cre/loxP recombination approach. Interestingly, our findings indicate the importance of EC talin1 in the stability and barrier function of the intestinal microvasculature. Furthermore, we present both *in vivo* and *in vitro* data that support a role for talin in VE-cadherin organization and show that talin-dependent activation of β1 integrin is a key node in this pathway required for AJ stability and integrity of the endothelium.

3.2 Methods

Mice

To delete talin1 postnatally in endothelial cells, *Tln1*$^{f/f}$;Cdh5-C**r**eERT2$^{+/-}$ [182, 202] (a gift from Ralf Adams, Max Planck Institute) male mice were crossed with *Tln1*$^{f/f}$ female mice to generate *Tln1*$^{f/f}$;Cdh5-CreERT2$^{-/-}$ (Tln1 CTRL) and *Tln1*$^{f/f}$;Cdh5-CreERT2$^{+/-}$ (Tln1 EC-KO) offspring. Studies using the tdTomato reporter were done by comparing mice with genotype *Tln1*$^{f/f}$;Cdh5-CreERT2$^{+/-}$;Rosa26-tdTomato$^{+/-}$ with *Tln1*$^{f/wt}$;Cdh5-CreERT2$^{+/-}$;Rosa26-tdTomato$^{+/-}$ mice. Adult mice, 8-10 week old mice were treated with tamoxifen (Cayman Chemicals) dissolved in corn oil via intraperitoneal injection (2mg/mouse/day) for 3 consecutive days. For retinal angiogenesis studies, pups received tamoxifen (dissolved in corn oil) via intragastric injection (50μg/mouse/day) for 3 consecutive days starting on postnatal day 2. Similar ratios of males and female mice were used for experiments and experimenters were blinded to the genotypes of mice until all data was collected. In control experiments to test the effects of tamoxifen versus corn oil on survival mice were randomly assigned to treatment groups.

Statistical Analysis

All statistical tests were performed using Prism Software 8.0. The specific test that was used to analyze individual experiments is noted in the figure legends but briefly for comparison of parametric data from two groups, an unpaired t-test was used. Data sets analyzed with parametric statistical tests were tested for a normal distribution using a Shapiro-Wilk test. For comparison of vessel leak in mouse organs, we performed multiple unpaired t-tests as only two groups (CTRL vs EC-KO) were compared. Where noted in the legends, we performed one-way analysis of variance with either a Dunnet's, Tukey or Sidak's Multiple comparison test. The number of animals and experimental repeats is listed in individual legends. Detailed methods can be found in the supplement.

3.3 Results

Endothelial-specific deletion of talin1 in established blood vessels causes intestinal vascular hemorrhage and death.

To test the contribution of talin-dependent integrin activation in endothelial cells in the maintenance and stability of mature vasculature, we generated endothelial cell (EC)-specific talin1 knock-out mice utilizing *Tln1* floxed mice [165, 166] expressing a tamoxifen-inducible Cre driven by the VE-cadherin (*Cdh5*) promoter[182]. Adult *Tln1*$^{f/f}$;Cdh5-CreERT2$^{-/-}$ (referred to as Tln1 CTRL) and *Tln1*$^{f/f}$;Cdh5-CreERT2$^{+/-}$ (Tln1 EC-KO) mice were administered tamoxifen at 8-10 weeks of age. Strikingly, Tln1 EC-KO mice developed sudden-onset morbidity, including inactivity and hunched posture, starting approximately 14 days after tamoxifen treatment and died 16-21 days after tamoxifen treatment (Fig 3.1A). Neither Tln1 EC-KO mice treated with corn oil vehicle nor *Tln1*$^{f/f}$;Cdh5-CreERT2$^{-/-}$ mice treated with tamoxifen showed adverse effects

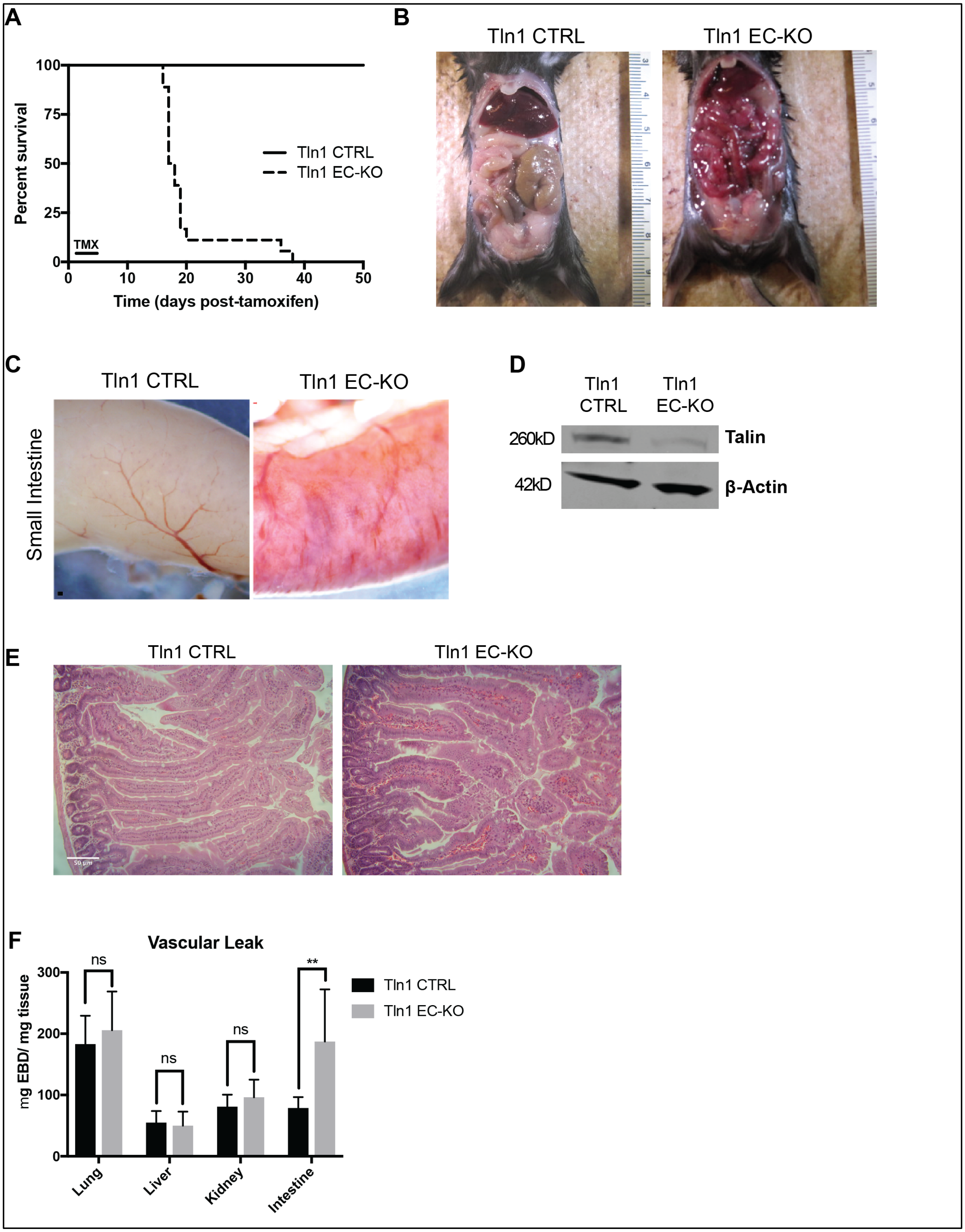
A
100
75
50
25
0
Percent survival
TMX
0
10
20
30
40
50
Time (days post-tamoxifen)
Tln1 CTRL
Tln1 EC-KO
B
Tln1 CTRL
Tln1 EC-KO
C
Tln1 CTRL
Tln1 EC-KO
Small Intestine
D
Tln1 CTRL
Tln1 EC-KO
260kD
Talin
42kD
β-Actin
E
Tln1 CTRL
Tln1 EC-KO
F
Vascular Leak
ns
ns
ns
**
300
200
100
0
mg EBD/ mg tissue
Lung
Liver
Kidney
Intestine
Tln1 CTRL
Tln1 EC-KO

Figure 3.1: Endothelial cell-specific deletion of talin1 in established blood vessels causes intestinal vascular hemorrhage and death.

A-C. Adult Tln1 EC-KO (*Tln1*$^{fl/fl}$;Cdh5creERT2$^{+/-}$) and Tln1 CTRL (*Tln1*$^{fl/fl}$;Cdh5creERT2$^{-/-}$) mice were administered tamoxifen once a day for 3 consecutive days via intraperitoneal injection. **A.** Survival of Tln1 EC-KO and Tln1 CTRL mice following tamoxifen treatment (n=15, Tln1 CTRL; n=14, Tln1 EC-KO). **B.** Pictures of exposed peritoneum of adult Tln1 EC-KO and CTRL mice sacrificed 16 days after tamoxifen treatment. **C.** Macroscopic images of intestinal vascular hemorrhage in Tln1 EC-KO adult mice 16 days after tamoxifen treatment. **D.** Western blot analysis of talin expression in mouse lung endothelial cell cultures isolated from Tln1 CTRL or Tln1 EC-KO mice. Cultures were treated with 4-hydroxy-tamoxifen for 4 days and protein lysates subjected to Western blotting with talin and β-actin antibodies. (n=2). **E**. Hematoxylin/eosin staining of small intestine isolated from Tln1 CTRL and Tln1 EC-KO mice 16 days after tamoxifen treatment showing the presence of extravascular red blood cells in Tln1 EC-KO villi. (n=3; scale=50 μm). **F**. Measurements of Evan's Blue Dye (EBD) in lung, liver, intestine, brain and kidney of Tln1 CTRL and Tln1 EC-KO mice 2 hours after intravenous injection. (n=12, Tln1 CTRL; n=10, Tln1 EC-KO; **p = 0.0013 two-tailed unpaired t-test).

or reduced survival (data not shown and Fig 3.1A). Gross examination of Tln1 EC-KO adult mice 16 days after deletion of talin1 deletion revealed bloody intestines whereas abnormalities in other organs were not observed (Fig 3.1B and 3.1C). Talin protein expression was reduced by 82% in ECs isolated from lungs of Tln1 EC-KO mice treated with tamoxifen *in vitro* (Fig 3.1D). In light of the observed extravascular red blood cells in the intestinal capillaries of Tln1 EC-KO mice visualized by Hematoxylin and eosin staining (Fig 3.1E), we measured the leak of circulating Evan's Blue Dye (EBD), a well-established *in vivo* assay to assess vascular permeability[203]. Two hours after intravenous injection of EBD, which binds tightly to serum albumin, Tln1 EC-KO mice showed approximately a 2.5-fold increase in EBD content in the small intestines compared to Tln1 CTRL mice indicating impaired endothelial barrier function in the intestines of Tln1 EC-KO mice (Fig 3.1F). We also deleted *Tln1* utilizing a second EC-specific, tamoxifen-inducible PDGFβ-CreERT2 mouse line[204]. Tamoxifen treatment of *Tln1*$^{f/f}$,PDGFβ-CreERT+/- mice resulted in similar intestinal bleeding and death as when *Tln1* was deleted with *Cdh5*-CreERT2 (Fig S3.1A-C). The possibility of Cre-mediated recombination in hematopoietic cells in Cdh5-CreERT2 and PDGFβ-CreERT2 mice was examined with a Rosa26-flox-stop-flox-TdTomato (TdTom) Cre reporter mouse (Jackson Labs #007914). Flow cytometry of peripheral blood isolated from tamoxifen-treated PDGFβ-CreERT2$^{+/-}$;TdTom mice showed TdTomato expression in approximately 10% of platelets consistent with the previous characterization of these mice[204]. In contrast, TdTomato expression was not detected in any peripheral hematopoietic cells isolated from tamoxifen-treated Cdh5-CreERT2$^{+/-}$;TdTom mice (Fig S3.1D). Since talin expression in platelets is essential for hemostasis[165, 166], we utilized Cdh5-CreERT2 to delete EC talin1 in all subsequent experiments.

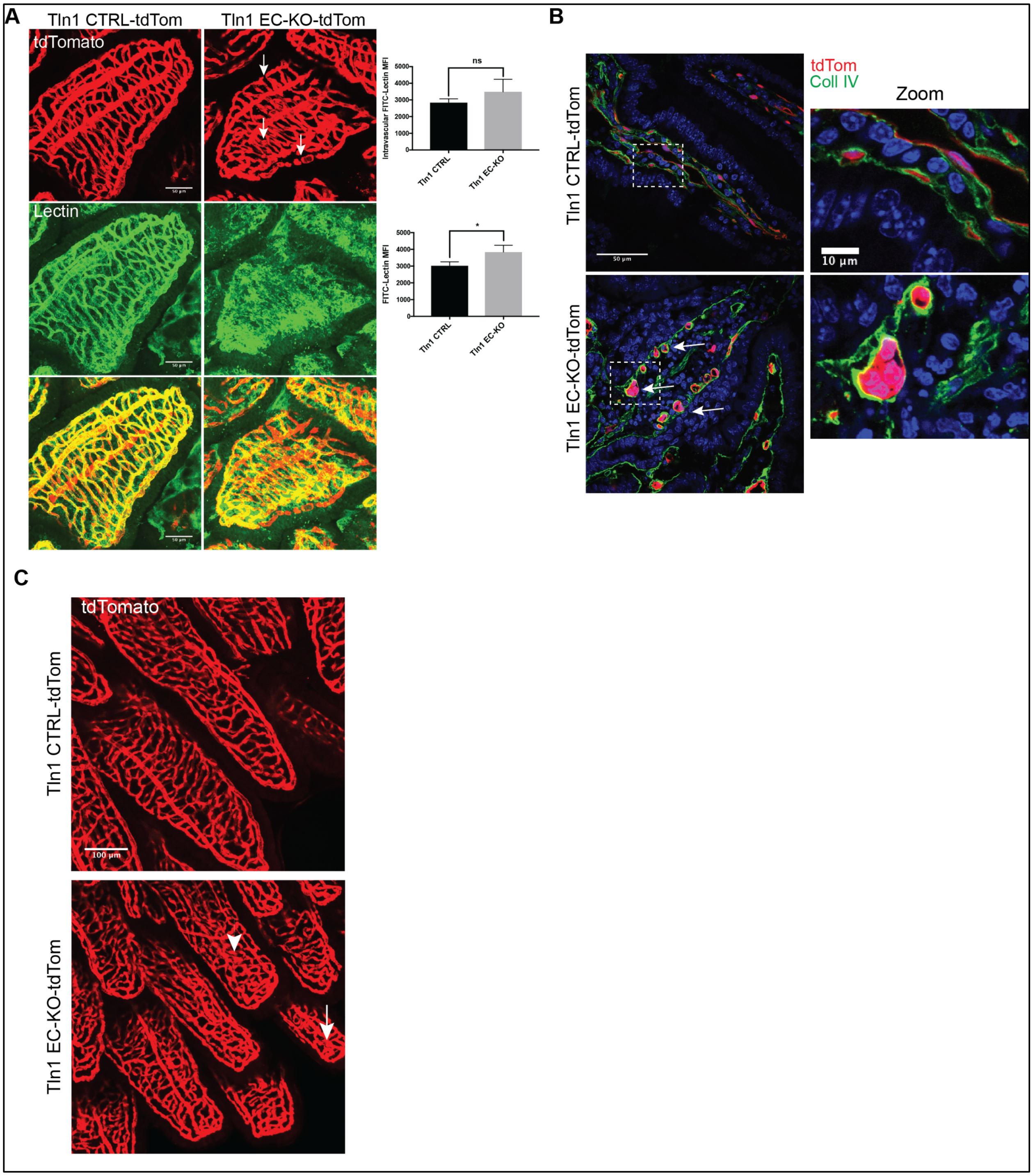
A
Tln1 CTRL-tdTom
Tln1 EC-KO-tdTom
tdTomato
Lectin
ns
Intravascular FITC-Lectin MFI
Tln1 CTRL
Tln1 EC-KO
*
FITC-Lectin MFI
B
tdTom
Coll IV
Zoom
Tln1 CTRL-tdTom
Tln1 EC-KO-tdTom
50 µm
10 µm
C
tdTomato
Tln1 CTRL-tdTom
Tln1 EC-KO-tdTom
100 µm

Figure 3.2: Endothelial talin is required for maintenance of intestinal vascular integrity and barrier function.

A. TdTomato and FITC-lectin were visualized in the villi of mice 16 days after tamoxifen injection. Mice were injected intravenously with FITC-lectin 30 minutes prior to sacrifice. (n=3;scale=50 µm). Total FITC-lectin fluorescence and intravascular lectin levels were quantitated indicating increased extravascular leak in Tln1 EC-KO-tdTom mice relative to Tln1 CTRL-tdTom (n=3 mice/group; *p=0.039 two-tailed unpaired t-test) **B.** Confocal microscopic analysis of cryosections of intestine showing tdTomoto fluorescence and collagen IV immunofluorescence. Inset shows a zoomed region demonstrating endothelial cell rounding (white arrows) and detachment from neighboring cells in the intestinal villi of Tln1 EC-KO-tdTom mice. (n=3; scale=50 µm; zoom scale=10 µm). **C.** TdTomato fluorescence showing disorganized capillaries and cyst-like structures (white arrows) in Tln1 EC-KO-tdTom intestinal wall and villi 12 days after tamoxifen injections. (n=3; scale=100 µm).

Endothelial talin1 is required for intestine vascular barrier function

To visualize vascular morphology in cre-recombined cells, the above-described TdTomato Cre-reporter was bred into Tln1 EC-KO and CTRL mouse lines to create *Tln1*$^{wt/f}$;Cdh5-CreERT2$^{+/-}$,TdTomato^{+} (Tln1 CTRL-TdTom) and *Tln1*$^{f/f}$;Cdh5-CreERT2$^{+/-}$,TdTomato^{+} (Tln1 EC-KO-TdTom) mice. Intravascular labeling of the endothelium with FITC-lectin for 30 minutes revealed extravascular accumulation of FITC-lectin in surrounding intestinal tissue in Tln1 EC-KO-TdTom mice 16 days after tamoxifen suggestive of vascular leak despite comparable intravascular FITC-lectin labeling (Fig 3.2A). Confocal microscopic analysis of Tln1 EC-KO-TdTom villi revealed disorganized villi capillary beds with the appearance of round cyst-like malformations composed of multiple ECs (Fig 3.2B) that were not observed in Tln1 CTRL-TdTom littermates. We examined the vasculature of whole-mounted segments of small intestine from adult mice as early as 12 days after tamoxifen injection and observed morphological defects in the microvasculature of Tln1 EC-KO-TdTom mice, characterized by small cyst-like structures and widening of the villi capillaries (Fig 3.2C). Importantly, TdTomato was expressed in the blood vessels of all organs examined including the brain, liver and heart, of Tln1 CTRL-TdTom and Tln1 EC-KO-TdTom mice indicating efficient activation of Cre after tamoxifen treatment (Fig S3.2). Deletion of *Tln1* transcript in intestinal ECs was confirmed by reverse transcription and real-time PCR analysis of RNA isolated from FACS-sorted intestinal ECs (Fig S3.3). Together, the foregoing data support an important function of talin in the maintenance and stability of intestinal microvasculature.

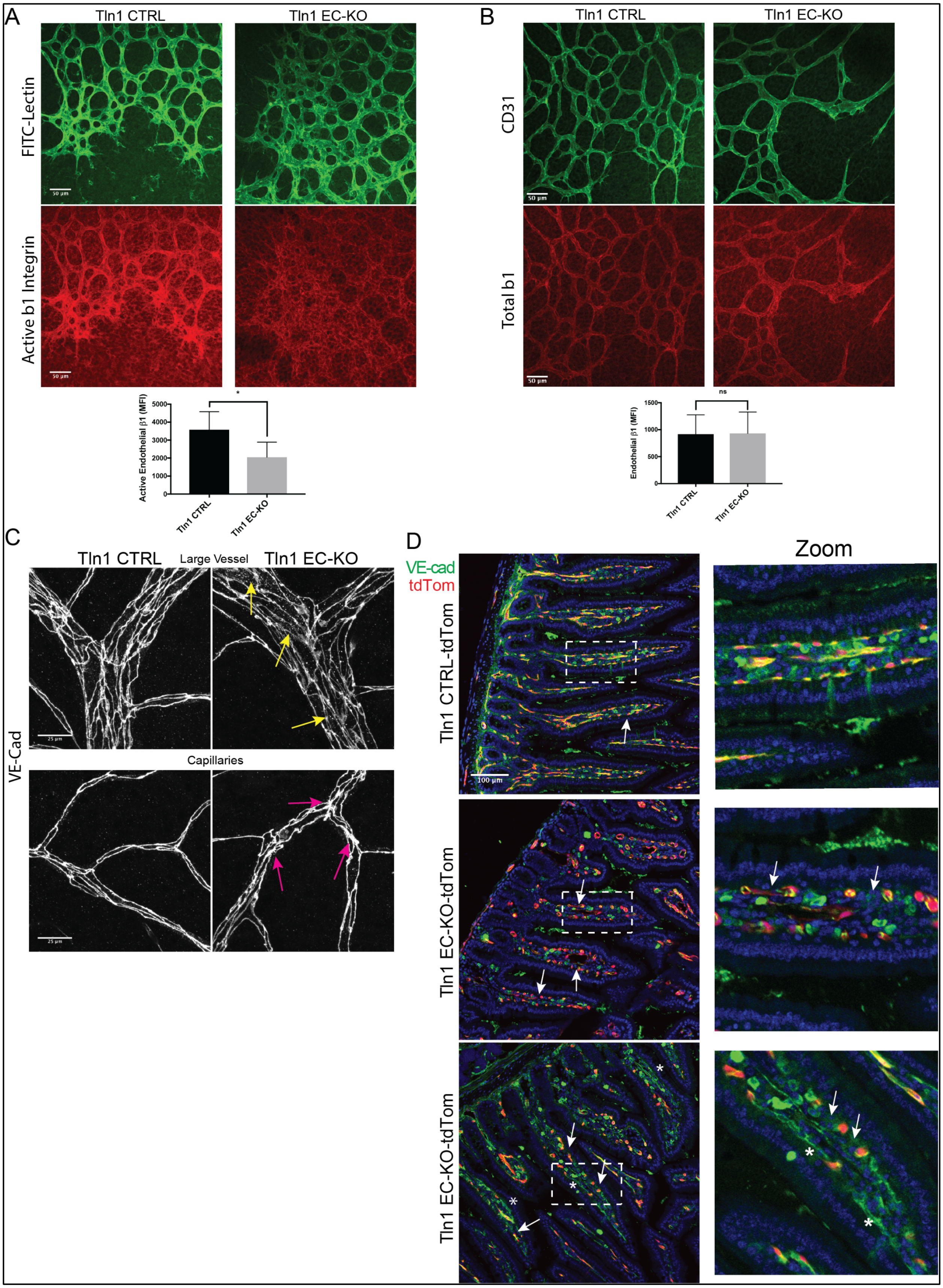
A
Tln1 CTRL
Tln1 EC-KO
FITC-Lectin
Active b1 Integrin
50 µm
Active Endothelial β1 (MFI)
Tln1 CTRL
Tln1 EC-KO
B
Tln1 CTRL
Tln1 EC-KO
CD31
Total b1
50 µm
Endothelial β1 (MFI)
ns
C
Tln1 CTRL
Large Vessel
Tln1 EC-KO
Capillaries
VE-Cad
25 µm
D
VE-cad
tdTom
Zoom
Tln1 CTRL-tdTom
Tln1 EC-KO-tdTom
Tln1 EC-KO-tdTom
100 µm

Figure 3.3: Reduced β1 integrin activation and disorganized adherens junctions in established vessels of Talin1 EC-KO mice.

A-B. Immunofluorescence analysis of active β1 integrin with the activation-sensitive antibody 9EG7 (A) or total β1 integrin with an activation insensitive β1 integrin antibody HMb1-1 (n=3-4; *p=0.03 two-tailed unpaired t-test) (B) in whole mounted retinas from Tln1 EC-KO and Tln1 CTRL mice. Neonates were treated with tamoxifen on P1-3 and sacrificed on postnatal day 7 (P7) at which time retina whole mounts were prepared for staining. (n=3-4; ns=not significant unpaired t-test; scale=50 μm). **C**. Altered junctional thickness (magenta arrows) and localization of VE-Cadherin (yellow arrows) in retinal vessels and capillaries of Tln1 EC-KO mice 16 days after tamoxifen injections compared to Tln1 CTRL mice. (n=3; scale=25 μm). **D**. VE-cadherin immunofluorescence of intestine cryosections showing disrupted cell-cell junctions in villi (white arrows) of Tln1 EC-KO-tdTom mice 16 days after tamoxifen treatment. Changes in cell-cell junctions appear cell autonomous as junctions between non-recombined ECs in Tln1 EC-KO-tdTom villi (asterisks) are intact. (n=3; scale=100 μm).

Reduced β1 integrin activation and disorganized adherens junctions in established vessels of Talin1 EC-KO mice.

Consistent with the established role of talin as a key regulator of integrin activation, immunofluorescence analysis of retinas of P7 Tln1 EC-KO and CTRL neonates with a β1 integrin activation-sensitive antibody indicated a significant reduction in active β1 integrin in Tln1 EC-KO endothelium (Fig 3.3A). Importantly, total β1 integrin expression in the retina appeared similar between groups (Fig 3.3B). Furthermore, similar levels of β1 integrin surface expression were observed in acutely isolated lung ECs from adult Tln1 EC-KO and CTRL mice 15-days after tamoxifen treatment (Fig S3.4A). Endothelial barrier function depends on VE-cadherin (VE-Cad)[37, 190]. Recent work highlighting the requirement of endothelial β1-integrin in maintaining vessel stability by regulating VE-cadherin localization[138] suggested that VE-Cad localization might be altered in the endothelium of Tln1 EC-KO mice. Whole-mount staining of retinal vasculature from adult Tln1 EC-KO and CTRL mice 15 days after tamoxifen treatment revealed disorganized capillary cell-cell junctions and increased intracellular VE-Cad staining relative to Tln1 CTRL mice (Fig 3.3C). Interestingly, intestinal capillary junctions visualized by immunofluorescence of VE-Cad were discontinuous with ECs detached from neighboring ECs (Fig 3.3D). Analysis of zonula occludens-1 (ZO-1), a component of tight junctions, similarly showed altered organization in P7 Tln1 EC-KO retinas (Fig S3.5B). Together, these data indicate that talin expression is necessary for β1 integrin activation in ECs *in vivo* and suggest an important mechanistic link between talin-dependent β1 integrin activation and the regulation of cell-cell junction organization in ECs.

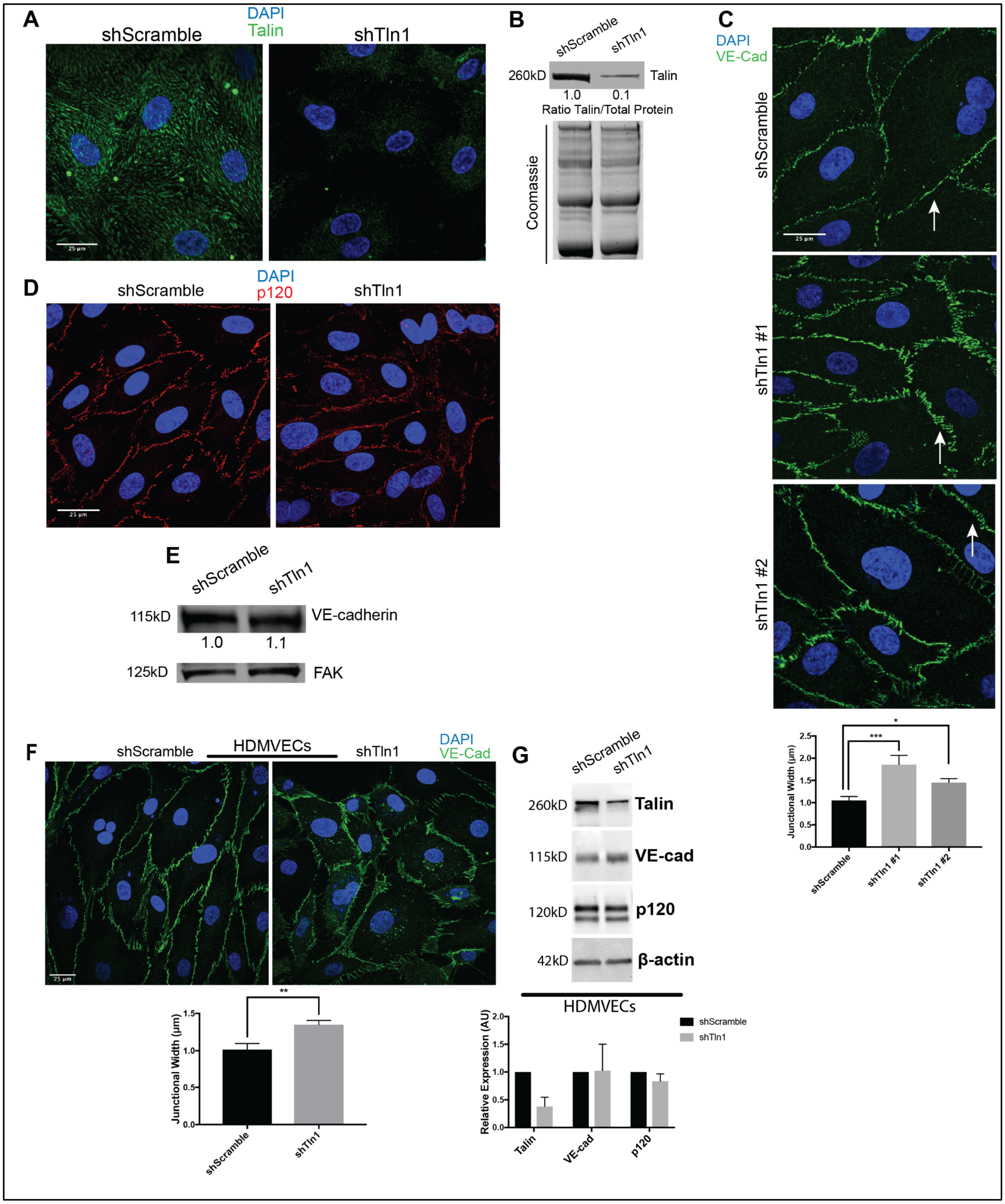
A
DAPI
Talin
shScramble
shTln1
B
shScramble
shTln1
260kD
Talin
1.0
0.1
Ratio Talin/Total Protein
Coomassie
C
DAPI
VE-Cad
shScramble
shTln1 #1
shTln1 #2
D
DAPI
p120
shScramble
shTln1
E
shScramble
shTln1
115kD
VE-cadherin
1.0
1.1
125kD
FAK
Junctional Width (µm)
shScramble
shTln1 #1
shTln1 #2
F
shScramble
HDMVECs
shTln1
DAPI
VE-Cad
Junctional Width (µm)
shScramble
shTln1
G
shScramble
shTln1
260kD
Talin
115kD
VE-cad
120kD
p120
42kD
β-actin
HDMVECs
Relative Expression (AU)
shScramble
shTln1
Talin
VE-cad
p120

Figure 3.4: Increased width of adherens junctions formed by talin-deficient endothelial cells. **A**. HUVECs were infected with talin1 shRNA (shTln1) or scramble sequence shRNA (shScramble) lentivirus. Immunostaining for talin1/2 72 hours after shRNA infection shows efficient knockdown of talin protein in shTln1 cells (n=5; scale=25 μm). **B**. Western blot analysis and quantitation of talin1 protein levels relative to total protein in shScramble and shTln1 treated HUVECs (n=5). **C**. Max-intensity projections depicting Immunofluorescence of VE-Cadherin in cells infected with two different shTln1 lentiviruses. shTln1 HUVECs shows disorganized cell-cell junctions and increased junctional width (white arrows) compared to shScramble HUVECs. (n=3; ***p=0.0007, *p=0.0225 one-way ANOVA with Dunnett's multiple comparisons test). **D**. Immunofluorescence of p120-catenin in shTln1 and shScramble HUVECs. (n=3). **E.** Western blot analysis of VE-cadherin protein levels in shScramble and shTln1 HUVECs show similar levels of expression (n=6). **F**. Human dermal microvascular cells (HDMVECs) treated with shTln1 lentivirus exhibit increased junctional width relative to shScramble treated cells (n=3; scale=25 μm; **p=0.0042 two-tailed unpaired t-test). **G.** Western blot analysis and quantitation of talin1/VE-cad/p120 protein levels in shScramble and shTln1 HDMVECs. Efficient deletion of talin1 does not appear to affect relative expression of VE-cad or p120 protein (n=3).

Disorganized cell-cell junctions in talin-deficient endothelial cells.

To further investigate the mechanisms by which EC talin1 contributes to cell-cell junction stability, we deleted talin1 using short hairpin RNAs in human umbilical vein endothelial cells (HUVECs) as measured by immunofluorescence and western blot analysis (Fig 3.4A and 3.4B). Deletion of talin1 did not alter surface expression of the major endothelial integrins as measured by flow cytometry (Fig S3.4B). Talin-deficient cells exhibited a striking difference in the junctional organization of VE-cadherin (Fig 3.4C) and ZO-1 (Fig S3.5A) with significantly wider cell junctions in shTln1 cells relative to shScramble control cells. p120 staining at the cell-cell junctions was discontinuous and diffuse in shTln1 cells consistent with altered AJ organization (Fig 3.4D). Altered junctional organization in talin-deficient ECs was not accompanied by any consistent detectable changes to VE-cadherin or p120 protein expression relative to shScramble cells (Fig 3.4E, Fig S3.6B). Changes to junctional organization in talin-deficient ECs were also evident in human dermal blood microvascular endothelial cells (HDMVECs). Deletion of talin1 in HDMVECs increased junctional width (Fig 3.4F) with no consequence to the total expression of adherens junction components VE-cadherin and p120 (Fig 3.4G). Because of the junctional alterations exhibited in talin-deficient ECs, we speculated that increased cell contraction[138] might be responsible for changes in junctional morphology of talin-deficient ECs. Indeed, talin-deficient HUVECs and HDMVECs displayed increased actin stress fiber formation relative to shScramble cells (Fig 3.5A and Fig S3.6D). Phosphorylation of myosin light chain was also increased in talin-deficient HUVECs, consistent with increased contractility in the absence of talin (Figure 3.5B). Pharmacological inhibition of Rho-Kinase in talin-deficient HUVECs mitigated the alterations in VE-Cad organization and actin stress fiber formation (Fig 3.5C). These findings indicate that talin stabilizes endothelial AJs at least in part by suppressing actin-myosin contractility.

Reduced barrier function of talin-deficient endothelial cells.

To test whether altered cell-cell junctions of talin-deficient ECs was due to increased cell-cell junctional tension, we performed immunofluorescence co-localization of VE-cadherin and vinculin to identify tensile AJs. Previous work has described changes in junctional VE-cad organization in response to increased actin cytoskeleton tension demarcated by co-localization of vinculin and VE-cadherin at cell-cell contacts[71, 94]. Deletion of talin1 in HUVECs resulted in pronounced co-localization of VE-cadherin and increased junctional pools of vinculin (Fig 3.5D-E) as measured by line-scanning of cell junctions. Interestingly, the appearance of tensile VE-cadherin+/vinculin+ cell-cell contacts could be reversed by Rho Kinase inhibition supporting the role of increased contraction in the change in tensile junction formation (Fig 3.5F-G). To test whether the increased appearance of tensile cell-cell contacts and wider junctions of shTln1 cells coincided with altered EC barrier function, we performed Electric Cell-Substrate Impedance Sensing (ECIS Z0; Applied Biophysics) experiments to assess basal impedance of EC monolayers in response to talin depletion. shTln1 HUVECs exhibited a 39% reduction in endothelial monolayer impedance compared to shScramble-treated control cells (Fig 3.5H). Defects in monolayer resistance were similarly observed in shTln1 HDMVECs relative to control cells (Fig 3.5I). Together, these results are consistent with the observation of leaky blood vessels in Tln1 EC-KO mice and indicates that talin1 is required for EC barrier function *in vitro* and *in vivo*.

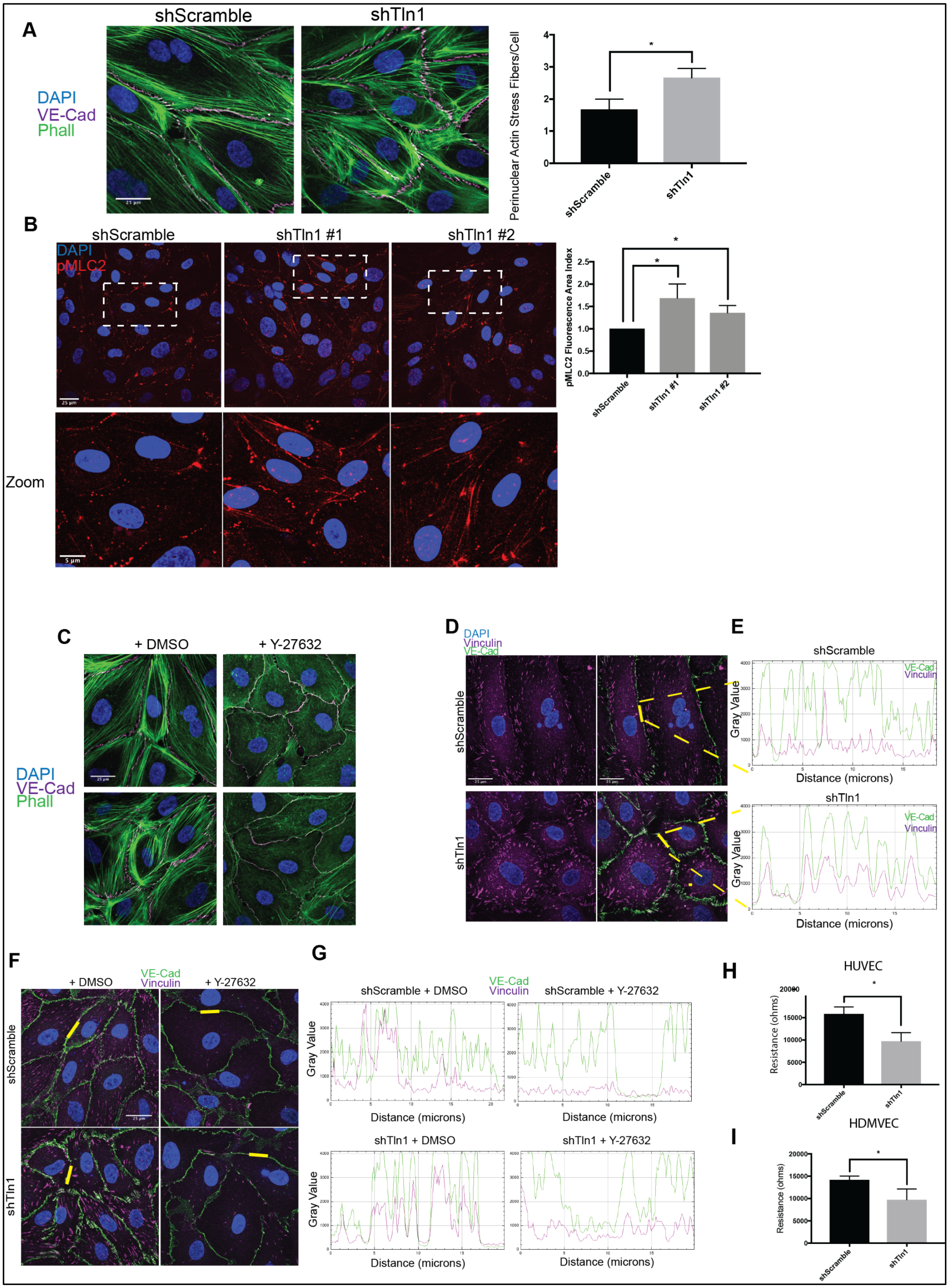
A
shScramble
shTln1
DAPI
VE-Cad
Phall
Perinuclear Actin Stress Fibers/Cell
shScramble
shTln1
B
shScramble
shTln1 #1
shTln1 #2
DAPI
pMLC2
Zoom
pMLC2 Fluorescence Area Index
shScramble
shTln1 #1
shTln1 #2
C
+ DMSO
+ Y-27632
DAPI
VE-Cad
Phall
D
DAPI
Vinculin
VE-Cad
shScramble
shTln1
E
shScramble
VE-Cad
Vinculin
Gray Value
Distance (microns)
shTln1
VE-Cad
Vinculin
Gray Value
Distance (microns)
F
+ DMSO
VE-Cad
Vinculin
+ Y-27632
shScramble
shTln1
G
shScramble + DMSO
VE-Cad
Vinculin
shScramble + Y-27632
Gray Value
Distance (microns)
Distance (microns)
shTln1 + DMSO
shTln1 + Y-27632
Gray Value
Distance (microns)
Distance (microns)
H
HUVEC
Resistance (ohms)
shScramble
shTln1
I
HDMVEC
Resistance (ohms)
shScramble
shTln1

Figure 3.5: Increased cell contraction and tensile adherens junctions in talin-deficient endothelial cell.

A. Phalloidin and VE-cadherin immunofluorescence on shScramble and shTln1 HUVECs. The number of perinuclear stress fibers per cell were quantified as described in methods. (n=3; scale=25 µm *p=0.016 two-tailed unpaired t-test) **B**. Max-intensity immunofluorescence projections of HUVECs stained with anti-pMLC2 antibody indicate increased pMLC2+ cell area in shTln1#1 and shTln1#2 cells relative to shScramble (n=2-4; scale=25 µm; *p=0.0105, *p=0.0405 one-way ANOVA with Kruskal Wallis multiple comparisons test) **C.** Inhibition of cytoskeletal contraction by treating cells with Rho-associated kinase inhibitor Y-27632 (50nM, 12 hours) reduces junctional disorganization and FAJ formation in talin-deficient HUVECs. (n=3; scale=25 µm). **D.** Co-localization of VE-Cadherin (magenta) and Vinculin (green) at cell-cell junctions is increased in shTln1 cells compared to shScramble HUVECs (scale=25 µm). **E.** Intensity profile plot of VE-Cadherin and vinculin immunofluorescence shown in D. (n=4) **F.** Inhibition of ROCK-mediated cellular contraction (Y-27623) reduces vinculin localization at cell-cell junctions of shTln1 HUVECs relative to vehicle treated cells (n=3; scale=25 µm). **G.** Intensity profile plot of VE-cadherin and vinculin immunofluorescence depicted in G (n=3). **H.** HUVEC monolayer resistance measured using electrical cell impedance sensing (ECIS) of shTln1 infected monolayers is reduced relative to shScramble (n=3; *p=0.0131; two-tailed unpaired t-test). **I.** HDMVEC monolayer resistance measured by ECIS of shTln1 infected monolayers is reduced relative to shScramble (n=3; *p=0.0399; two-tailed unpaired t-test).

β1 integrin localizes to cell junctions and β1 activation is required for junctional stability. The expression of β1-integrin in endothelial cells has been shown to promote VE-cadherin stability [138]. Interestingly, a pool of β1 integrin has previously been reported to localize to EC junctions[137]. To investigate whether *active* β1 integrin contributes to AJ stability we first examined the localization of active β1 integrin by immunofluorescence with an activation-sensitive β1 integrin antibody in HUVECs. As expected, active β1 integrin localized to focal adhesions (Fig 3.6A). In addition, we observed a pool of active β1 integrin at VE-cadherin-containing cell-cell junctions (Fig 3.6A). We confirmed these findings using higher resolution 3D structure illuminated microscopy (3D-SIM) (Fig 3.6B). In addition, a pool of talin was localized at cell-cell junctions (Fig 3.6C). Treatment of HUVECs with the ligand blocking β1 integrin antibody P5D2 induced VE-cadherin disorganization and reduced endothelial barrier function compared to cells treated with the non-function altering β1 integrin antibody K20. (Fig 3.6D-E). To test whether impaired β1 integrin activation contributed to the altered VE-cadherin junction organization we observed in talin-deficient HUVECs, we treated shTln1 and shScramble HUVECs with either β1 integrin activating antibody (9EG7) or nonimmune IgG. 9EG7 treatment largely reversed the increased AJ width of talin-deficient HUVECs (Fig 3.6F). Treatment of shTln1 and shScramble HUVECs with 9EG7 did not alter total protein expression of VE-cadherin relative to control groups treated with rat isotype IgG (Fig 3.6G). Functionally, treatment of talin-deficient HUVECs with 9EG7, but not the non-function altering β1 integrin antibody K20, rescued EC barrier function up to 6 hours after treatment (Fig 3.6H). Together, these results indicate that talin-dependent activation of β1 integrin is required for maintaining VE-cadherin organization and EC barrier function.

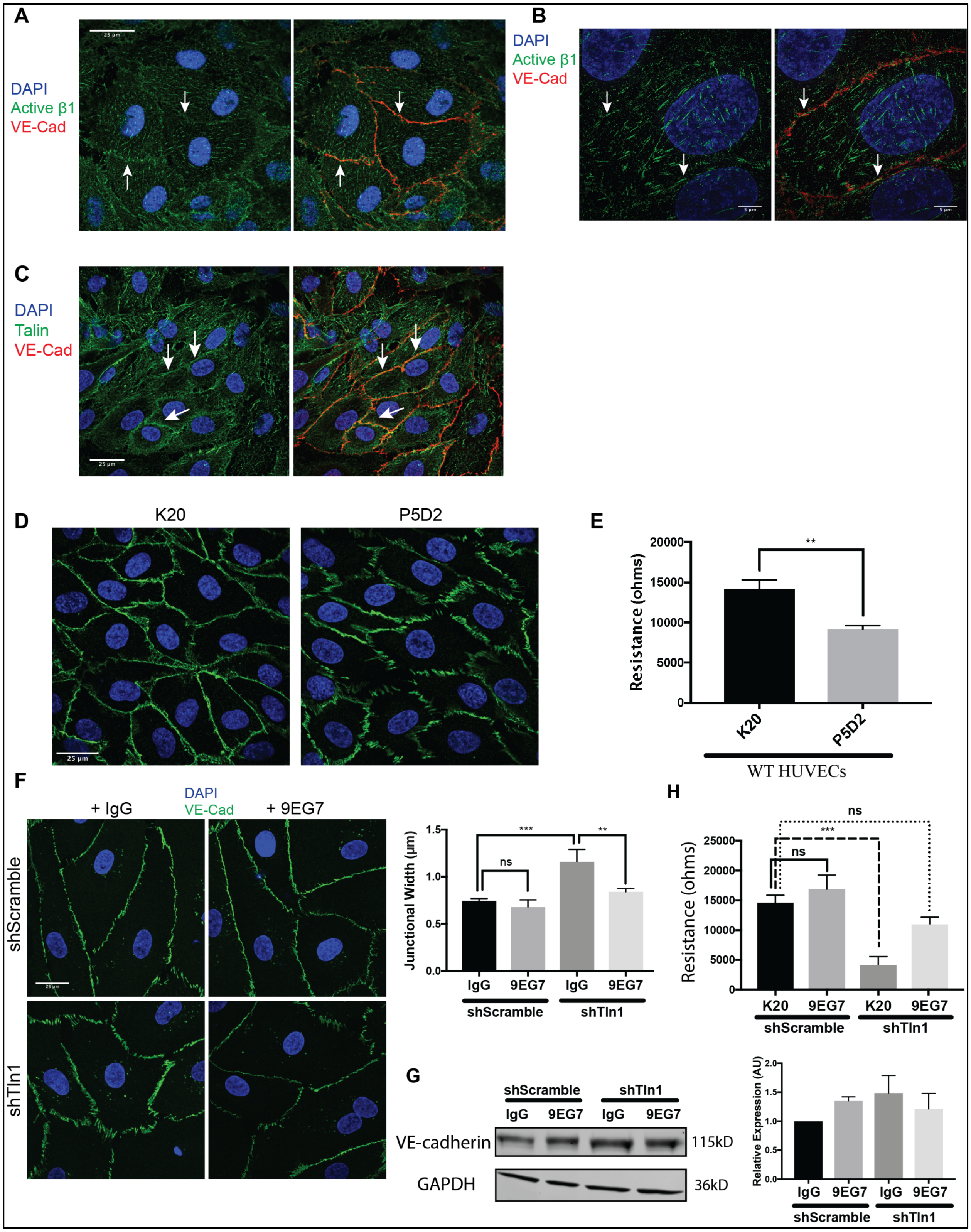

A
DAPI
Active β1
VE-Cad
B
DAPI
Active β1
VE-Cad
C
DAPI
Talin
VE-Cad
D
K20
P5D2
E
Resistance (ohms)
20000
15000
10000
5000
0
**
K20
P5D2
WT HUVECs
F
+ IgG
DAPI
VE-Cad
+ 9EG7
shScramble
shTln1
Junctional Width (µm)
***
**
ns
IgG
9EG7
IgG
9EG7
shScramble
shTln1
H
Resistance (ohms)
25000
20000
15000
10000
5000
0
ns
***
ns
K20
9EG7
K20
9EG7
shScramble
shTln1
G
shScramble
shTln1
IgG
9EG7
IgG
9EG7
VE-cadherin
115kD
GAPDH
36kD
Relative Expression (AU)
IgG
9EG7
IgG
9EG7
shScramble
shTln1

Figure 3.6: Talin-dependent β1-integrin activation is required for endothelial barrier function. **A**. Z-stack projections of immunofluorescence using an activation-sensitive β1 integrin antibody (9EG7) (green) and VE-Cadherin antibody (red) on HUVECs showing the appearance of a subpopulation of β1 integrin near AJs of confluent HUVECs. White arrows highlight cell-cell border regions enriched for β1 integrin. (n=3; scale=25 μm). **B.** Super resolution 3D structured illumination (3D-SIM) immunostaining of active β1 integrin and VE-cadherin in HUVECs highlight a subset of β1 integrin (white arrows) at VE-cadherin-positive junctions (n=3; scale=5 μm). **C.** Immunofluorescence on HUVECs with antibodies against talin (green) and VE-cadherin (red). A subset of talin localized to cell-cell contacts (white arrows) in addition to the expected pool of talin at focal adhesions (n=3; scale=25 μm). **D**. Treatment of HUVEC monolayers with a β1 integrin blocking antibody (P5D2) alters cell-cell junction organization relative to cells treated with a non-function altering β1 integrin antibody (K20). (n=3; scale=25 μm). **E**. HUVEC monolayers treated with a β1 integrin blocking antibody (P5D2) exhibit reduced barrier function as measured by electrical cell-substrate impedance sensing (4000 Hz) relative to HUVECs treated with a non-function altering β1 integrin antibody (K20). Measurements were made 3 hours after antibody incubation and remained stable for up to 6 hours post-treatment. (n=3; p=0.0019 unpaired t-test). **F**. Junctional width measured by VE-Cadherin immunofluorescence (green) is normalized by antibody-mediated β1 integrin activation (9EG7) in shTln1 HUVECs relative to talin-deficient HUVECs treated with a non-function altering antibody (K20). (n=3; scale=25 μm; *** p=0.0006, ** p=0.0036 ordinary one-way ANOVA with Sidak's multiple comparisons test). **G.** VE-cadherin protein expression measured by western blot in shScramble and shTln1 HUVECs treated with 5 μg/mL Rat Isotype IgG or β1 integrin activating antibody 9EG7 for 12 hours. (n=2; ns; One-way anova with a Tukey multiple comparisons test) **H**. Electrical resistance of shScramble and shTln1 HUVECs treated with either the activating β1 integrin antibody 9EG7 or the non-function altering β1 antibody K20. (n=3; *** p=0.0002 one-way ANOVA with a Tukey multiple comparisons test).

Talin-dependent β1 integrin activation stabilizes VE-cadherin.

To test whether changes in talin-dependent β1 integrin activation altered turnover of VE-cadherin, we performed an antibody internalization assay[45, 46] to visualize VE-cadherin internalization in talin-deficient HUVECs. Whereas total pools of VE-cadherin appeared similar, shTln1 cells exhibited a 37% increase in internalized VE-cadherin (Fig 3.7A). The increased VE-cadherin width in talin-deficient ECs was abrogated by transfecting shTln1 cells with GFP-talin but not GFP (Fig 3.7B). Reconstitution of HUVECs with GFP-tagged talin head domain (GFP-THD) which activates integrins[205] but lacks most actin binding sites appears to partially rescue junctional width while expression of GFP-THD-L325R, capable of binding to, but not activating integrins[205] failed to normalize AJ organization compared to GFP-Tln1 (Fig 3.7B). These data reveal a critical role of talin-dependent integrin activation in regulating the junctional organization of VE-cadherin: when β1 integrin is activated, either by expression of talin or by treating talin-deficient cells with β1 integrin activating antibodies, cell-cell junctions are stabilized. Importantly, changes to junctional organization in response to stimulation of β1 integrin activation or blockade of β1 integrin correspond functionally with altered monolayer barrier function.

3.4 Discussion

Here we tested the requirement for EC talin in the maintenance of established blood vessels. Deletion of EC talin in adult mice results in vascular leak and lethal intestinal hemorrhage 16-21 days after *Tln1* deletion. EC-specific talin1 knockout mice exhibit altered cell-cell junction organization and intestinal EC detachment from adjacent ECs. Mechanistically, depletion of talin with *Tln1* shRNA in HUVECs resulted in cell-cell junction remodeling, increased cytoskeletal

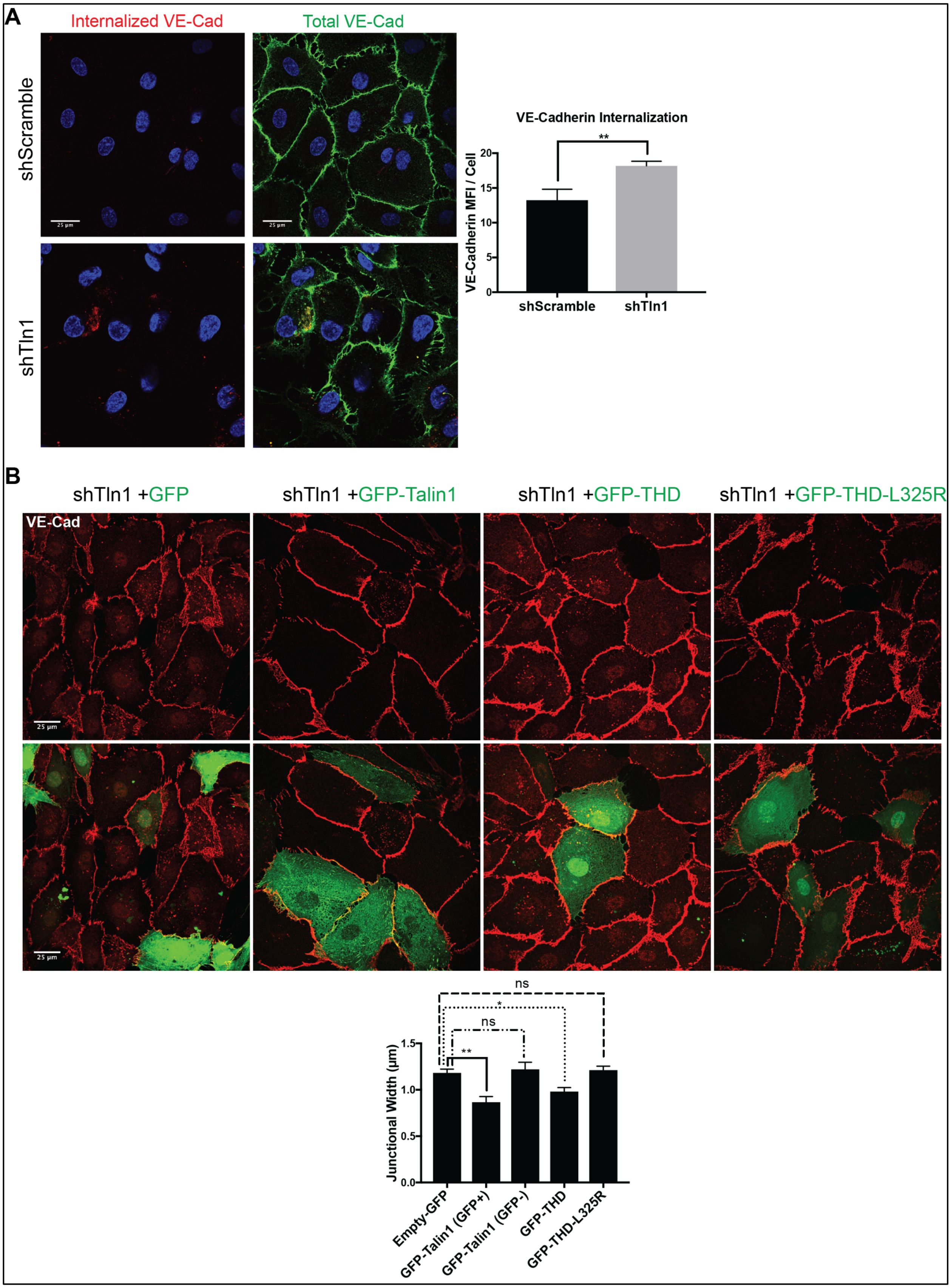

A
Internalized VE-Cad
Total VE-Cad
shScramble
shTln1
25 µm
VE-Cadherin Internalization
**
VE-Cadherin MFI / Cell
0
5
10
15
20
shScramble
shTln1
B
shTln1 +GFP
shTln1 +GFP-Talin1
shTln1 +GFP-THD
shTln1 +GFP-THD-L325R
VE-Cad
25 µm
ns
*
ns
**
Junctional Width (µm)
0.0
0.5
1.0
1.5
Empty-GFP
GFP-Talin1 (GFP+)
GFP-Talin1 (GFP-)
GFP-THD
GFP-THD-L325R

Figure 3.7: Talin-dependent integrin activation is indispensable for endothelial adherens junction organization.

A. Antibody internalization assay in which mouse VE-Cadherin (red) antibody was incubated with either shTln1 or shScramble HUVECs for 30min prior to fixation after which excess surface-bound antibody was removed by acid washing as described in Methods. After fixation/permeabilization, total levels of VE-Cadherin (green) were visualized using a rabbit VE-Cadherin antibody. (n=3; scale= 25 μm; **p=0.0077 two-tailed unpaired t-test). **B.** shTln1 HUVECs were transfected with either Empty-GFP, GFP-Talin1, GFP-THD or GFP-THD-L325R after which junctional width was assessed as described above and in Methods. GFP-Talin1 (GFP+) and GFP-Talin1 (GFP-) cells junctional widths were quantitated as an internal control for transfected groups. (n=3; scale=25 μm; *** p=0.0007, ** p=0.0099, ns=not significant, one-way ANOVA with a Tukey multiple comparisons test.

contraction and increased junctional width. Loss of talin promoted the appearance of tensile Focal Adherens Junctions (FAJs) suggesting increased junctional tension. Activation of β1-integrin rescued junctional VE-cadherin organization while β1-integrin blockade in WT HUVECs phenocopied shRNA-mediated talin depletion suggesting a critical role for talin-dependent integrin activation in maintaining cell-cell junctions. Functionally, deletion of talin in HUVECs increased VE-cadherin internalization and reduced EC barrier electrical resistance. Defects in cell-cell junction organization and EC barrier function in talin-deficient ECs were rescued by treating cells with a β1 activating antibody. Furthermore, reconstitution of talin-deficient HUVECs with either full length talin1 or an integrin-activating talin1 head-domain normalized VE-cadherin organization. Collectively, these studies reveal an important role of talin-dependent β1-integrin activation in the maintenance of vascular barrier function.

Our observation that inducible genetic deletion of talin1 in ECs of adult mice causes defects predominantly in the intestinal microvasculature is striking. Similar phenotypes were observed utilizing two widely-used tamoxifen-inducible EC-specific Cre mice limiting the chances that the phenotype could be attributed to deletion of talin in non-ECs. While EC turnover appears to be similar across various established vascular beds [21], the concept of vascular heterogeneity and organ-specific EC function is well-supported[16, 17, 206]. For example, the unique structures and functions of the blood brain barrier (BBB)[207, 208], blood retinal barrier (BRB)[209, 210] and the gut vascular barrier (GVB)[19] each play context-dependent roles in regulating paracellular permeability.[18, 20, 190] The endothelium of the BBB lacks fenestrations and contains continuous intercellular tight/adherens junctions.[207] In contrast, the endothelium of the outer BRB and of the GVB are characterized by fenestrated capillaries and increased permeability to components of the blood, immune cells and, in the case of the GVB, microbiota[19, 192]. Furthermore, compelling evidence suggests that fenestrated microvasculature and endocrine organ vasculature are preferentially dependent on VEGF-VEGFR2 signaling as pharmacological VEGF inhibition reduces fenestrations and vessel growth[211, 212]. The reasons for Tln1 EC-KO mice developing defects predominantly in the intestinal microvasculature is not clear. Integrin signaling has been shown to promote VEGFR2 function[130, 213, 214]. It is therefore plausible that VEGFR2 activity may be reduced in the endothelium of Tln1 EC-KO mice. If the fenestrated[215] capillaries of the intestine are more dependent on VEGF signaling than other vascular beds, this could contribute to the observed dysfunction of the intestinal microvasculature of Tln1 EC-KO mice.

A key regulator of vascular permeability is the AJ molecule, VE-cadherin[190, 194]. As cell-matrix and cell-cell adhesions are linked through their independent interactions with the actin cytoskeleton[60, 216], their downstream signaling pathways converge at a number of molecular hubs which act downstream of mechanosensory stimuli.[217] Small GTPases, cytoskeletal adaptors and mechanosensitive proteins such as vinculin play critical roles in establishing and maintaining both cell-cell and cell-matrix adhesions. Our observation that talin-deficient HUVECs exhibit altered vinculin localization to cell-cell borders (Fig 3.5D) is reminiscent of recent work which showed thrombin-induced cell contraction promotes weakening of the endothelial barrier and the appearance of FAJs. [71] FAJs are demarcated by VE-Cad-vinculin co-localization at cell-cell contacts. As talin1 contains several vinculin-binding sites [147, 218] and the actin cytoskeleton is disorganized in talin-deficient ECs (Fig 3.5A), loss of EC talin may promote the association of vinculin with the AJ complex by promoting vinculin-α-catenin binding and thereby altering cellular tension. Interestingly, the altered organization of tight junction component ZO-1 would suggest that changes in cellular tension likely affect the junctional stability of other adhesive structures, an observation that warrants further future investigation (Fig S3.6).

Together, our *in vitro* and *in vivo* results provide evidence for a link between inside-out integrin activation and the maintenance of the endothelial barrier in the intestinal microvasculature. Early studies established the importance of endothelial α5β1 integrin in barrier function as antibody-mediated blockade of α5β1, but not αvβ3 integrin, weakened barrier function *in vitro* [137]. Subsequent studies have revealed the importance of β1 integrin during developmental angiogenesis as it dictates endothelial cell polarity[197] and functions in the stabilization of established and maturing vessels [138]. Together, these studies highlight the requirement of EC β1 integrin expression in the growth, maintenance and stability of blood vessels. Our results here build on these concepts by demonstrating that talin-dependent integrin activation controls the organization of cell-cell junctions in the intestinal microvasculature. Our *in vitro* results, utilizing both pharmacological and genetic approaches, indicate that it is the capacity of talin to activate integrins, not mechanically linking integrins to the actin cytoskeleton, that contributes to VE-cadherin organization. Importantly, this finding suggests the exciting possibility that pharmacological manipulation of integrin activation may represent a novel therapeutic strategy for modifying the endothelial barrier in the context of a variety of human diseases.

Acknowledgements

The authors thank the following investigators for generously providing mice used in these studies: David Critchley and Susan Monkley (*Tln1*$^{fl/fl}$ mice), Ralf Adams (Cdh5-CreERT2 mice), and Marcus Fruttiger (PDGFβ-CreERT2 mice). We are also grateful for support from Children's Healthcare of Atlanta and Emory University Pediatric Flow Cytometry Core and the Emory University Integrated Cellular Imaging Core.

3.5 Supplement

Methods

Cell and Tissue Culture

Human umbilical vein endothelial cells (HUVECs) were purchased from Lonza (C-2519A) and cultured in endothelial cell growth medium (Lonza). Cells used for experiments were not cultured beyond passage 8. For mouse lung endothelial cell cultures, lungs were harvested and pooled from 2 adult mice and enzymatically dissociated with collagenase I (Worthington Chemical) for 50 minutes at 37°C. Endothelial cell enrichment and culture was performed as previously described.[219, 220] Briefly, sheep anti-rat Dynal Beads (Fisher) coated with CD31 antibody (BD Pharm- MEC 13.3) were incubated with the lung single-cell suspension. Magnetically sorted cells were plated in flasks coated with 5µg/mL human fibronectin (Sigma). Upon reaching confluency, ECs were magnetically sorted a second time using sheep anti-rat Dynal beads coated with CD102 antibody (Life Technologies). Cre-mediated deletion of *Tln1* was induced by adding 500nM 4-hyrdoxy-tamoxifen (Cayman) to the culture media.

Immunostaining, Western blot and Antibodies

For detection of talin1/2 protein levels by Western blotting, cells were lysed in RIPA buffer (150mM NaCl, 50mM Tris pH 7.4, 0.1% SDS, 1% Triton X-100, 1% Sodium deoxycholate, 1mM PMSF, 1mM NaVO4, 1mM NaF, 1mM EDTA, complete protease inhibitor (Roche) and samples were clarified by centrifugation at 13,000g for 10 min at 4°C. Protein samples were boiled for 5 minutes in Laemmli buffer containing 10mM DTT and separated on 6% Tris-glyine gels (Invitrogen). Immunoblotting was done using a goat anti-mouse Talin1/2 (Santa Cruz, sc-7534, 1:1000) antibody. Primary antibody was detected using donkey anti-goat IR800 (Thermo, 1:10000) with an Odyssey CLx imager (LI-COR). For retinal preparations, retinas were fixed and whole-mounted as described below and immunofluorescence was performed using activation-sensitive integrin β1 9EG7 antibody (BD Biosciences, 550531, 1:100), hamster anti-β1 integrin HMβ1-1 (Biolegend,102206, 1:100), rat anti-mouse VE-cadherin (BD Biosciences, 550548, 1:50), and Rabbit anti-mouse ZO-1 (ThermoFisher, 61-7300, 1:200). Immunofluorescence on cryosections of 4% PFA-fixed, 10μm frozen sections was performed using rabbit anti-collagen IV (Thermo, NC0530614, 1:500), rabbit anti-mouse Laminin (Sigma, L9393, 1:400). Fixed-cell immunofluorescence was performed as described below with antibodies rabbit anti-mouse VE-cadherin (Enzo- ALX-210-232-C100, 1:300), mouse anti-VE-cadherin (Enzo, ALX-803-305-C100, 1:200), goat anti-mouse talin1/2 (Santa Cruz, sc-7534, 1:300), mouse anti-p120 catenin (BD Labs, 610133, 1:200), Vinculin (Sigma- V9131, 1:500), β1 Integrin TS2/16 (Biolegend, 303002, 1:100), phalloidin- Alexa568 (Life Technologies, A12380, 1:500), Secondary antibodies used were goat anti-mouse Alexa488 and Alexa568 (Life Tech, 1:400), goat anti-rabbit Alexa-488/568/647 (Life Tech, 1:400), donkey anti-goat Alexa-488/647 (Life Tech, 1:400). For antibody internalization assays rabbit anti-mouse VE-cadherin (Enzo, ALX-210-232-C100, 1:300) and mouse anti-VE-cadherin (Enzo, ALX-803-305-C100, 1:200) were utilized.

Flow Cytometry

For flow cytometry assessment of surface β1 integrin expression, whole lungs were enzymatically dissociated in collagenase I (Worthington) as described below, antibody staining was performed for 15 minutes on ice with mouse anti-CD31-PE (Biolegend, 102408, 1:100) and mouse anti-CD45-APC (Biolegend, 103112, 1:100). For flow cytometry assessment of surface integrin subunit expression in cultured ECs, staining was performed as mentioned above using anti-α1-PE (Biolegend, 328303, 1:50), anti-α2-PE (Biolegend, 359307, 1:50), anti-α3-PE (Biolegend, 343803, 1:50), anti-α4-PE (Biolegend, 304303, 1:50), anti-α5-PE (Biolegend, 328009, 1:50), anti-α6-PE (Biolegend, 313611, 1:50), anti-αv-PE (Biolegend, 327909, 1:50), anti-β1-PE (Biolegend, 303003, 1:50), or anti-β3-PE (Biolegend, 336405, 1:50). Mouse IgG1-PE (Biolegend, 400111, 1:50), mouse IgG2a-PE (Biolegend, 400211, 1:50) or mouse-IgG2b-PE (Biolegend, 401207, 1:50) were used as isotype controls.

shRNA Transduction and Plasmid Transfection

Lentivirus was generated using the pLKO.1 backbone expressing either human Talin1 or scramble shRNAs sequences (Talin1 #1: 5'- GCCTCAGATAATCTGGTGAAA, Talin1 #2: 5'-TCCGAATGACCAAGGGTATTA, scramble: 5'- CGAGGGCGACTTAACCTTAGG). HUVECs were infected with virus overnight, puromycin selected 24 hours after infection and 48 hours after infection trypsinized and replated onto glass coverslips coated with human fibronectin or gelatin or seeded into ECIS electrode arrays as described below.

HUVECs were transfected with DNA plasmids encoding GFP fused to the N-terminus of either full-length mouse talin or talin head head domain (amino acids 1-435) using an Amaxa Nucleofector IIb (Lonza) and nucleofector kit for HUVECs (Lonza) per manufacturer's instruction. Transfection was done 48 hours after lentiviral transduction of shScramble or shTln1 shRNA and cells were fixed and analyzed by confocal microscopy 24 hours after transfection.

Cell and Tissue Immunofluorescence

For *in vitro* immunofluorescence, HUVECs were transduced with either shScramble or shTln1 shRNA and replated as described above on fibronectin (5µg/mL, Sigma) or gelatin (0.1%, Sigma) coated coverslips. Cells were fixed for 10 minutes with 4% paraformaldehyde and washed with PBS+ (Ca^{2+}/Mg^{2+}). Cells were then permeabilized with 0.1% Triton X-100/PBS+ for 10 minutes and washed with PBS+. Primary and secondary antibody incubations were performed in 0.1% BSA/PBS+ for 30 minutes at 37°C. Cells were mounted using Vectashield with DAPI (Vector Labs) and sealed with nail polish. Where noted, antibodies used for β1 integrin activation (9EG7, Biolegend), function-blocking (P5D2, Abcam) and non-functional (K-20, Santa Cruz) were added during cell seeding and incubated for 24 hours or after seeding for blocking experiments.

Retinal mounts and immunofluorescence were performed as previously described[202]. Briefly, retinas were dissected out of mice at specified times after tamoxifen treatment, fixed in 4% PFA and whole-mounted following antibody staining. Tissue was mounted using Fluoromount (Life Technologies) and imaging was performed on an Olympus FV1000 inverted confocal microscope. For intestinal whole-mount imaging, mice were euthanized at the specified time after tamoxifen injection and a small piece of the small intestine was splayed onto a silicon plate with micro dissecting pins and fixed in 4% PFA at 4°C for 2 hours before being mounted on glass coverslips in Fluoromount. Total and Active β1 integrin levels in P7 Tln1 CTRL and Tln1 EC-KO retinal vessels were visualized using hamster anti-β1 integrin HMβ1-1 (Biolegend, 102206, 1:100) or β1 9EG7 antibody (BD Biosciences, 550531, 1:100) respectively from 3 mice per group. 5-6 images per retina were acquired with endothelium specifically visualized with either CD31 (BD Biosciences, 550274, 1:100) or FITC-lectin (Vector Labs, FL1101-5, 1:25). Mean fluorescence of either total or active β1 integrin levels were measured only in CD31+ or

FITC-lectin+ areas of the acquired images to exclude any non-endothelial integrin signal using FIJI software's threshold masking (Li Threshold) and selection.

For analysis of frozen tissue sections, mice were perfused through the heart with 4% PFA, further fixed overnight in 4% PFA at 4°C and incubated in 30% sucrose/PBS at 4°C overnight. Organs were washed with PBS, embedded in O.C.T Compound (TissueTek),snap frozen in liquid nitrogen and 10μm cryosections were cut at 50μm intervals. Tissue was permeablized and blocked with PBS containing 0.3% Triton-X and 1% BSA. Primary antibody incubation was performed overnight at 4 degrees in perm/block buffer. Secondary antibody incubation was performed in PBS with 0.1% BSA at 37 degrees for 2 hours. Sections were mounted using Vectashield with DAPI (Vector Labs). Data collected from frozen sections and animal tissue was done so by annotating microscope slides with the animal ID number and without the genotype of each animal. Only after all pertinent data was collected and organized was the user unblinded to the genotypes of the mice in order to analyze the groups being compared in each experiment. For quantitative fluorescence analysis through FIJI, datasets were thresholded using FIJI software's triangle or default algorithm where appropriate to ensure unbiased quantitation of datasets. As a negative control for immunostaining experiments, a secondary antibody only condition was included in at least one biological replicate of each assay presented. Negative control data was collected alongside experimental groups to ensure specificity of the antibody signals detected.

Junctional Width Quantitation, Line Intensity Profiles, Internalization Quantitation and Cell Contraction Analysis

HUVEC junctions were visualized by immunostaining for VE-cadherin (Enzo). Junctional width was measured using FIJI software using the line tool to select 3 unique parts of a cell-cell edge. The average of the 3 measurements is reported as the junctional width of a single cell-cell border. Cell junctions between 40-50 cells from 5-6 fields of view were measured and the data shown is from 3 independent experiments.

Line intensity profiling was done using FIJI to plot pixel intensity (Grey Values) of 20µm regions of cell-cell contacts. Profiles of VE-cadherin and vinculin staining were separately collected and overlayed to generate co-localization line-intensity profiles.

Antibody internalization assays were performed as previously described[45, 46] and analyzed using FIJI software. Mean fluorescence intensity (MFI) was measured by calculating the area of fluorescence signal of the internalized antibody per field of view from 4-6 fields of view for the two conditions analyzed. MFI was divided across the number of cells counted per field view as determined by DAPI staining and MFI/cell was compared across the groups.
Cell contraction was measured in talin-deficient and control HUVECs by staining for pMLC2 (Cell Signaling, 3674s, 1:100). Staining was performed as described above. 4-6 images (~20 cells per image) were collected per group and unbiasedly analyzed using FIJI software's threshold algorithm, triangle. pMLC2+ area was reported as a representation of pMLC2 activity and statistically analyzed as indicated in the figure legend. Actin stress fiber formation in talin-deficient and control HUVECs/HDMVECs was analyzed by immunofluorescence staining using FITC-Phalloidin (Sigma, P5282, 1:300). Staining was performed in conditions as described above and quantitated by counting the number of actin stress fiber positive cells (>3 perinuclear stress fibers/cell) from 4-6 fields of view (~15-20 cells/field) per condition tested. Where indicated, the number of perinuclear actin stress fibers/cell was also analyzed in HUVECs treated

with either shTln1#1, shTln1#2 or shScramble shRNA by assessing the number of perinuclear fibers in each cell from 4-6 fields of view. Statistical analysis was performed as indicated in each figure legend.

Electrical Cell-Substrate Impedance Sensing

Barrier function of endothelial monolayers was assessed using an ECIS-Z-Theta (Applied Biophysics) instrument. Electrode arrays (8W1E; iBidi) were pre-treated with 10mM L-cysteine for 10 minutes at room temperature and coated with 0.1% gelatin and 5µg/ml human fibronectin for 1 hour at 37°C. 1.0 x 10^5 cells were seeded into each well 24 hours prior to starting time-point for multiple-frequency measurements. Cells were cultured at 37°C in 5% CO_2 for 24 hours and experimental groups were averaged from 2-3 wells of a standard 8-well set-up. Monolayer resistance values reported were measured at 24 hours after seeding and normalized to basal resistance in a cell-free well. All resistance values were recorded at a frequency of 4000 Hz. For β1-integrin activating/blocking antibody analyses at the 24 hour point, ECIS measurements were paused, media was changed to 400µL of fresh EGM-2 media containing antibody and wells brought to 37°C by equilibrating in the incubator for 15 minutes prior to restarting data collection. Data points reported are 3 hours after antibody addition. For antibody functional assays, cells were treated with β1 integrin K20 (Santa Cruz, sc-18887, 5µg/mL), β1 integrin 9EG7 (BD Biosciences, 550531, 5µg/mL), and β1 integrin P5D2 (R and D Systems, MAB17781, 5µg/mL).

***In vivo* Permeability**

To measure vascular leak, we performed an Evans blue dye (EBD) assay with slight modifications[221]. (Sigma, St Louis, MO, USA, 1%) was injected into the retroorbital plexus of mice. Blood was taken 5 and 120 minuntes post-injection. Two hours following EBD injection, mice were euthanized and organs (kidney, liver, brain and intestine) were excised. Organs were then weighed and incubated in formamide for 48 hours at 56°C to extract EBD from the tissue. The extravasation of dye was measured spectrophotometrically at 620nm and 740nm. Values were corrected for hemoglobin with the following formula: OD620-(1.426×OD740+0.03). Concentrations were calculated by using a standard curve of known concentrations of EBD and normalized by tissue weight.

Vascular leak in the intestinal villi was also assessed by retro-orbital injections of 200 µL of FITC-lectin (2.5 µg/mL, Vector Labs, FL1101-5) into adult 8-12 week old Tln1 CTRL and EC-KO mice 15 days following tamoxifen injections. lectin was allowed to circulate for 30 minutes and mouse tissue was perfusion fixed with 4% PFA. Following several PBS washes, a piece of the small intestine proximal to the stomach was splayed and mounted onto a silicon plate to reduce tissue elasticity overnight. A piece of the flattened tissue was mounted onto a slide where 4-6 whole villi per mouse were imaged. Max-intensity z-stack projections were quantitated using FIJI. Intravascular levels of FITC-lectin mean fluorescence were measured by first creating a mask on all tdTomato positive areas. Extravascular areas were assessed by excluding the tdTomato+ areas followed by quantitation of FITC-lectin fluorescence.

<u>Quantitative real-time PCR</u>

Total RNA was isolated from CD31+,TdTomato+ and CD31+, TdTomato- cells with a miRNeasy Mini Kit (Qiagen) according to the manufacturer's protocol and reverse transcribed to cDNA using oligodT primers and SuperScript IV reverse transcriptase (Life Technologies) according to the manufacturer's protocol. RNA concentrations were quantified at 260/280 using the Nanodrop 2000 (Thermofisher) and 50 ng of RNA was used for first strand cDNA synthesis. A non-reverse transcribed sample control was used in which the reaction lacked reverse transcriptase. Quantitative PCR was performed using Fast SYBR Green Master Mix (Applied Biosystems) with primers specific for *Tln1* (5'-GGCTGGGAAAGCTTTGGAC, 5'-CATCTCATTGAGCCGCTGG) and β-actin (*Actb*) (5'-GGGAAATCGTGCGTGACATCAAAG, 5'-CATACCCAAGAAGGAAGGCTGGAA) using a CFX96 Touch real-time PCR detection system (Bio-Rad Laboratories). qPCR reactions were carried out in 20μL volumes containing relevant primers at 250nM and 10ng of cDNA template in duplicates. Data was analyzed and presented using the $2^{-\Delta Ct}$ method[222] for relative gene expression analysis.

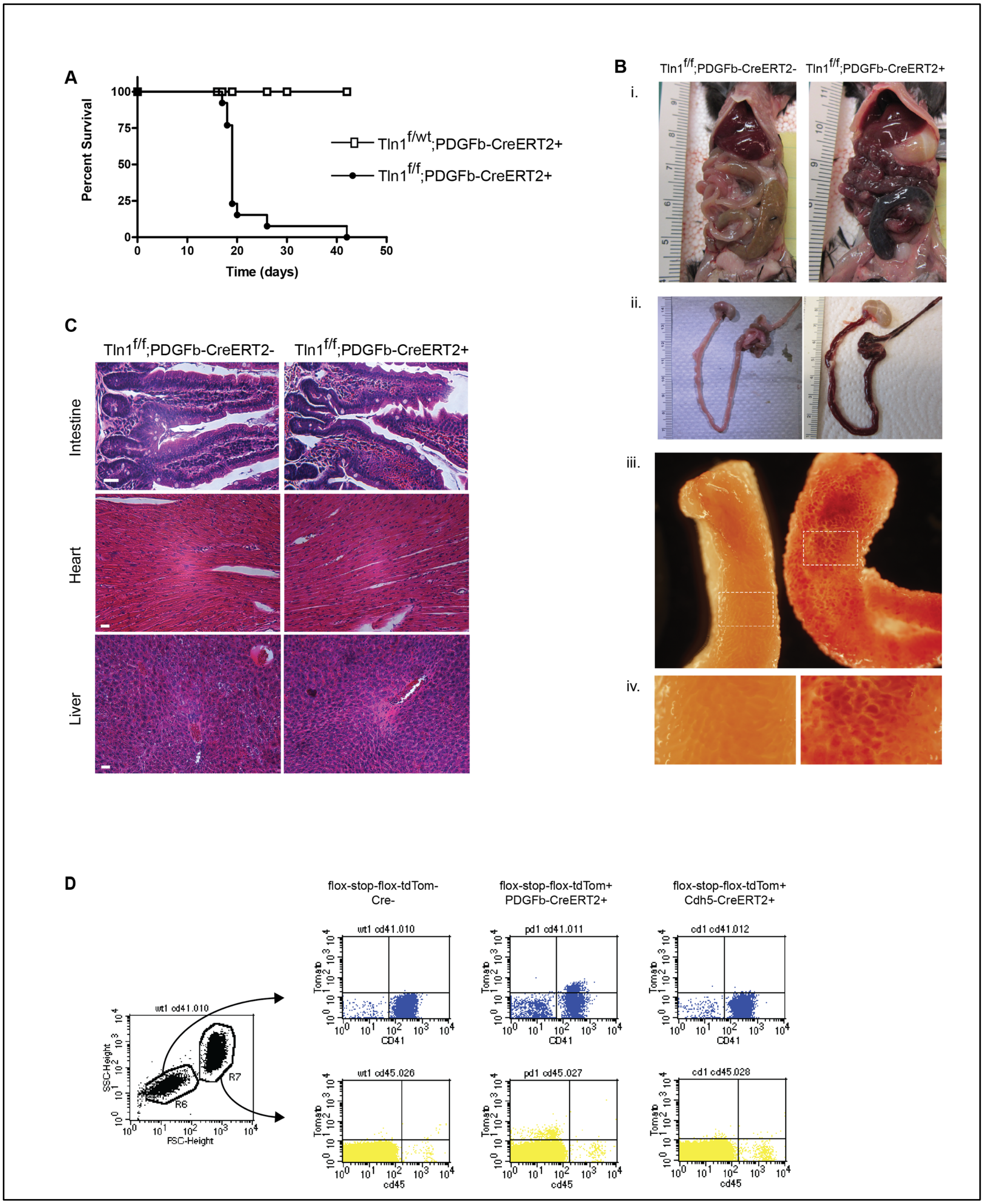
A
Percent Survival
Time (days)
Tln1f/wt;PDGFb-CreERT2+
Tln1f/f;PDGFb-CreERT2+
B
Tln1f/f;PDGFb-CreERT2-
Tln1f/f;PDGFb-CreERT2+
i.
ii.
iii.
iv.
C
Tln1f/f;PDGFb-CreERT2-
Tln1f/f;PDGFb-CreERT2+
Intestine
Heart
Liver
D
flox-stop-flox-tdTom-
Cre-
flox-stop-flox-tdTom+
PDGFb-CreERT2+
flox-stop-flox-tdTom+
Cdh5-CreERT2+
wt1 cd41.010
pd1 cd41.011
cd1 cd41.012
wt1 cd45.026
pd1 cd45.027
cd1 cd45.028
SSC-Height
FSC-Height
R6
R7
Tomato
CD41
cd45

Figure S3.1. Inducible endothelial cell-specific deletion of talin in *Tln1*$^{f/f}$;PDGFβ-iCreERT2+ mice causes defects in the integrity of intestinal capillaries.

A. Adult, 8-12 week old, *Tln1*$^{f/f}$;PDGFβ-iCreERT2$^{+/-}$, *Tln1*$^{f/wt}$;PDGβ-iCreERT2$^{+/-}$ and *Tln1*$^{f/f}$;PDGFβ-iCreERT2$^{-/-}$ mice were treated with tamoxifen once a day for three consecutive days and survival was monitored. *Tln1*$^{f/f}$;PDGFβ-iCreERT2$^{-/-}$ mice all survived for more than 42 days and for clarity are not depicted. **B.** Intestinal vascular hemorrhage was observed 16 days after tamoxifen treatment in *Tln1*$^{f/f}$;PDGFβ-iCreERT2+ mice (i-ii). Bleeding was observed in the intestinal wall of small intestines that were cut longitudinally and everted (iii) with bleeds prominent in the villi (iv). **C.** Hematoxylin/eosin staining of organs isolated from *Tln1*$^{f/f}$;PDGFβ-iCreERT2$^{+/-}$ and *Tln1*$^{f/f}$;PDGFβ-iCreERT2$^{-/-}$ mice 16 days after tamoxifen treatment. Scale bar= 25μm. **D.** Flow cytometry of peripheral blood of mice with the indicated genotypes 7 days after tamoxifen treatment. Platelets were analyzed by gating on region R6 and staining with a FITC-CD41 antibody. Leukocytes were analyzed by gating on region R7 and staining with a FITC-CD45 antibody.

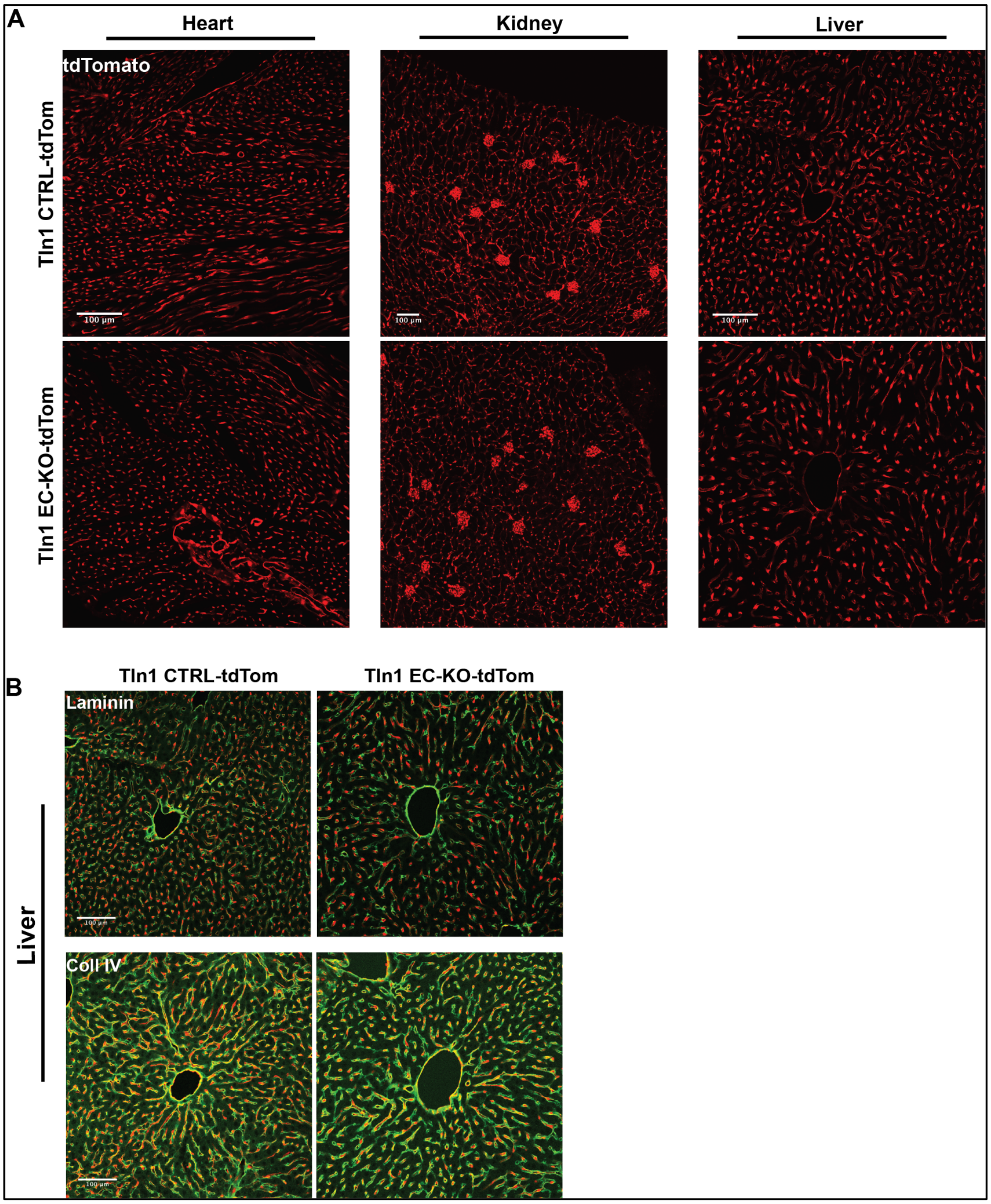

Figure S3.2. Cdh5-creERT2 is efficiently activated by tamoxifen in the endothelium of several organs.

Talin1 EC-KO-tdTom and Tln1 CTRL-tdTom were treated with tamoxifen and after 16days organs were fixed and frozen sections were prepared and analyzed by confocal microscopy. **A**. TdTomato expression in sections of heart, kidney, and liver. (n=3; scale=100 μm) **B**. TdTomato and either collagen IV or laminin immunofluorescence were examined in liver sections. (n=2; scale = 100 μm).

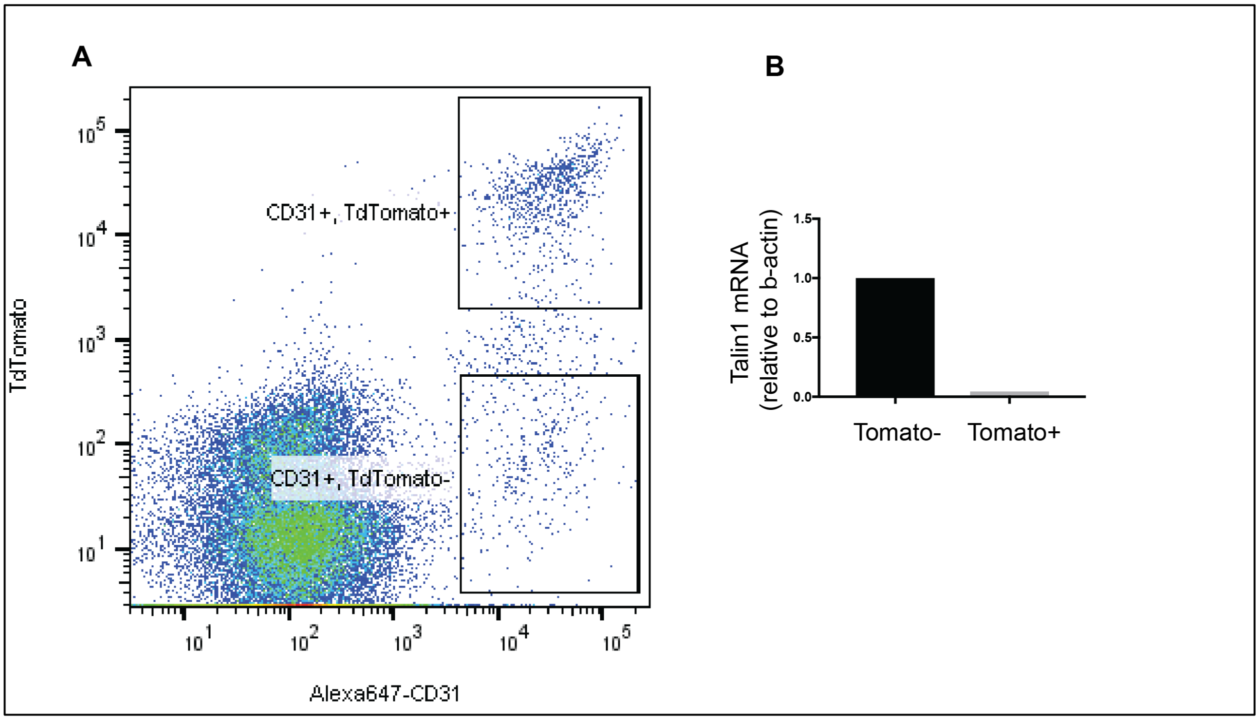

Figure S3.3. Talin1 is deleted in intestinal ECs.

A. Tln1 EC-KO-tdTom mice were injected with a low dose of tamoxifen (250µg, once) and 10 days later small intestine from 3 mice were pooled, enzymatically dissociated and live, CD45- cells were FACS-sorted to isolate CD31+ cells that were either TdTomato positive or TdTomato negative. **B.** Reverse transcription of RNA isolated from the sorted populations was analyzed by real time PCR with primers specific for talin1 and β-actin transcripts and talin1 expression was normalized to β-actin.

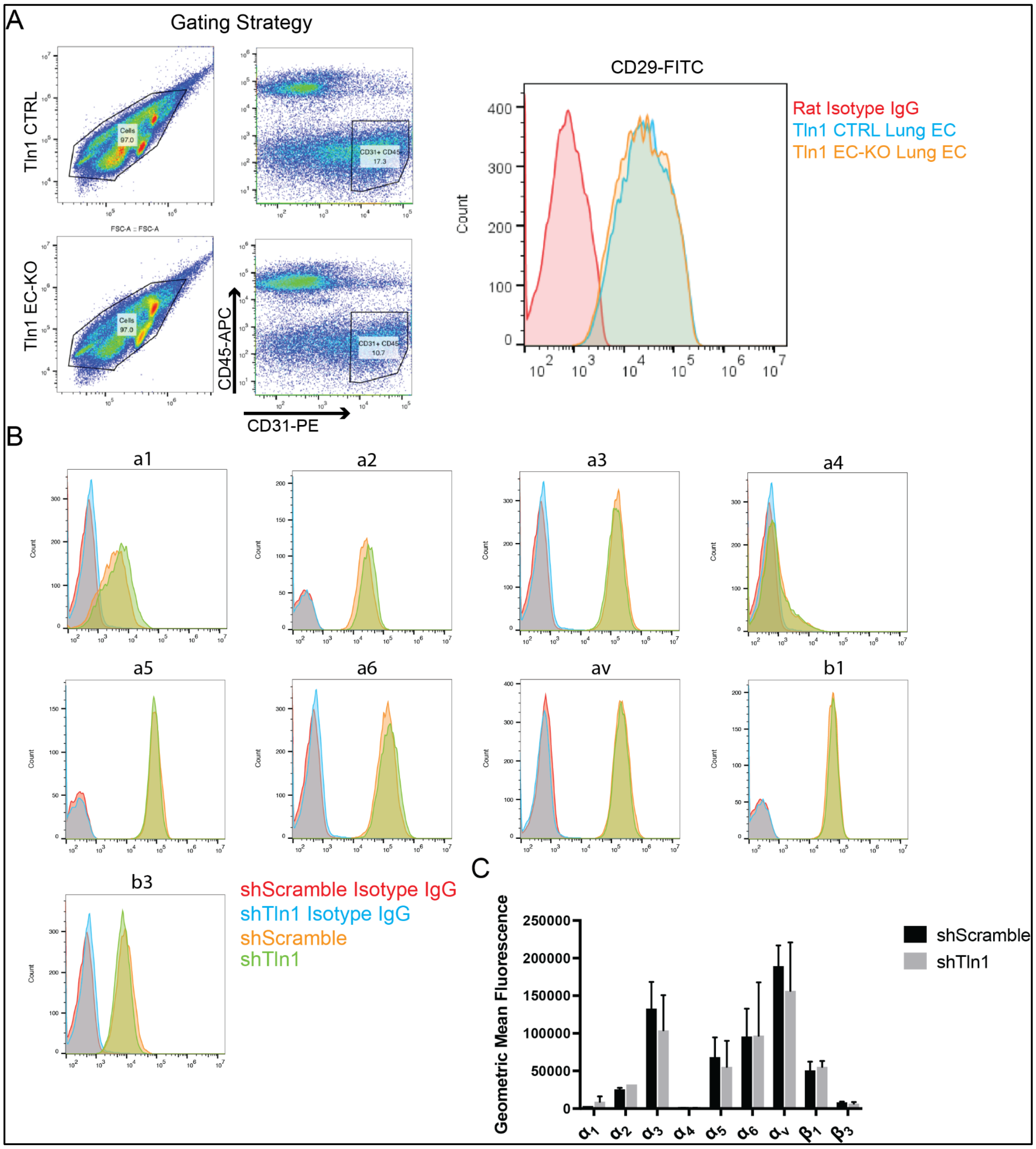

Figure S3.4. Deletion of talin1 does not alter endothelial cell integrin surface expression. A. Flow cytometry analysis of surface β1 integrin expression of lung endothelial cells of Tln1 EC-KO and Tln1 CTRL mice. Single cell suspensions were prepared from enzymatically-dissociated lungs. β1 integrin expression was quantified on EC populations defined as CD31+,CD45-. (n=2). B. Flow cytometry analysis of surface integrin subunit expression (α1, α2, α3, α4, α5, α6, αv, β1, β3) is comparable in shScramble and shTln1 HUVECs (n=2).

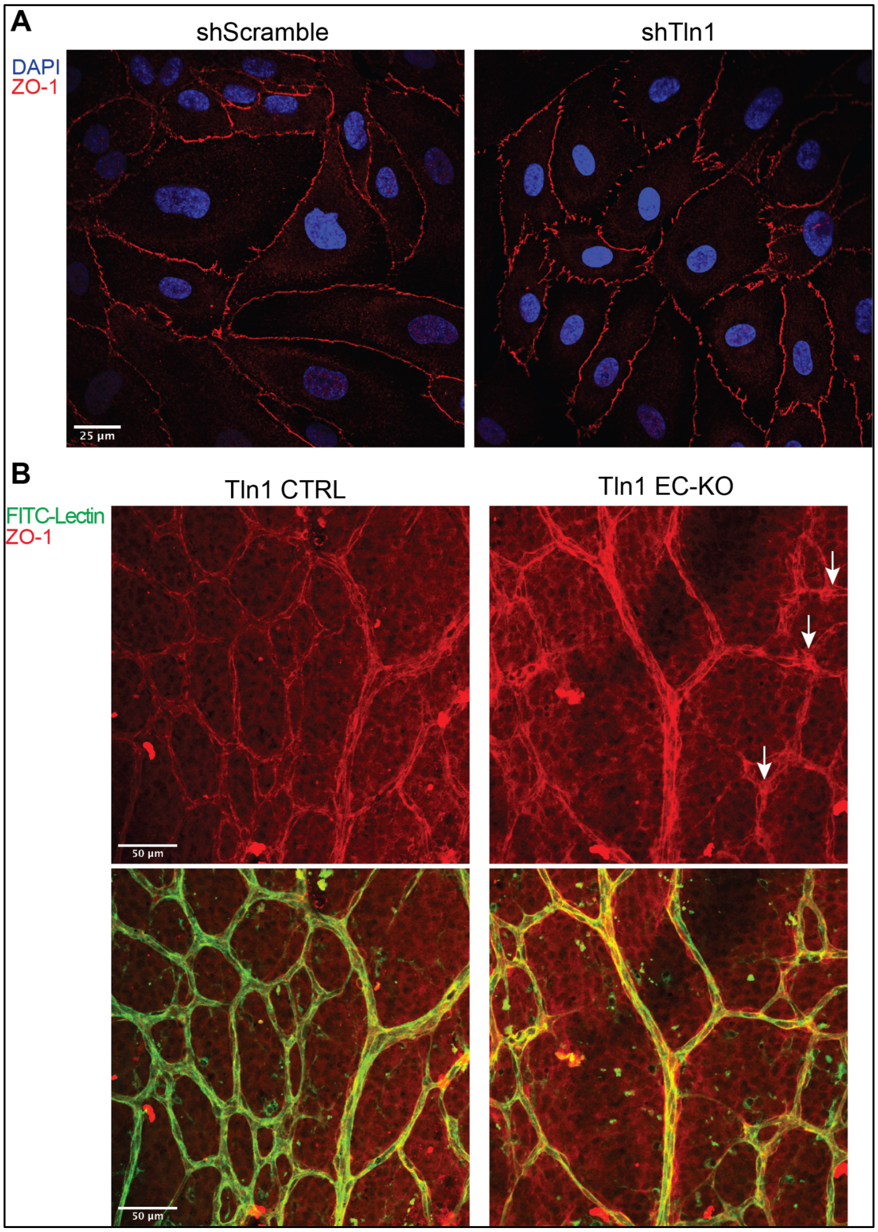

Figure S3.5. Loss of talin1 in cultured ECs and retinal vasculature alters ZO-1 junctional organization

A. Immunofluorescence staining of ZO-1 in shTln1 HUVECs shows junctional widening and discontinuity of tight junctions relative to shScramble cells (n=2; scale=25 µm). **B.** P7 retinal mounts from Tln1 CTRL and Tln1 EC-KO mice stained with FITC-lectin and ZO-1. White arrows identify junctional disorganization in retinal capillaries consistent with changes observed in VE-cadherin stained retinal capillaries (n=3; scale=25 µm).

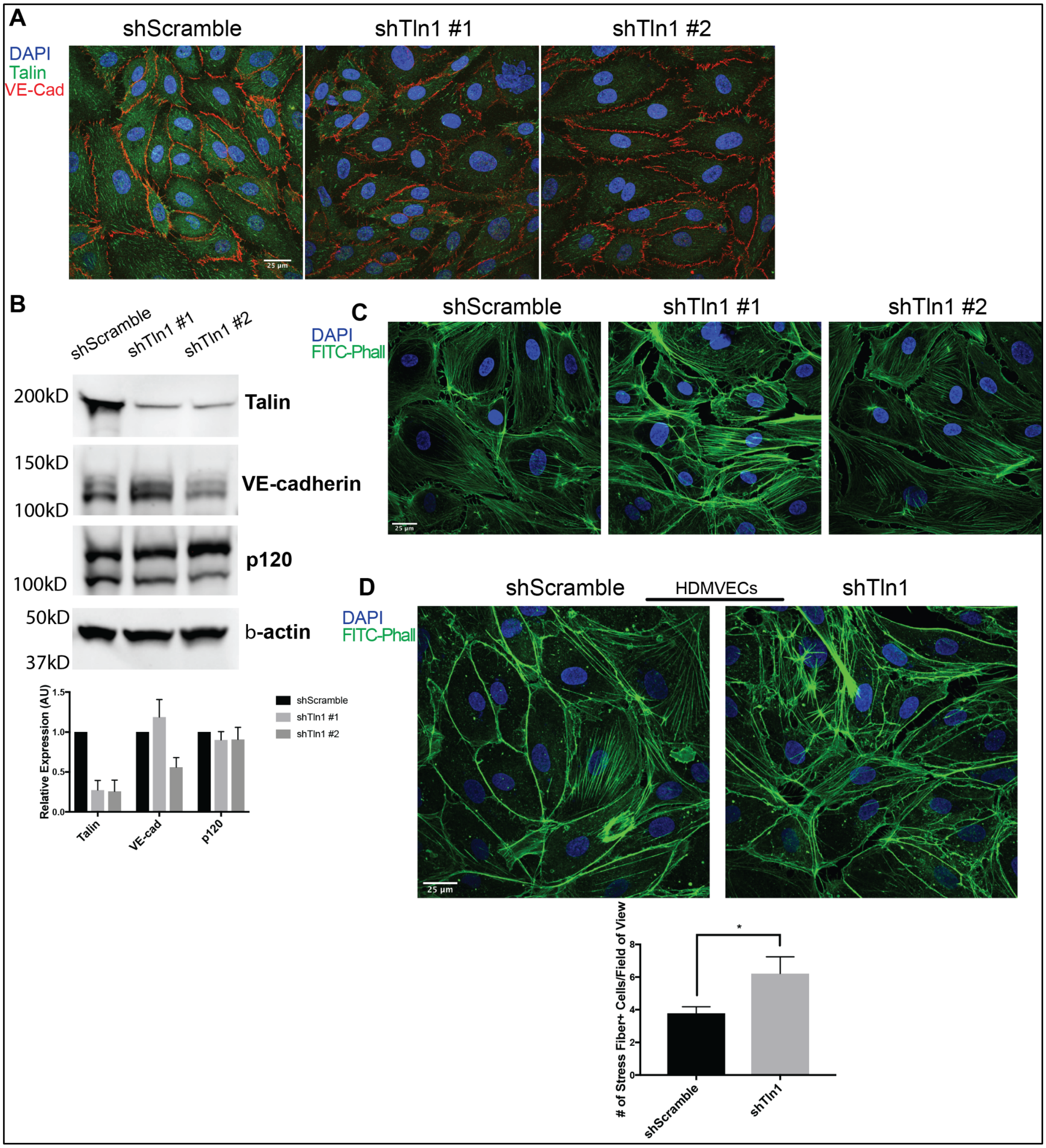
A
shScramble
shTln1 #1
shTln1 #2
DAPI
Talin
VE-Cad
25 µm
B
shScramble
shTln1 #1
shTln1 #2
200kD
Talin
150kD
VE-cadherin
100kD
p120
100kD
50kD
b-actin
37kD
Relative Expression (AU)
1.5
1.0
0.5
0.0
Talin
VE-cad
p120
shScramble
shTln1 #1
shTln1 #2
C
shScramble
shTln1 #1
shTln1 #2
DAPI
FITC-Phall
D
shScramble
HDMVECs
shTln1
DAPI
FITC-Phall
25 µm
# of Stress Fiber+ Cells/Field of View
8
6
4
2
0
*
shScramble
shTln1

Figure S3.6. Tln1 deletion in venous and dermal microvascular ECs alters cell-cell junction organization and promotes cytoskeletal contraction

A. Immunofluorescence analysis of talin1-depleted HUVECs with multiple shRNAs against *Tln1* showing junctional disorganization relative to control cells (n=3; scale=25 μm). **B.** Efficient deletion of talin1 in HUVECs does not appear to consistently reduce total VE-cadherin and p120 protein expression as measured by western blot (n=3). **C.** Deletion of talin1 using two different *Tln1* shRNAs promotes cellular contraction as highlighted by qualitative changes in actin stress fiber formation (n=3; scale=25 μm). **D.** HDMVECs treated with shTln1 lentivirus increases the number of stress fiber positive cells per field of view relative to shScramble control cells (n=3; scale=25 μm; *p=.0186 two-tailed unpaired t-test).

Chapter 4: Discussion and Future Directions

Understanding the mechanisms by which endothelial cells regulate their adhesive properties during pathological blood vessel growth and barrier function in disease states has long been of interest to researchers seeking to identify therapies that target EC adhesion in these contexts. An example of this research focus has been the targeting of integrins in a number of cancers[81, 223] wherein early pre-clinical success have not yielded the hypothesized efficacy indicating a better need to understand the molecular mechanisms at play[224-226]. Independent research efforts have also focused on understanding adherens junction dysregulation in diseases characterized by increased vascular permeability, yet only recently have reports focused on how crosstalk between focal adhesions and adherens junctions might coordinate endothelial dysfunction[73, 113, 139]. To better understand the global contributions of integrin signaling in diseased endothelium in the context of cancer or chronic inflammatory states, I have concentrated my research focus on understanding how talin, a key regulator of integrins, contributes to barrier function and postnatal angiogenesis. In doing so, research presented in the 2nd chapter has identified the indispensable role of EC talin1 in postnatal angiogenesis through its contributions to postnatal vascular development, EC proliferation and lumen formation during tumor angiogenesis. The 3rd chapter of my thesis research asked the question of whether talin1 is required in the ECs of established vessels and specifically whether it plays a role in the maintenance of the vascular barrier (Fig 4.1). Collectively, my doctoral research has provided intriguing insights into the role of talin in EC function and offers novel information into the basic signaling mechanisms whereby cell-cell and cell-matrix contributes to vascular maintenance and pathological states.

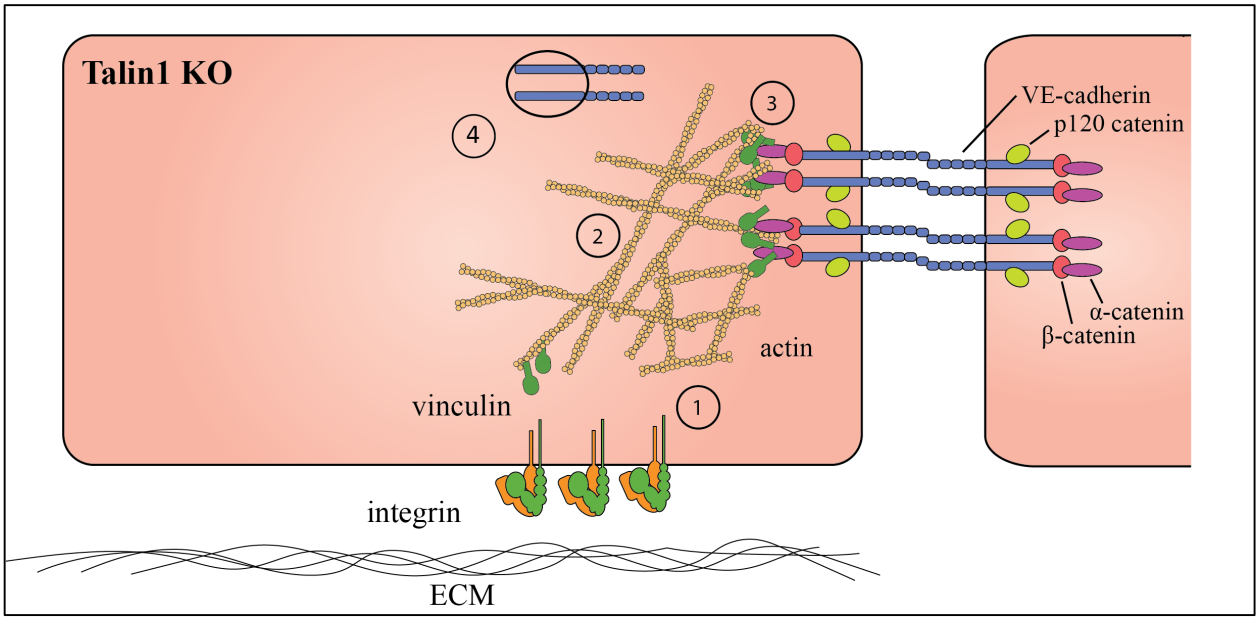

Figure 4.1. Summary model depicting the role of EC talin1 in the maintenance cell-cell junction stability and barrier function
1. Deletion of talin1 results in impaired β1 integrin activation. **2.** Loss of talin promotes cytoskeletal contraction in a myosin light chain-rho kinase-dependent manner. **3.** Increased tension promotes the formation of tensile focal adherens junctions characterized by widening of cell-cell junctions and vinculin/VE-cad co-localization. **4.** Increased cell contraction promotes barrier weakening and VE-cadherin internalization.

4.1 The Role of EC Talin1 in Postnatal Angiogenesis

Our lab and others reported the indispensable role of endothelial talin1 during embryonic angiogenesis. Inducible deletion of talin1 in ECs during mouse development resulted in embryonic lethality due to defects in endothelial cell spreading in angiogenic vessels while established vessels appeared intact[176]. Furthermore, the role of talin1 in endothelial cells was investigated *in vitro* wherein ablation of talin1 or reconstitution of integrin-activation deficient mutant L325R in talin-depleted cells was found to inhibit adhesion and spreading[174]. It remained unclear whether the function of EC talin1 during postnatal angiogenesis, both in physiological and pathological contexts, was similar to the observed requirement of EC talin1 in embryonic angiogenesis. As the talin rod links integrins to the actin cytoskeleton and interacts with a host of other cytoskeletal adaptors, the Monkley et al study whereby talin1 is deleted in ECs is limited in specifically determining whether defects in integrin activation are responsible for the observed phenotype. Therefore, the approach in the 2nd chapter utilizes two inducible, EC-specific mouse models to delete talin1 (Tln1 EC-KO) or to exclusively express a mutant talin1 L325R (Tln1 L325R) to address this question. Intriguingly, deletion of talin1 and induction of talin1 L325R expression during early postnatal development resulted in defects in retinal angiogenesis (Fig 2.2. and Fig 2.3). However, Tln1 EC-KO pups exhibited vascular hemorrhaging in several vascular beds, reduced EC proliferation and early lethality by P8 (Fig 2.1) which was not observed in Tln1 L325R pups despite comparable defects in retinal vascularization. Tln1 L325R pups survive to adulthood but are dramatically undersized relative to littermate controls (Fig 2.3) and have defects in in tumor angiogenesis that gives rise to smaller primary tumors (Fig 2.3). These results, though informative in determining the indispensable function of talin, in part through its integrin-activating function, raise a number of questions to be answered in future work.

For example, the talin rod contains multiple actin binding sites and cryptic binding sites for a number of cytoskeletal adaptor proteins like vinculin that become exposed only when tension is applied across the length of the talin molecule[160, 187-189]. Is the obvious retention of these interactions in Tln1 L325R ECs which are absent in Tln1 EC-KO ECs a source of the disparity between these two models? In the Haling et al study, defects in clot retraction of talin1 L325R platelets were rescued with manganese that stabilizes the high-affinity conformation of integrin (effectively bypassing inside-out signaling). In turn, clot retraction was abrogated by Cytochalasin D pre-treatment which inhibits actin polymerization[168]. These experiments point to the importance of the integrin-talin-actin linkage in platelet function and it likely may play a critical, unappreciated role in ECs during developmental angiogenesis. Interestingly, a recent study discovered a strong association between mutations in *tln1* with familial and sporadic cases of spontaneous coronary artery dissection[227]. Of the 11 unique mutations described, all but one was located in the talin-rod with a high frequency of these occurring in ABSs indicating that the cytoskeletal linkage of talin to actin may play a prominent role in arterial vessel stability. It is plausible that the mechanical linkage of talin in connecting the outside of the cell to the cytoskeleton is of critical importance in intestinal microvasculature and its inhibition directly tied to the leak observed in Tln1 EC-KO mice.

Given the observed vascular defects in multiple organs in Tln1 EC-KO mice that were not present in Tln1 L325R neonates, it is plausible to consider that there exist functions of talin in the endothelium that may regulate vascular stability in already established or newly developing vessels outside of the known involvement of talin in mediating integrin function. The idea of integrin-independent functions of talin have been somewhat explored in an early report analyzing the role of talin1 in follicle cells during *Drosophila* oogenesis[228]. Bécam and colleagues sought to understand the contributions of talin in this context as regulation of adhesive interactions both with the basement membrane and adjoining cells is critical for the proper development and localization of oocytes. Curiously, deletion of talin but not β-integrin expression in follicle cells resulted in increased expression of DE-cadherin, a key component of *Drosophila* adherens junctions which resulted in defective cell-cell adhesion and impaired oocyte localization during development. In light of the observation that DE-cadherin mRNA was reduced in talin-null cells, this report concluded that talin functions to repress DE-cadherin overexpression by affecting transcription factor control of DE-cadherin transcription[228]. This intriguing study suggests that a canonical cell-matrix protein plays a direct role in modulating the transcription, expression and function of adhesion molecules at cell-cell junctions that is important in the context of oogenesis. Although we found no changes in VE-cad expression in talin-depleted HUVECs and HDMVECs (Fig 3.6F and S3.6) nor did we observe differences in VE-cad expression by IF in Tln1 EC-KO retinal and intestinal ECs, we did not measure VE-cad expression in talin1-depleted cells during angiogenesis. Future work ought to explore VE-cad expression during angiogenesis in Tln1 EC-KO and Tln1 L325R pups. Is it possible that the phenotype in Tln1 EC-KO pups is due to altered VE-cadherin expression or stability at cell-cell junctions that is not observed when talin1 L325R is expressed in ECs? Future work is required to test this hypothesis specifically in the context of angiogenesis, however an intriguing and related finding was the focus of the findings presented in the third chapter.

4.2 The Role of EC Talin1 in the Regulation of Barrier Function in Established Vessels

In the 3rd chapter of this dissertation, I explored the requirement of talin-dependent integrin activation in ECs of already established vessels. The role of various EC integrins and to a lesser extent talin1 during angiogenesis has been considered, but whether talin1 plays a role in maintenance of the quiescent vasculature in any capacity was unexplored. Given the recent report from Yamamoto and colleagues which reported that EC deletion of β1 integrin during postnatal angiogenesis resulted in reduced stability of VE-cadherin at cell-cell junctions[138] and the earlier study from Bécam et al linking talin expression to DE-cadherin transcriptional regulation, we hypothesized that EC talin1 could play a role in the regulation of EC barrier function in established vessels. Strikingly, deletion of talin1 in ECs of adults 8-10 weeks resulted in early lethality within 16-20 days after tamoxifen-mediated activation of cre-recombinase, increased vascular permeability in the gut and altered VE-cadherin localization in intestinal and retinal ECs (Fig 3.1-3.3). Depletion of talin1 by shRNA in HUVECs phenocopied the weakened barrier observed *in vivo* and interestingly was partially restored through exogenous antibody-mediated activation of β1 integrin. Furthermore, altered junctional VE-cad organization was restored when shTln1 HUVECs were reconstituted with either GFP-Tln1 or GFP-THD but not a GFP-THD-L325R mutant which is incapable of activating integrins suggesting that the observed junctional defects are at least in part dependent on changes in inside-out integrin activation. These collective data posit a unique and previously unappreciated role for talin-mediated integrin activation in maintaining adherens junction organization and in-turn EC barrier function. However, this study and the specificity of the phenotype *in vivo* to the gut and retina of Tln1 EC-KO mice leave open a few outstanding questions concerning the role of talin1 in vascular barrier maintenance.

First, whereas talin1 is expressed in all endothelium, it is surprising that changes in vascular permeability were not observed in other vascular beds outside of the gastrointestinal system in Tln1 EC-KO mice. In light of the observation that VE-cad disorganization in talin1-depleted EC monolayers is normalized by Rho-kinase inhibition (Fig 3.5), is it possible that the absence of talin in the intestinal endothelium causes a tensional imbalance which lends itself to a leaky gut vascular barrier? Elegant work from Spadoni and colleagues identified and characterized a gut vascular barrier which functions to exclude microbial access to the circulation[19, 192]. In a separate report, the ablation of integrin-linked kinase in the pancreas inhibited vascularization of pancreatic islets due to disrupted islet cell-endothelial adhesive interactions which are required for islet vascularization [229]. As the intestinal tract is subject to considerable tension due to peristalsis, could the absence of talin in ECs in the gut promote dysregulation of the gut-vascular barrier? Given the specialized gut-vascular barrier described by Spadoni and colleagues, it may be prudent to investigate whether the stability of this barrier is dependent on regulation of endothelial cytoskeletal tension and more interestingly whether targeting it pharmacologically may offer an approach to treating diseases associated with a leaky gut vasculature. This recent finding is yet another indication of the extremely specialized nature of vascular networks and the regulation of their barrier properties across different tissues.

Interestingly, the only other vascular bed wherein cell-cell junctions appeared altered was in retinal vessels of Tln1 EC-KO mice. Curiously, microvasculature in these two vascular beds contains a fenestrated endothelium which accommodates a heightened permeability to solutes through diaphragm-restricted pores[215] on the luminal side of ECs[14, 15]. It is possible that the role of inside-out integrin activation in these vessels is in part linked to the regulation of these fenestrations although this observation requires further study. It has also been reported that

VEGF-A/VEGFR-2 signaling is a critical regulator in maintaining fenestrations[211, 212] and given the well-described link between VEGF signaling and integrin signaling during angiogenesis[130, 230], there may be reason to consider whether diminished integrin activation due to talin1 loss pre-disposes vascular beds reliant on VEGF signaling such as those in the BRB, GVB or endocrine organs to the defects in VE-cadherin localization observed in Tln1 EC-KO mice.

Although loss of talin1 results in early lethality due to defects in basal intestinal permeability which are due, in part, to reduced β1 integrin activation, it remains less clear whether this regulatory function extends to contexts of induced permeability. A number of gut-driven pathologies are associated with pathophysiological intestinal leakage, although most efforts have exclusively examined the contributions of the gut epithelial barrier in contexts such as chronic cholitis, inflammatory bowel syndrome and diabetes-induced leak[231]. In light of the finding that the GVB restricts bacterial dissemination from entering the circulation through tight adherens junctions, it would be prudent to examine whether the aforementioned pathologies exhibit defective cell-cell junctions[19]. Perhaps vascular hyperpermeability in the gut may be attenuated through strategies that activate endothelial β1 integrin which would agree with our findings that inhibition of β1 integrin in WT HUVECs impairs the EC barrier whereas treatment of leaky talin-depleted monolayers with β1 integrin activating antibodies attenuates increased leak (Fig 3.6). Furthermore, confocal and 3D structure illuminated microscopy of WT HUVECs revealed a pool of active β1 integrin and talin at the cell-periphery (Fig 3.6) suggesting perhaps that these molecules which are thought to function exclusively at cell-matrix adhesion may well behave at cell-cell contacts, perhaps in complex with other adherens junction components.

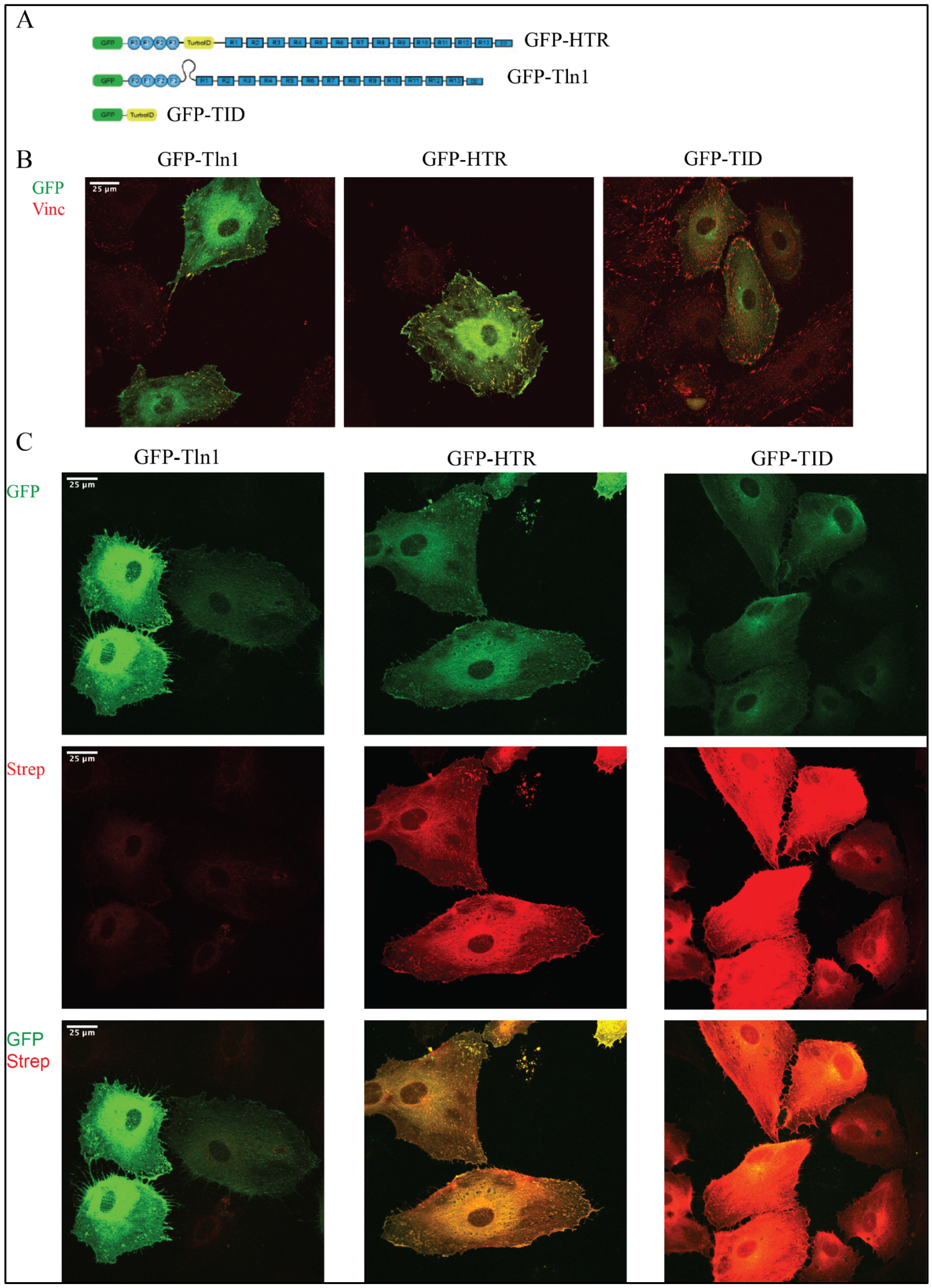

Figure 4.2. Establishment of a GFP-talin-turboID construct for proximity biotinylation of novel talin-interacting proteins
A. Schematic showing the constructs used in characterizing and validating GFP-HTR construct. **B.** All GFP constructs (green) are expressed in a human microvascular endothelial cell (HMECs) line but only GFP-Tln1 and GFP-HTR co-localize with vinculin (green) at focal adhesions. **C.** GFP-HTR, GFP-Tln1 and GFP-TID transfected HMECs cultured with exogenous biotin to permit TID-mediated labeling of proximal proteins. IF using fluorescently tagged streptavidin to visualize biotinylation reveals GFP-HTR biotinylation of vinculin positive structures whereas GFP-TID mediated biotinylation is observed throughout the cell (red). GFP-Tln1 transfected cells were used as a negative control where no biotinylation was expected or observed.

4.3 Future Directions

The surprising role of talin1 in ECs of established vessels in the 3rd chapter is indicative of a largely unappreciated role for integrin signaling in coordinating barrier function in ECs through cross-talk with cell-cell junctions. Although the observation that impaired barrier function in talin1-null monolayers can be partially rescued through exogenous β1 integrin activation, the restriction of this phenotype *in vivo* to the gut microvasculature indicates that there are likely unappreciated mechanisms that are talin-dependent which may be critical to regulation of the vascular barrier. To identify and determine the extent to which EC talin1 may regulate barrier function independent of its role in activating β1 integrin, our lab has adapted an *in vitro* proximity biotinylation approach [232]to identify novel interactions of talin1 in resting and hyperpermeable conditions. Conceptually, this approach coupled with mass spectrometry can identify novel interactions that may mediated talin-dependent regulation of the barrier. The recent development of a new generation of a promiscuous biotin ligase termed TurboID by Branon and colleagues enables the identification of weak and transient interactions in response to pro-inflammatory/pro-angiogenic agonists[233]. TurboID, when fused to bait protein, biotinylates proteins within a 30nm radius of the tagged protein within 10min[233]. Biotinylated proteins are then pulled down using Neutravidin conjugated beads and isolated proteins are identified by mass spectrometry. A comparison of proteins identified in untreated and treated groups should reveal how talin interactions change in response to agonists known to promote vascular leak. Our preliminary work utilized 3 GFP-fusion constructs to characterize the localization pattern of the GFP-Talin Head-TurboID-Talin Rod construct hereafter referred to as GFP-HTR by comparing it to GFP-TurboID (GFP-TID) and full length GFP-Talin1 (GFP-Tln1) (Fig 4.2A). I expressed these three constructs into HUVECs and co-stained with vinculin

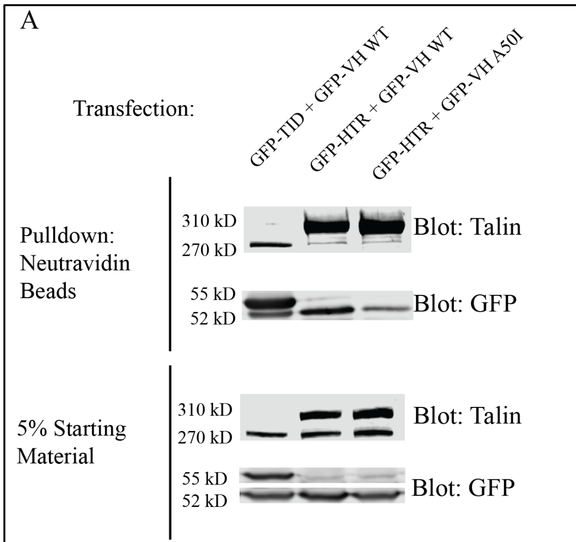

B

protein name	Peptide Spectrum Match (PSM) GFP	TurboID-Talin
paxillin	0	37
lammelipodin	0	36
zyxin	5	34
beta1 integrin	3	16
vinculin	1	14
Kank2	0	47
rap1b	2	7
kindlin2	1	82
tensin1	0	78
tensin3	0	22
moesin	3	12
MAP4K4	0	11

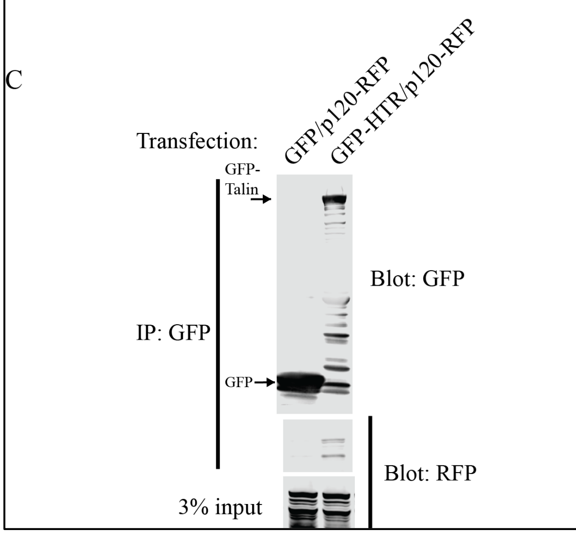

Figure 4.3. GFP-HTR proximity biotinylation coupled with mass spectrometry identifies known talin-interacting proteins as well as novel interactors
A. Co-transfection of HEK 293Ts: 1) GFP-TID + GFP-VH WT 2) GFP-HTR + GFP-VH WT 3) GFP-HTR + GFP-VH A50I pull down of biotinylated proteins with neutravidin beads. Immunoblot of pulled down material identifies reduced biotinylation of mutant GFP-VH A50I relative to GFP-VH WT. GFP-TID was used as a negative non-specific control. (55 kD band = GFP-TID / 52 kD band = GFP-VH)**B.** Mass spectrometry raw data. HMECs transfected with GFP or GFP-HTR were culture din presence of biotin for 3 hours. Peptide Spectrum Match which is a quantitatve representation of biotinylation by GFP-HTR reveals labeling of many known talin interacting proteins. **C.** Co-transfection and immunoprecipitation of HMECs expressing GFP-HTR/GFP and RFP-p120. IP of GFP-HTR transfected cells with anti-GFP conjugated beads but not GFP transfected followed by immunoblotting for RFP reveals association of p120 with GFP-HTR.

antibody to validate the localization of the GFP-HTR and GFP-Tln1 constructs to focal adhesions (Fig 4.2B). Furthermore, the functionality of the biotin ligase was assessed by transfecting cells with GFP-TurboID, GFP-Tln1 and GFP-HTR independently followed by co-staining with fluorescently tagged anti-streptavidin antibody to visualize biotinylation by IF. Indeed, only GFP-HTR and GFP-TID were positive for streptavidin signal and streptavidin signal was observed at focal adhesions in GFP-HTR but not GFP-TID transfected cells indicating specificity of biotinylation to known localization sites of talin1 (Fig 4.2C). As further proof of principle, we co-expressed GFP-HTR with either WT GFP-vinculin head (GFP-VH) or mutant vinculin head A50I (GFP-VH A50I)[234] which is known to have reduced binding affinity for talin1 and pulled down all biotinylated material using neutravidin-conjugated beads. Indeed, GFP-VH was pulled down indicating GFP-HTR induced biotinylation of this known interacting protein had occurred while considerably less GFP-VH A50I was pulled down indicating reduced biotinylation and reduced interaction with GFP-HTR relative to WT GFP-VH (Fig 4.3A). Furthermore, a pilot experiment was performed wherein ECs were transfected with GFP or GFP-HTR. Mass spectrometry analysis of isolated proteins revealed efficient labeling of a number of known talin-binding proteins including β1 integrin, vinculin and kank2 (Fig 4.3B). These data also revealed an intriguing interaction of GFP-HTR with p120-catenin (p120), a canonical VE-cad binding protein which stabilizes VE-cadherin at cell-cell junctions. Initial validation of the interaction between talin and p120 was performed by co-immunoprecipitation of GFP-HTR and RFP-p120 (Fig 4.3C). Collectively, my results suggest the feasibility of using this proteomic approach to identify novel talin-interacting proteins that may contribute to regulation of the barrier during agonist stimulation. Future efforts will look to test the functional significance of these as well as other interactions by using *in vitro* techniques to measure permeability in resting and hyperpermeable states in the absence/presence of newly identified talin interactors. I envision that novel talin interactors that function to promote increased leak in agonist-induced states may be tested in *in vivo* in murine models of cancer, diabetes or sepsis wherein pathophysiological permeability drives disease progression.

References

1. Matsumoto K, Yoshitomi H, Rossant J and Zaret KS. Liver organogenesis promoted by endothelial cells prior to vascular function. *Science*. 2001;294:559-63.
2. Pardanaud L, Yassine F and Dieterlen-Lievre F. Relationship between vasculogenesis, angiogenesis and haemopoiesis during avian ontogeny. *Development*. 1989;105:473-85.
3. Pardanaud L, Luton D, Prigent M, Bourcheix LM, Catala M and Dieterlen-Lievre F. Two distinct endothelial lineages in ontogeny, one of them related to hemopoiesis. *Development*. 1996;122:1363-71.
4. Flamme I, Frolich T and Risau W. Molecular mechanisms of vasculogenesis and embryonic angiogenesis. *J Cell Physiol*. 1997;173:206-10.
5. Cox CM and Poole TJ. Angioblast differentiation is influenced by the local environment: FGF-2 induces angioblasts and patterns vessel formation in the quail embryo. *Dev Dyn*. 2000;218:371-82.
6. Vokes SA and Krieg PA. Endoderm is required for vascular endothelial tube formation, but not for angioblast specification. *Development*. 2002;129:775-85.
7. Ribatti D, Nico B and Crivellato E. Morphological and molecular aspects of physiological vascular morphogenesis. *Angiogenesis*. 2009;12:101-11.
8. Sherwood L. *Human Physiology: From Cells to Systems*: Thomson Brooks/Cole, Belmont.; 2007.
9. Hall JE. *Guyton and Hall Textbook of Medical Physiology.* 12th Edition ed: Saunders El Sevier; 2011.
10. Torres-Vazquez J, Kamei M and Weinstein BM. Molecular distinction between arteries and veins. *Cell Tissue Res*. 2003;314:43-59.
11. You LR, Lin FJ, Lee CT, DeMayo FJ, Tsai MJ and Tsai SY. Suppression of Notch signalling by the COUP-TFII transcription factor regulates vein identity. *Nature*. 2005;435:98-104.
12. Wang HU, Chen ZF and Anderson DJ. Molecular distinction and angiogenic interaction between embryonic arteries and veins revealed by ephrin-B2 and its receptor Eph-B4. *Cell*. 1998;93:741-53.
13. Zhong TP, Childs S, Leu JP and Fishman MC. Gridlock signalling pathway fashions the first embryonic artery. *Nature*. 2001;414:216-20.
14. Aird WC. Phenotypic heterogeneity of the endothelium: II. Representative vascular beds. *Circ Res*. 2007;100:174-90.
15. Aird WC. Phenotypic heterogeneity of the endothelium: I. Structure, function, and mechanisms. *Circ Res*. 2007;100:158-73.
16. Aird WC. Endothelial cell heterogeneity. *Cold Spring Harb Perspect Med*. 2012;2:a006429.
17. Aird WC. Endothelium in health and disease. *Pharmacol Rep*. 2008;60:139-43.
18. Lampugnani MG, Dejana E and Giampietro C. Vascular Endothelial (VE)-Cadherin, Endothelial Adherens Junctions, and Vascular Disease. *Cold Spring Harb Perspect Biol*. 2017.
19. Spadoni I, Zagato E, Bertocchi A, Paolinelli R, Hot E, Di Sabatino A, Caprioli F, Bottiglieri L, Oldani A, Viale G, Penna G, Dejana E and Rescigno M. A gut-vascular barrier controls the systemic dissemination of bacteria. *Science*. 2015;350:830-4.

20. Giannotta M, Trani M and Dejana E. VE-cadherin and endothelial adherens junctions: active guardians of vascular integrity. *Dev Cell*. 2013;26:441-54.

21. Tannock IF and Hayashi S. The proliferation of capillary endothelial cells. *Cancer Res*. 1972;32:77-82.

22. Kim KJ, Li B, Winer J, Armanini M, Gillett N, Phillips HS and Ferrara N. Inhibition of vascular endothelial growth factor-induced angiogenesis suppresses tumour growth in vivo. *Nature*. 1993;362:841-4.

23. Potente M, Gerhardt H and Carmeliet P. Basic and therapeutic aspects of angiogenesis. *Cell*. 2011;146:873-87.

24. Shalaby F, Ho J, Stanford WL, Fischer KD, Schuh AC, Schwartz L, Bernstein A and Rossant J. A requirement for Flk1 in primitive and definitive hematopoiesis and vasculogenesis. *Cell*. 1997;89:981-90.

25. Shalaby F, Rossant J, Yamaguchi TP, Gertsenstein M, Wu XF, Breitman ML and Schuh AC. Failure of blood-island formation and vasculogenesis in Flk-1-deficient mice. *Nature*. 1995;376:62-6.

26. Hirschi KK, Rohovsky SA and D'Amore PA. PDGF, TGF-beta, and heterotypic cell-cell interactions mediate endothelial cell-induced recruitment of 10T1/2 cells and their differentiation to a smooth muscle fate. *J Cell Biol*. 1998;141:805-14.

27. Dickson MC, Martin JS, Cousins FM, Kulkarni AB, Karlsson S and Akhurst RJ. Defective haematopoiesis and vasculogenesis in transforming growth factor-beta 1 knock out mice. *Development*. 1995;121:1845-54.

28. Carmeliet P, Ferreira V, Breier G, Pollefeyt S, Kieckens L, Gertsenstein M, Fahrig M, Vandenhoeck A, Harpal K, Eberhardt C, Declercq C, Pawling J, Moons L, Collen D, Risau W and Nagy A. Abnormal blood vessel development and lethality in embryos lacking a single VEGF allele. *Nature*. 1996;380:435-9.

29. Ferrara N, Carver-Moore K, Chen H, Dowd M, Lu L, O'Shea KS, Powell-Braxton L, Hillan KJ and Moore MW. Heterozygous embryonic lethality induced by targeted inactivation of the VEGF gene. *Nature*. 1996;380:439-42.

30. Gaengel K, Genove G, Armulik A and Betsholtz C. Endothelial-mural cell signaling in vascular development and angiogenesis. *Arterioscler Thromb Vasc Biol*. 2009;29:630-8.

31. Hellstrom M, Kalen M, Lindahl P, Abramsson A and Betsholtz C. Role of PDGF-B and PDGFR-beta in recruitment of vascular smooth muscle cells and pericytes during embryonic blood vessel formation in the mouse. *Development*. 1999;126:3047-55.

32. Lindahl P, Johansson BR, Leveen P and Betsholtz C. Pericyte loss and microaneurysm formation in PDGF-B-deficient mice. *Science*. 1997;277:242-5.

33. Suri C, Jones PF, Patan S, Bartunkova S, Maisonpierre PC, Davis S, Sato TN and Yancopoulos GD. Requisite role of angiopoietin-1, a ligand for the TIE2 receptor, during embryonic angiogenesis. *Cell*. 1996;87:1171-80.

34. Puri MC, Partanen J, Rossant J and Bernstein A. Interaction of the TEK and TIE receptor tyrosine kinases during cardiovascular development. *Development*. 1999;126:4569-80.

35. Dumont DJ, Gradwohl G, Fong GH, Puri MC, Gertsenstein M, Auerbach A and Breitman ML. Dominant-negative and targeted null mutations in the endothelial receptor tyrosine kinase, tek, reveal a critical role in vasculogenesis of the embryo. *Genes Dev*. 1994;8:1897-909.

36. Sato TN, Tozawa Y, Deutsch U, Wolburg-Buchholz K, Fujiwara Y, Gendron-Maguire M, Gridley T, Wolburg H, Risau W and Qin Y. Distinct roles of the receptor tyrosine kinases Tie-1 and Tie-2 in blood vessel formation. *Nature*. 1995;376:70-4.
37. Corada M, Mariotti M, Thurston G, Smith K, Kunkel R, Brockhaus M, Lampugnani MG, Martin-Padura I, Stoppacciaro A, Ruco L, McDonald DM, Ward PA and Dejana E. Vascular endothelial-cadherin is an important determinant of microvascular integrity in vivo. *Proc Natl Acad Sci U S A*. 1999;96:9815-20.
38. Carmeliet P, Lampugnani MG, Moons L, Breviario F, Compernolle V, Bono F, Balconi G, Spagnuolo R, Oosthuyse B, Dewerchin M, Zanetti A, Angellilo A, Mattot V, Nuyens D, Lutgens E, Clotman F, de Ruiter MC, Gittenberger-de Groot A, Poelmann R, Lupu F, Herbert JM, Collen D and Dejana E. Targeted deficiency or cytosolic truncation of the VE-cadherin gene in mice impairs VEGF-mediated endothelial survival and angiogenesis. *Cell*. 1999;98:147-57.
39. Gory-Faure S, Prandini MH, Pointu H, Roullot V, Pignot-Paintrand I, Vernet M and Huber P. Role of vascular endothelial-cadherin in vascular morphogenesis. *Development*. 1999;126:2093-102.
40. Breviario F, Caveda L, Corada M, Martin-Padura I, Navarro P, Golay J, Introna M, Gulino D, Lampugnani MG and Dejana E. Functional properties of human vascular endothelial cadherin (7B4/cadherin-5), an endothelium-specific cadherin. *Arterioscler Thromb Vasc Biol*. 1995;15:1229-39.
41. Dejana E, Tournier-Lasserve E and Weinstein BM. The control of vascular integrity by endothelial cell junctions: molecular basis and pathological implications. *Dev Cell*. 2009;16:209-21.
42. Pokutta S, Choi HJ, Ahlsen G, Hansen SD and Weis WI. Structural and thermodynamic characterization of cadherin.beta-catenin.alpha-catenin complex formation. *J Biol Chem*. 2014;289:13589-601.
43. Desai R, Sarpal R, Ishiyama N, Pellikka M, Ikura M and Tepass U. Monomeric alpha-catenin links cadherin to the actin cytoskeleton. *Nat Cell Biol*. 2013;15:261-73.
44. Oas RG, Xiao K, Summers S, Wittich KB, Chiasson CM, Martin WD, Grossniklaus HE, Vincent PA, Reynolds AB and Kowalczyk AP. p120-Catenin is required for mouse vascular development. *Circ Res*. 2010;106:941-51.
45. Nanes BA, Chiasson-MacKenzie C, Lowery AM, Ishiyama N, Faundez V, Ikura M, Vincent PA and Kowalczyk AP. p120-catenin binding masks an endocytic signal conserved in classical cadherins. *J Cell Biol*. 2012;199:365-80.
46. Chiasson CM, Wittich KB, Vincent PA, Faundez V and Kowalczyk AP. p120-catenin inhibits VE-cadherin internalization through a Rho-independent mechanism. *Mol Biol Cell*. 2009;20:1970-80.
47. Gerhardt H, Golding M, Fruttiger M, Ruhrberg C, Lundkvist A, Abramsson A, Jeltsch M, Mitchell C, Alitalo K, Shima D and Betsholtz C. VEGF guides angiogenic sprouting utilizing endothelial tip cell filopodia. *J Cell Biol*. 2003;161:1163-77.
48. Bentley K, Franco CA, Philippides A, Blanco R, Dierkes M, Gebala V, Stanchi F, Jones M, Aspalter IM, Cagna G, Westrom S, Claesson-Welsh L, Vestweber D and Gerhardt H. The role of differential VE-cadherin dynamics in cell rearrangement during angiogenesis. *Nat Cell Biol*. 2014;16:309-21.

49. Jakobsson L, Franco CA, Bentley K, Collins RT, Ponsioen B, Aspalter IM, Rosewell I, Busse M, Thurston G, Medvinsky A, Schulte-Merker S and Gerhardt H. Endothelial cells dynamically compete for the tip cell position during angiogenic sprouting. *Nat Cell Biol*. 2010;12:943-53.
50. Hellstrom M, Phng LK, Hofmann JJ, Wallgard E, Coultas L, Lindblom P, Alva J, Nilsson AK, Karlsson L, Gaiano N, Yoon K, Rossant J, Iruela-Arispe ML, Kalen M, Gerhardt H and Betsholtz C. Dll4 signalling through Notch1 regulates formation of tip cells during angiogenesis. *Nature*. 2007;445:776-80.
51. Suchting S, Freitas C, le Noble F, Benedito R, Breant C, Duarte A and Eichmann A. The Notch ligand Delta-like 4 negatively regulates endothelial tip cell formation and vessel branching. *Proc Natl Acad Sci U S A*. 2007;104:3225-30.
52. Lobov IB, Renard RA, Papadopoulos N, Gale NW, Thurston G, Yancopoulos GD and Wiegand SJ. Delta-like ligand 4 (Dll4) is induced by VEGF as a negative regulator of angiogenic sprouting. *Proc Natl Acad Sci U S A*. 2007;104:3219-24.
53. Lee S, Jilani SM, Nikolova GV, Carpizo D and Iruela-Arispe ML. Processing of VEGF-A by matrix metalloproteinases regulates bioavailability and vascular patterning in tumors. *J Cell Biol*. 2005;169:681-91.
54. Arroyo AG and Iruela-Arispe ML. Extracellular matrix, inflammation, and the angiogenic response. *Cardiovasc Res*. 2010;86:226-35.
55. Hynes RO. Integrins: bidirectional, allosteric signaling machines. *Cell*. 2002;110:673-87.
56. Desgrosellier JS and Cheresh DA. Integrins in cancer: biological implications and therapeutic opportunities. *Nat Rev Cancer*. 2010;10:9-22.
57. Stupack DG and Cheresh DA. Integrins and angiogenesis. *Curr Top Dev Biol*. 2004;64:207-38.
58. Arnaout MA, Goodman SL and Xiong JP. Structure and mechanics of integrin-based cell adhesion. *Curr Opin Cell Biol*. 2007;19:495-507.
59. Morse EM, Brahme NN and Calderwood DA. Integrin cytoplasmic tail interactions. *Biochemistry*. 2014;53:810-20.
60. Bershadsky AD, Balaban NQ and Geiger B. Adhesion-dependent cell mechanosensitivity. *Annu Rev Cell Dev Biol*. 2003;19:677-95.
61. Fantin A, Vieira JM, Gestri G, Denti L, Schwarz Q, Prykhozhij S, Peri F, Wilson SW and Ruhrberg C. Tissue macrophages act as cellular chaperones for vascular anastomosis downstream of VEGF-mediated endothelial tip cell induction. *Blood*. 2010;116:829-40.
62. Nicoli S, Standley C, Walker P, Hurlstone A, Fogarty KE and Lawson ND. MicroRNA-mediated integration of haemodynamics and Vegf signalling during angiogenesis. *Nature*. 2010;464:1196-200.
63. Makanya AN, Hlushchuk R and Djonov VG. Intussusceptive angiogenesis and its role in vascular morphogenesis, patterning, and remodeling. *Angiogenesis*. 2009;12:113-23.
64. Lampugnani MG, Orsenigo F, Gagliani MC, Tacchetti C and Dejana E. Vascular endothelial cadherin controls VEGFR-2 internalization and signaling from intracellular compartments. *J Cell Biol*. 2006;174:593-604.
65. Grazia Lampugnani M, Zanetti A, Corada M, Takahashi T, Balconi G, Breviario F, Orsenigo F, Cattelino A, Kemler R, Daniel TO and Dejana E. Contact inhibition of VEGF-induced proliferation requires vascular endothelial cadherin, beta-catenin, and the phosphatase DEP-1/CD148. *J Cell Biol*. 2003;161:793-804.

66. Lee S, Chen TT, Barber CL, Jordan MC, Murdock J, Desai S, Ferrara N, Nagy A, Roos KP and Iruela-Arispe ML. Autocrine VEGF signaling is required for vascular homeostasis. *Cell*. 2007;130:691-703.

67. Rudini N, Felici A, Giampietro C, Lampugnani M, Corada M, Swirsding K, Garre M, Liebner S, Letarte M, ten Dijke P and Dejana E. VE-cadherin is a critical endothelial regulator of TGF-beta signalling. *EMBO J*. 2008;27:993-1004.

68. Rho SS, Ando K and Fukuhara S. Dynamic Regulation of Vascular Permeability by Vascular Endothelial Cadherin-Mediated Endothelial Cell-Cell Junctions. *J Nippon Med Sch*. 2017;84:148-159.

69. Pulous FE and Petrich BG. Integrin-dependent regulation of the endothelial barrier. *Tissue Barriers*. 2019:1685844.

70. Timmerman I, Heemskerk N, Kroon J, Schaefer A, van Rijssel J, Hoogenboezem M, van Unen J, Goedhart J, Gadella TW, Jr., Yin T, Wu Y, Huveneers S and van Buul JD. A local VE-cadherin and Trio-based signaling complex stabilizes endothelial junctions through Rac1. *J Cell Sci*. 2015;128:3514.

71. Huveneers S, Oldenburg J, Spanjaard E, van der Krogt G, Grigoriev I, Akhmanova A, Rehmann H and de Rooij J. Vinculin associates with endothelial VE-cadherin junctions to control force-dependent remodeling. *J Cell Biol*. 2012;196:641-52.

72. Hynes RO, Lively JC, McCarty JH, Taverna D, Francis SE, Hodivala-Dilke K and Xiao Q. The diverse roles of integrins and their ligands in angiogenesis. *Cold Spring Harb Symp Quant Biol*. 2002;67:143-53.

73. Hakanpaa L, Sipila T, Leppanen VM, Gautam P, Nurmi H, Jacquemet G, Eklund L, Ivaska J, Alitalo K and Saharinen P. Endothelial destabilization by angiopoietin-2 via integrin beta1 activation. *Nat Commun*. 2015;6:5962.

74. Saharinen P, Eklund L, Miettinen J, Wirkkala R, Anisimov A, Winderlich M, Nottebaum A, Vestweber D, Deutsch U, Koh GY, Olsen BR and Alitalo K. Angiopoietins assemble distinct Tie2 signalling complexes in endothelial cell-cell and cell-matrix contacts. *Nat Cell Biol*. 2008;10:527-37.

75. Carmeliet P and Jain RK. Molecular mechanisms and clinical applications of angiogenesis. *Nature*. 2011;473:298-307.

76. Bergers G, Brekken R, McMahon G, Vu TH, Itoh T, Tamaki K, Tanzawa K, Thorpe P, Itohara S, Werb Z and Hanahan D. Matrix metalloproteinase-9 triggers the angiogenic switch during carcinogenesis. *Nat Cell Biol*. 2000;2:737-44.

77. Nikitenko LL. Vascular endothelium in cancer. *Cell Tissue Res*. 2009;335:223-40.

78. Criscuoli ML, Nguyen M and Eliceiri BP. Tumor metastasis but not tumor growth is dependent on Src-mediated vascular permeability. *Blood*. 2005;105:1508-14.

79. Jain RK. Normalization of tumor vasculature: an emerging concept in antiangiogenic therapy. *Science*. 2005;307:58-62.

80. Carmeliet P and Jain RK. Angiogenesis in cancer and other diseases. *Nature*. 2000;407:249-57.

81. Avraamides CJ, Garmy-Susini B and Varner JA. Integrins in angiogenesis and lymphangiogenesis. *Nat Rev Cancer*. 2008;8:604-17.

82. Brooks PC, Clark RA and Cheresh DA. Requirement of vascular integrin alpha v beta 3 for angiogenesis. *Science*. 1994;264:569-71.

83. Boudreau NJ and Varner JA. The homeobox transcription factor Hox D3 promotes integrin alpha5beta1 expression and function during angiogenesis. *J Biol Chem*. 2004;279:4862-8.
84. Kim S, Bell K, Mousa SA and Varner JA. Regulation of angiogenesis in vivo by ligation of integrin alpha5beta1 with the central cell-binding domain of fibronectin. *Am J Pathol*. 2000;156:1345-62.
85. Silva R, D'Amico G, Hodivala-Dilke KM and Reynolds LE. Integrins: the keys to unlocking angiogenesis. *Arterioscler Thromb Vasc Biol*. 2008;28:1703-13.
86. Brooks PC, Montgomery AM, Rosenfeld M, Reisfeld RA, Hu T, Klier G and Cheresh DA. Integrin alpha v beta 3 antagonists promote tumor regression by inducing apoptosis of angiogenic blood vessels. *Cell*. 1994;79:1157-64.
87. Zhang Z, Ramirez NE, Yankeelov TE, Li Z, Ford LE, Qi Y, Pozzi A and Zutter MM. alpha2beta1 integrin expression in the tumor microenvironment enhances tumor angiogenesis in a tumor cell-specific manner. *Blood*. 2008;111:1980-8.
88. Pozzi A, Moberg PE, Miles LA, Wagner S, Soloway P and Gardner HA. Elevated matrix metalloprotease and angiostatin levels in integrin alpha 1 knockout mice cause reduced tumor vascularization. *Proc Natl Acad Sci U S A*. 2000;97:2202-7.
89. Malinin NL, Pluskota E and Byzova TV. Integrin signaling in vascular function. *Curr Opin Hematol*. 2012;19:206-11.
90. Mahabeleshwar GH, Feng W, Reddy K, Plow EF and Byzova TV. Mechanisms of integrin-vascular endothelial growth factor receptor cross-activation in angiogenesis. *Circ Res*. 2007;101:570-80.
91. De S, Razorenova O, McCabe NP, O'Toole T, Qin J and Byzova TV. VEGF-integrin interplay controls tumor growth and vascularization. *Proc Natl Acad Sci U S A*. 2005;102:7589-94.
92. Huynh J, Nishimura N, Rana K, Peloquin JM, Califano JP, Montague CR, King MR, Schaffer CB and Reinhart-King CA. Age-related intimal stiffening enhances endothelial permeability and leukocyte transmigration. *Sci Transl Med*. 2011;3:112ra122.
93. Mazzone M, Dettori D, de Oliveira RL, Loges S, Schmidt T, Jonckx B, Tian YM, Lanahan AA, Pollard P, de Almodovar CR, De Smet F, Vinckier S, Aragones J, Debackere K, Luttun A, Wyns S, Jordan B, Pisacane A, Gallez B, Lampugnani MG, Dejana E, Simons M, Ratcliffe P, Maxwell P and Carmeliet P. Heterozygous deficiency of PHD2 restores tumor oxygenation and inhibits metastasis via endothelial normalization. *Cell*. 2009;136:839-851.
94. Dorland YL, Malinova TS, van Stalborch AM, Grieve AG, van Geemen D, Jansen NS, de Kreuk BJ, Nawaz K, Kole J, Geerts D, Musters RJ, de Rooij J, Hordijk PL and Huveneers S. The F-BAR protein pacsin2 inhibits asymmetric VE-cadherin internalization from tensile adherens junctions. *Nat Commun*. 2016;7:12210.
95. Dejana E and Giampietro C. Vascular endothelial-cadherin and vascular stability. *Curr Opin Hematol*. 2012;19:218-23.
96. Crosby CV, Fleming PA, Argraves WS, Corada M, Zanetta L, Dejana E and Drake CJ. VE-cadherin is not required for the formation of nascent blood vessels but acts to prevent their disassembly. *Blood*. 2005;105:2771-6.
97. Tanihara H, Kido M, Obata S, Heimark RL, Davidson M, St John T and Suzuki S. Characterization of cadherin-4 and cadherin-5 reveals new aspects of cadherins. *J Cell Sci*. 1994;107 (Pt 6):1697-704.

98. Peifer M, Berg S and Reynolds AB. A repeating amino acid motif shared by proteins with diverse cellular roles. *Cell*. 1994;76:789-91.
99. Vestweber D, Winderlich M, Cagna G and Nottebaum AF. Cell adhesion dynamics at endothelial junctions: VE-cadherin as a major player. *Trends Cell Biol*. 2009;19:8-15.
100. Schulte D, Kuppers V, Dartsch N, Broermann A, Li H, Zarbock A, Kamenyeva O, Kiefer F, Khandoga A, Massberg S and Vestweber D. Stabilizing the VE-cadherin-catenin complex blocks leukocyte extravasation and vascular permeability. *EMBO J*. 2011;30:4157-70.
101. Gavard J and Gutkind JS. VEGF controls endothelial-cell permeability by promoting the beta-arrestin-dependent endocytosis of VE-cadherin. *Nat Cell Biol*. 2006;8:1223-34.
102. Wallez Y, Cand F, Cruzalegui F, Wernstedt C, Souchelnytskyi S, Vilgrain I and Huber P. Src kinase phosphorylates vascular endothelial-cadherin in response to vascular endothelial growth factor: identification of tyrosine 685 as the unique target site. *Oncogene*. 2007;26:1067-77.
103. Angelini DJ, Hyun SW, Grigoryev DN, Garg P, Gong P, Singh IS, Passaniti A, Hasday JD and Goldblum SE. TNF-alpha increases tyrosine phosphorylation of vascular endothelial cadherin and opens the paracellular pathway through fyn activation in human lung endothelia. *Am J Physiol Lung Cell Mol Physiol*. 2006;291:L1232-45.
104. Adam AP, Lowery AM, Martino N, Alsaffar H and Vincent PA. Src Family Kinases Modulate the Loss of Endothelial Barrier Function in Response to TNF-alpha: Crosstalk with p38 Signaling. *PLoS One*. 2016;11:e0161975.
105. Nottebaum AF, Cagna G, Winderlich M, Gamp AC, Linnepe R, Polaschegg C, Filippova K, Lyck R, Engelhardt B, Kamenyeva O, Bixel MG, Butz S and Vestweber D. VE-PTP maintains the endothelial barrier via plakoglobin and becomes dissociated from VE-cadherin by leukocytes and by VEGF. *J Exp Med*. 2008;205:2929-45.
106. Broermann A, Winderlich M, Block H, Frye M, Rossaint J, Zarbock A, Cagna G, Linnepe R, Schulte D, Nottebaum AF and Vestweber D. Dissociation of VE-PTP from VE-cadherin is required for leukocyte extravasation and for VEGF-induced vascular permeability in vivo. *J Exp Med*. 2011;208:2393-401.
107. Frye M, Dierkes M, Kuppers V, Vockel M, Tomm J, Zeuschner D, Rossaint J, Zarbock A, Koh GY, Peters K, Nottebaum AF and Vestweber D. Interfering with VE-PTP stabilizes endothelial junctions in vivo via Tie-2 in the absence of VE-cadherin. *J Exp Med*. 2015;212:2267-87.
108. Fukuhara S, Sakurai A, Sano H, Yamagishi A, Somekawa S, Takakura N, Saito Y, Kangawa K and Mochizuki N. Cyclic AMP potentiates vascular endothelial cadherin-mediated cell-cell contact to enhance endothelial barrier function through an Epac-Rap1 signaling pathway. *Mol Cell Biol*. 2005;25:136-46.
109. Noda K, Zhang J, Fukuhara S, Kunimoto S, Yoshimura M and Mochizuki N. Vascular endothelial-cadherin stabilizes at cell-cell junctions by anchoring to circumferential actin bundles through alpha- and beta-catenins in cyclic AMP-Epac-Rap1 signal-activated endothelial cells. *Mol Biol Cell*. 2010;21:584-96.
110. van Wetering S, van Buul JD, Quik S, Mul FP, Anthony EC, ten Klooster JP, Collard JG and Hordijk PL. Reactive oxygen species mediate Rac-induced loss of cell-cell adhesion in primary human endothelial cells. *J Cell Sci*. 2002;115:1837-46.
111. Gorovoy M, Neamu R, Niu J, Vogel S, Predescu D, Miyoshi J, Takai Y, Kini V, Mehta D, Malik AB and Voyno-Yasenetskaya T. RhoGDI-1 modulation of the activity of monomeric

RhoGTPase RhoA regulates endothelial barrier function in mouse lungs. *Circ Res*. 2007;101:50-8.
112. Mikelis CM, Simaan M, Ando K, Fukuhara S, Sakurai A, Amornphimoltham P, Masedunskas A, Weigert R, Chavakis T, Adams RH, Offermanns S, Mochizuki N, Zheng Y and Gutkind JS. RhoA and ROCK mediate histamine-induced vascular leakage and anaphylactic shock. *Nat Commun*. 2015;6:6725.
113. Mui KL, Chen CS and Assoian RK. The mechanical regulation of integrin-cadherin crosstalk organizes cells, signaling and forces. *J Cell Sci*. 2016;129:1093-100.
114. Stupack DG and Cheresh DA. ECM remodeling regulates angiogenesis: endothelial integrins look for new ligands. *Sci STKE*. 2002;2002:pe7.
115. Shattil SJ, Kim C and Ginsberg MH. The final steps of integrin activation: the end game. *Nat Rev Mol Cell Biol*. 2010;11:288-300.
116. Calderwood DA, Zent R, Grant R, Rees DJ, Hynes RO and Ginsberg MH. The Talin head domain binds to integrin beta subunit cytoplasmic tails and regulates integrin activation. *J Biol Chem*. 1999;274:28071-4.
117. Tadokoro S, Shattil SJ, Eto K, Tai V, Liddington RC, de Pereda JM, Ginsberg MH and Calderwood DA. Talin binding to integrin beta tails: a final common step in integrin activation. *Science*. 2003;302:103-6.
118. Wegener KL, Partridge AW, Han J, Pickford AR, Liddington RC, Ginsberg MH and Campbell ID. Structural basis of integrin activation by talin. *Cell*. 2007;128:171-82.
119. Ma YQ, Qin J, Wu C and Plow EF. Kindlin-2 (Mig-2): a co-activator of beta3 integrins. *J Cell Biol*. 2008;181:439-46.
120. Horton ER, Byron A, Askari JA, Ng DHJ, Millon-Fremillon A, Robertson J, Koper EJ, Paul NR, Warwood S, Knight D, Humphries JD and Humphries MJ. Definition of a consensus integrin adhesome and its dynamics during adhesion complex assembly and disassembly. *Nat Cell Biol*. 2015;17:1577-1587.
121. Humphries JD, Chastney MR, Askari JA and Humphries MJ. Signal transduction via integrin adhesion complexes. *Curr Opin Cell Biol*. 2019;56:14-21.
122. Payne S, De Val S and Neal A. Endothelial-Specific Cre Mouse Models. *Arterioscler Thromb Vasc Biol*. 2018;38:2550-2561.
123. van der Flier A, Badu-Nkansah K, Whittaker CA, Crowley D, Bronson RT, Lacy-Hulbert A and Hynes RO. Endothelial alpha5 and alphav integrins cooperate in remodeling of the vasculature during development. *Development*. 2010;137:2439-49.
124. Zovein AC, Luque A, Turlo KA, Hofmann JJ, Yee KM, Becker MS, Fassler R, Mellman I, Lane TF and Iruela-Arispe ML. Beta1 integrin establishes endothelial cell polarity and arteriolar lumen formation via a Par3-dependent mechanism. *Dev Cell*. 2010;18:39-51.
125. Lei L, Liu D, Huang Y, Jovin I, Shai SY, Kyriakides T, Ross RS and Giordano FJ. Endothelial expression of beta1 integrin is required for embryonic vascular patterning and postnatal vascular remodeling. *Mol Cell Biol*. 2008;28:794-802.
126. Ghatak S, Niland S, Schulz JN, Wang F, Eble JA, Leitges M, Mauch C, Krieg T, Zigrino P and Eckes B. Role of Integrins alpha1beta1 and alpha2beta1 in Wound and Tumor Angiogenesis in Mice. *Am J Pathol*. 2016;186:3011-3027.
127. Hodivala-Dilke KM, McHugh KP, Tsakiris DA, Rayburn H, Crowley D, Ullman-Cullere M, Ross FP, Coller BS, Teitelbaum S and Hynes RO. Beta3-integrin-deficient mice are a model for

Glanzmann thrombasthenia showing placental defects and reduced survival. *J Clin Invest*. 1999;103:229-38.
128. Bader BL, Rayburn H, Crowley D and Hynes RO. Extensive vasculogenesis, angiogenesis, and organogenesis precede lethality in mice lacking all alpha v integrins. *Cell*. 1998;95:507-19.
129. Reynolds LE, Wyder L, Lively JC, Taverna D, Robinson SD, Huang X, Sheppard D, Hynes RO and Hodivala-Dilke KM. Enhanced pathological angiogenesis in mice lacking beta3 integrin or beta3 and beta5 integrins. *Nat Med*. 2002;8:27-34.
130. Mahabeleshwar GH, Feng W, Phillips DR and Byzova TV. Integrin signaling is critical for pathological angiogenesis. *J Exp Med*. 2006;203:2495-507.
131. Steri V, Ellison TS, Gontarczyk AM, Weilbaecher K, Schneider JG, Edwards D, Fruttiger M, Hodivala-Dilke KM and Robinson SD. Acute depletion of endothelial beta3-integrin transiently inhibits tumor growth and angiogenesis in mice. *Circ Res*. 2014;114:79-91.
132. Robinson SD, Reynolds LE, Wyder L, Hicklin DJ and Hodivala-Dilke KM. Beta3-integrin regulates vascular endothelial growth factor-A-dependent permeability. *Arterioscler Thromb Vasc Biol*. 2004;24:2108-14.
133. Su G, Atakilit A, Li JT, Wu N, Bhattacharya M, Zhu J, Shieh JE, Li E, Chen R, Sun S, Su CP and Sheppard D. Absence of integrin alphavbeta3 enhances vascular leak in mice by inhibiting endothelial cortical actin formation. *Am J Respir Crit Care Med*. 2012;185:58-66.
134. Alghisi GC, Ponsonnet L and Ruegg C. The integrin antagonist cilengitide activates alphaVbeta3, disrupts VE-cadherin localization at cell junctions and enhances permeability in endothelial cells. *PLoS One*. 2009;4:e4449.
135. Gonzalez AM, Bhattacharya R, deHart GW and Jones JC. Transdominant regulation of integrin function: mechanisms of crosstalk. *Cell Signal*. 2010;22:578-83.
136. Su G, Hodnett M, Wu N, Atakilit A, Kosinski C, Godzich M, Huang XZ, Kim JK, Frank JA, Matthay MA, Sheppard D and Pittet JF. Integrin alphavbeta5 regulates lung vascular permeability and pulmonary endothelial barrier function. *Am J Respir Cell Mol Biol*. 2007;36:377-86.
137. Lampugnani MG, Resnati M, Dejana E and Marchisio PC. The role of integrins in the maintenance of endothelial monolayer integrity. *J Cell Biol*. 1991;112:479-90.
138. Yamamoto H, Ehling M, Kato K, Kanai K, van Lessen M, Frye M, Zeuschner D, Nakayama M, Vestweber D and Adams RH. Integrin beta1 controls VE-cadherin localization and blood vessel stability. *Nat Commun*. 2015;6:6429.
139. Hakanpaa L, Kiss EA, Jacquemet G, Miinalainen I, Lerche M, Guzman C, Mervaala E, Eklund L, Ivaska J and Saharinen P. Targeting beta1-integrin inhibits vascular leakage in endotoxemia. *Proc Natl Acad Sci U S A*. 2018;115:E6467-E6476.
140. Burridge K and Connell L. A new protein of adhesion plaques and ruffling membranes. *J Cell Biol*. 1983;97:359-67.
141. Albiges-Rizo C, Frachet P and Block MR. Down regulation of talin alters cell adhesion and the processing of the alpha 5 beta 1 integrin. *J Cell Sci*. 1995;108 (Pt 10):3317-29.
142. Nuckolls GH, Romer LH and Burridge K. Microinjection of antibodies against talin inhibits the spreading and migration of fibroblasts. *J Cell Sci*. 1992;102 (Pt 4):753-62.
143. Priddle H, Hemmings L, Monkley S, Woods A, Patel B, Sutton D, Dunn GA, Zicha D and Critchley DR. Disruption of the talin gene compromises focal adhesion assembly in undifferentiated but not differentiated embryonic stem cells. *J Cell Biol*. 1998;142:1121-33.

144. Zhang X, Jiang G, Cai Y, Monkley SJ, Critchley DR and Sheetz MP. Talin depletion reveals independence of initial cell spreading from integrin activation and traction. *Nat Cell Biol*. 2008;10:1062-8.
145. Garcia-Alvarez B, de Pereda JM, Calderwood DA, Ulmer TS, Critchley D, Campbell ID, Ginsberg MH and Liddington RC. Structural determinants of integrin recognition by talin. *Mol Cell*. 2003;11:49-58.
146. Klapholz B and Brown NH. Talin - the master of integrin adhesions. *J Cell Sci*. 2017;130:2435-2446.
147. Calderwood DA, Campbell ID and Critchley DR. Talins and kindlins: partners in integrin-mediated adhesion. *Nat Rev Mol Cell Biol*. 2013;14:503-17.
148. Song X, Yang J, Hirbawi J, Ye S, Perera HD, Goksoy E, Dwivedi P, Plow EF, Zhang R and Qin J. A novel membrane-dependent on/off switch mechanism of talin FERM domain at sites of cell adhesion. *Cell Res*. 2012;22:1533-45.
149. Goult BT, Xu XP, Gingras AR, Swift M, Patel B, Bate N, Kopp PM, Barsukov IL, Critchley DR, Volkmann N and Hanein D. Structural studies on full-length talin1 reveal a compact auto-inhibited dimer: implications for talin activation. *J Struct Biol*. 2013;184:21-32.
150. Dedden D, Schumacher S, Kelley CF, Zacharias M, Biertumpfel C, Fassler R and Mizuno N. The Architecture of Talin1 Reveals an Autoinhibition Mechanism. *Cell*. 2019;179:120-131 e13.
151. Zeiler M, Moser M and Mann M. Copy number analysis of the murine platelet proteome spanning the complete abundance range. *Mol Cell Proteomics*. 2014;13:3435-45.
152. Zhu L, Yang J, Bromberger T, Holly A, Lu F, Liu H, Sun K, Klapproth S, Hirbawi J, Byzova TV, Plow EF, Moser M and Qin J. Structure of Rap1b bound to talin reveals a pathway for triggering integrin activation. *Nat Commun*. 2017;8:1744.
153. Gingras AR, Lagarrigue F, Cuevas MN, Valadez AJ, Zorovich M, McLaughlin W, Lopez-Ramirez MA, Seban N, Ley K, Kiosses WB and Ginsberg MH. Rap1 binding and a lipid-dependent helix in talin F1 domain promote integrin activation in tandem. *J Cell Biol*. 2019;218:1799-1809.
154. Lagarrigue F, Gingras AR, Paul DS, Valadez AJ, Cuevas MN, Sun H, Lopez-Ramirez MA, Goult BT, Shattil SJ, Bergmeier W and Ginsberg MH. Rap1 binding to the talin 1 F0 domain makes a minimal contribution to murine platelet GPIIb-IIIa activation. *Blood Adv*. 2018;2:2358-2368.
155. Goksoy E, Ma YQ, Wang X, Kong X, Perera D, Plow EF and Qin J. Structural basis for the autoinhibition of talin in regulating integrin activation. *Mol Cell*. 2008;31:124-33.
156. Wynne JP, Wu J, Su W, Mor A, Patsoukis N, Boussiotis VA, Hubbard SR and Philips MR. Rap1-interacting adapter molecule (RIAM) associates with the plasma membrane via a proximity detector. *J Cell Biol*. 2012;199:317-30.
157. Legate KR, Takahashi S, Bonakdar N, Fabry B, Boettiger D, Zent R and Fassler R. Integrin adhesion and force coupling are independently regulated by localized PtdIns(4,5)2 synthesis. *EMBO J*. 2011;30:4539-53.
158. Gingras AR, Ziegler WH, Frank R, Barsukov IL, Roberts GC, Critchley DR and Emsley J. Mapping and consensus sequence identification for multiple vinculin binding sites within the talin rod. *J Biol Chem*. 2005;280:37217-24.
159. del Rio A, Perez-Jimenez R, Liu R, Roca-Cusachs P, Fernandez JM and Sheetz MP. Stretching single talin rod molecules activates vinculin binding. *Science*. 2009;323:638-41.

160. Yao M, Goult BT, Klapholz B, Hu X, Toseland CP, Guo Y, Cong P, Sheetz MP and Yan J. The mechanical response of talin. *Nat Commun*. 2016;7:11966.
161. Liu J, Wang Y, Goh WI, Goh H, Baird MA, Ruehland S, Teo S, Bate N, Critchley DR, Davidson MW and Kanchanawong P. Talin determines the nanoscale architecture of focal adhesions. *Proc Natl Acad Sci U S A*. 2015;112:E4864-73.
162. Kanchanawong P, Shtengel G, Pasapera AM, Ramko EB, Davidson MW, Hess HF and Waterman CM. Nanoscale architecture of integrin-based cell adhesions. *Nature*. 2010;468:580-4.
163. Monkley SJ, Zhou XH, Kinston SJ, Giblett SM, Hemmings L, Priddle H, Brown JE, Pritchard CA, Critchley DR and Fassler R. Disruption of the talin gene arrests mouse development at the gastrulation stage. *Dev Dyn*. 2000;219:560-74.
164. Simonson WT, Franco SJ and Huttenlocher A. Talin1 regulates TCR-mediated LFA-1 function. *J Immunol*. 2006;177:7707-14.
165. Petrich BG, Marchese P, Ruggeri ZM, Spiess S, Weichert RA, Ye F, Tiedt R, Skoda RC, Monkley SJ, Critchley DR and Ginsberg MH. Talin is required for integrin-mediated platelet function in hemostasis and thrombosis. *J Exp Med*. 2007;204:3103-11.
166. Nieswandt B, Moser M, Pleines I, Varga-Szabo D, Monkley S, Critchley D and Fassler R. Loss of talin1 in platelets abrogates integrin activation, platelet aggregation, and thrombus formation in vitro and in vivo. *J Exp Med*. 2007;204:3113-8.
167. Petrich BG, Fogelstrand P, Partridge AW, Yousefi N, Ablooglu AJ, Shattil SJ and Ginsberg MH. The antithrombotic potential of selective blockade of talin-dependent integrin alpha IIb beta 3 (platelet GPIIb-IIIa) activation. *J Clin Invest*. 2007;117:2250-9.
168. Haling JR, Monkley SJ, Critchley DR and Petrich BG. Talin-dependent integrin activation is required for fibrin clot retraction by platelets. *Blood*. 2011;117:1719-22.
169. Sun H, Lagarrigue F, Gingras AR, Fan Z, Ley K and Ginsberg MH. Transmission of integrin beta7 transmembrane domain topology enables gut lymphoid tissue development. *J Cell Biol*. 2018;217:1453-1465.
170. Stefanini L, Ye F, Snider AK, Sarabakhsh K, Piatt R, Paul DS, Bergmeier W and Petrich BG. A talin mutant that impairs talin-integrin binding in platelets decelerates alphaIIbbeta3 activation without pathological bleeding. *Blood*. 2014;123:2722-31.
171. Monkley SJ, Pritchard CA and Critchley DR. Analysis of the mammalian talin2 gene TLN2. *Biochem Biophys Res Commun*. 2001;286:880-5.
172. Senetar MA and McCann RO. Gene duplication and functional divergence during evolution of the cytoskeletal linker protein talin. *Gene*. 2005;362:141-52.
173. Debrand E, Conti FJ, Bate N, Spence L, Mazzeo D, Pritchard CA, Monkley SJ and Critchley DR. Mice carrying a complete deletion of the talin2 coding sequence are viable and fertile. *Biochem Biophys Res Commun*. 2012;426:190-5.
174. Kopp PM, Bate N, Hansen TM, Brindle NP, Praekelt U, Debrand E, Coleman S, Mazzeo D, Goult BT, Gingras AR, Pritchard CA, Critchley DR and Monkley SJ. Studies on the morphology and spreading of human endothelial cells define key inter- and intramolecular interactions for talin1. *Eur J Cell Biol*. 2010;89:661-73.
175. Chen NT and Lo SH. The N-terminal half of talin2 is sufficient for mouse development and survival. *Biochem Biophys Res Commun*. 2005;337:670-6.

176. Monkley SJ, Kostourou V, Spence L, Petrich B, Coleman S, Ginsberg MH, Pritchard CA and Critchley DR. Endothelial cell talin1 is essential for embryonic angiogenesis. *Dev Biol*. 2011;349:494-502.
177. Bergers G and Benjamin LE. Tumorigenesis and the angiogenic switch. *Nat Rev Cancer*. 2003;3:401-10.
178. Foubert P and Varner JA. Integrins in tumor angiogenesis and lymphangiogenesis. *Methods Mol Biol*. 2012;757:471-86.
179. Bledzka K, Bialkowska K, Sossey-Alaoui K, Vaynberg J, Pluskota E, Qin J and Plow EF. Kindlin-2 directly binds actin and regulates integrin outside-in signaling. *J Cell Biol*. 2016;213:97-108.
180. Law DA, Nannizzi-Alaimo L and Phillips DR. Outside-in integrin signal transduction. Alpha IIb beta 3-(GP IIb IIIa) tyrosine phosphorylation induced by platelet aggregation. *J Biol Chem*. 1996;271:10811-5.
181. Pulous FE, Grimsley-Myers CM, Kansal S, Kowalczyk AP and Petrich BG. Talin-Dependent Integrin Activation Regulates VE-Cadherin Localization and Endothelial Cell Barrier Function. *Circ Res*. 2019;124:891-903.
182. Wang Y, Nakayama M, Pitulescu ME, Schmidt TS, Bochenek ML, Sakakibara A, Adams S, Davy A, Deutsch U, Luthi U, Barberis A, Benjamin LE, Makinen T, Nobes CD and Adams RH. Ephrin-B2 controls VEGF-induced angiogenesis and lymphangiogenesis. *Nature*. 2010;465:483-6.
183. Monvoisin A, Alva JA, Hofmann JJ, Zovein AC, Lane TF and Iruela-Arispe ML. VE-cadherin-CreERT2 transgenic mouse: a model for inducible recombination in the endothelium. *Dev Dyn*. 2006;235:3413-22.
184. Pitulescu ME, Schmidt I, Benedito R and Adams RH. Inducible gene targeting in the neonatal vasculature and analysis of retinal angiogenesis in mice. *Nat Protoc*. 2010;5:1518-34.
185. Zudaire E, Gambardella L, Kurcz C and Vermeren S. A computational tool for quantitative analysis of vascular networks. *PLoS One*. 2011;6:e27385.
186. Anthis NJ, Haling JR, Oxley CL, Memo M, Wegener KL, Lim CJ, Ginsberg MH and Campbell ID. Beta integrin tyrosine phosphorylation is a conserved mechanism for regulating talin-induced integrin activation. *J Biol Chem*. 2009;284:36700-10.
187. Gingras AR, Bate N, Goult BT, Patel B, Kopp PM, Emsley J, Barsukov IL, Roberts GC and Critchley DR. Central region of talin has a unique fold that binds vinculin and actin. *J Biol Chem*. 2010;285:29577-87.
188. Gingras AR, Bate N, Goult BT, Hazelwood L, Canestrelli I, Grossmann JG, Liu H, Putz NS, Roberts GC, Volkmann N, Hanein D, Barsukov IL and Critchley DR. The structure of the C-terminal actin-binding domain of talin. *EMBO J*. 2008;27:458-69.
189. Atherton P, Stutchbury B, Wang DY, Jethwa D, Tsang R, Meiler-Rodriguez E, Wang P, Bate N, Zent R, Barsukov IL, Goult BT, Critchley DR and Ballestrem C. Vinculin controls talin engagement with the actomyosin machinery. *Nat Commun*. 2015;6:10038.
190. Dejana E and Vestweber D. The role of VE-cadherin in vascular morphogenesis and permeability control. *Prog Mol Biol Transl Sci*. 2013;116:119-44.
191. Komarova YA, Kruse K, Mehta D and Malik AB. Protein Interactions at Endothelial Junctions and Signaling Mechanisms Regulating Endothelial Permeability. *Circ Res*. 2017;120:179-206.

192. Spadoni I, Fornasa G and Rescigno M. Organ-specific protection mediated by cooperation between vascular and epithelial barriers. *Nat Rev Immunol*. 2017;17:761-773.
193. Shechter R, London A and Schwartz M. Orchestrated leukocyte recruitment to immune-privileged sites: absolute barriers versus educational gates. *Nat Rev Immunol*. 2013;13:206-18.
194. Giannotta M, Trani M and Dejana E. VE-cadherin and endothelial adherens junctions: active guardians of vascular integrity. *Developmental Cell*. 2013;26:441-54.
195. Hynes RO, Lively JC, McCarty JH, Taverna D, Francis SE, Hodivala-Dilke K and Xiao Q. The diverse roles of integrins and their ligands in angiogenesis. *Cold Spring Harbor symposia on quantitative biology*. 2002;67:143-53.
196. Lei L, Liu D, Huang Y, Jovin I, Shai SY, Kyriakides T, Ross RS and Giordano FJ. Endothelial expression of beta1 integrin is required for embryonic vascular patterning and postnatal vascular remodeling. *Molecular and Cellular Biology*. 2008;28:794-802.
197. Zovein AC, Luque A, Turlo KA, Hofmann JJ, Yee KM, Becker MS, Fassler R, Mellman I, Lane TF and Iruela-Arispe ML. Beta1 integrin establishes endothelial cell polarity and arteriolar lumen formation via a Par3-dependent mechanism. *Developmental Cell*. 2010;18:39-51.
198. Ye F, Kim C and Ginsberg MH. Molecular mechanism of inside-out integrin regulation. *J Thromb Haemost*. 2011;9 Suppl 1:20-25.
199. Klann JE, Remedios KA, Kim SH, Metz PJ, Lopez J, Mack LA, Zheng Y, Ginsberg MH, Petrich BG and Chang JT. Talin Plays a Critical Role in the Maintenance of the Regulatory T Cell Pool. *J Immunol*. 2017;198:4639-4651.
200. Yago T, Petrich BG, Zhang N, Liu Z, Shao B, Ginsberg MH and McEver RP. Blocking neutrophil integrin activation prevents ischemia-reperfusion injury. *J Exp Med*. 2015;212:1267-81.
201. Monkley SJ, Kostourou V, Spence L, Petrich B, Coleman S, Ginsberg MH, Pritchard CA and Critchley DR. Endothelial cell talin1 is essential for embryonic angiogenesis. *Developmental Biology*. 2011;349:494-502.
202. Pitulescu ME, Schmidt I, Benedito R and Adams RH. Inducible gene targeting in the neonatal vasculature and analysis of retinal angiogenesis in mice. *Nature Protocols*. 2010;5:1518-34.
203. Lakshmikanthan S, Sobczak M, Chun C, Henschel A, Dargatz J, Ramchandran R and Chrzanowska-Wodnicka M. Rap1 promotes VEGFR2 activation and angiogenesis by a mechanism involving integrin alphavbeta(3). *Blood*. 2011;118:2015-26.
204. Claxton S, Kostourou V, Jadeja S, Chambon P, Hodivala-Dilke K and Fruttiger M. Efficient, inducible Cre-recombinase activation in vascular endothelium. *genesis*. 2008;46:74-80.
205. Kopp PM, Bate N, Hansen TM, Brindle NP, Praekelt U, Debrand E, Coleman S, Mazzeo D, Goult BT, Gingras AR, Pritchard CA, Critchley DR and Monkley SJ. Studies on the morphology and spreading of human endothelial cells define key inter- and intramolecular interactions for talin1. *European Journal of Cell Biology*. 2010;89:661-73.
206. Aird WC. Vascular bed-specific hemostasis: role of endothelium in sepsis pathogenesis. *Crit Care Med*. 2001;29:S28-34; discussion S34-5.
207. Obermeier B, Daneman R and Ransohoff RM. Development, maintenance and disruption of the blood-brain barrier. *Nat Med*. 2013;19:1584-96.
208. Reese TS and Karnovsky MJ. Fine structural localization of a blood-brain barrier to exogenous peroxidase. *J Cell Biol*. 1967;34:207-17.

209. Kaur C, Foulds WS and Ling EA. Blood-retinal barrier in hypoxic ischaemic conditions: basic concepts, clinical features and management. *Prog Retin Eye Res*. 2008;27:622-47.
210. Kim JH, Kim JH, Yu YS, Kim DH and Kim KW. Recruitment of pericytes and astrocytes is closely related to the formation of tight junction in developing retinal vessels. *J Neurosci Res*. 2009;87:653-9.
211. Kamba T, Tam BY, Hashizume H, Haskell A, Sennino B, Mancuso MR, Norberg SM, O'Brien SM, Davis RB, Gowen LC, Anderson KD, Thurston G, Joho S, Springer ML, Kuo CJ and McDonald DM. VEGF-dependent plasticity of fenestrated capillaries in the normal adult microvasculature. *Am J Physiol Heart Circ Physiol*. 2006;290:H560-76.
212. Yang Y, Zhang Y, Cao Z, Ji H, Yang X, Iwamoto H, Wahlberg E, Lanne T, Sun B and Cao Y. Anti-VEGF- and anti-VEGF receptor-induced vascular alteration in mouse healthy tissues. *Proc Natl Acad Sci U S A*. 2013;110:12018-23.
213. Mahabeleshwar GH and Byzova TV. Vascular integrin signaling. *Methods Enzymol*. 2008;443:199-226.
214. Plow EF, Meller J and Byzova TV. Integrin function in vascular biology: a view from 2013. *Curr Opin Hematol*. 2014;21:241-7.
215. Stan RV, Tse D, Deharvengt SJ, Smits NC, Xu Y, Luciano MR, McGarry CL, Buitendijk M, Nemani KV, Elgueta R, Kobayashi T, Shipman SL, Moodie KL, Daghlian CP, Ernst PA, Lee HK, Suriawinata AA, Schned AR, Longnecker DS, Fiering SN, Noelle RJ, Gimi B, Shworak NW and Carriere C. The diaphragms of fenestrated endothelia: gatekeepers of vascular permeability and blood composition. *Dev Cell*. 2012;23:1203-18.
216. Parsons JT, Horwitz AR and Schwartz MA. Cell adhesion: integrating cytoskeletal dynamics and cellular tension. *Nat Rev Mol Cell Biol*. 2010;11:633-43.
217. Mui KL, Chen CS and Assoian RK. The mechanical regulation of integrin-cadherin crosstalk organizes cells, signaling and forces. *Journal of Cell Science*. 2016;129:1093-100.
218. Goult BT, Zacharchenko T, Bate N, Tsang R, Hey F, Gingras AR, Elliott PR, Roberts GC, Ballestrem C, Critchley DR and Barsukov IL. RIAM and vinculin binding to talin are mutually exclusive and regulate adhesion assembly and turnover. *J Biol Chem*. 2013;288:8238-49.
219. Reynolds LE and Hodivala-Dilke KM. Primary mouse endothelial cell culture for assays of angiogenesis. *Methods Mol Med*. 2006;120:503-9.
220. Steri V, Ellison TS, Gontarczyk AM, Weilbaecher K, Schneider JG, Edwards D, Fruttiger M, Hodivala-Dilke KM and Robinson SD. Acute depletion of endothelial beta3-integrin transiently inhibits tumor growth and angiogenesis in mice. *Circulation Research*. 2014;114:79-91.
221. Lakshmikanthan S, Sobczak M, Li Calzi S, Shaw L, Grant MB and Chrzanowska-Wodnicka M. Rap1B promotes VEGF-induced endothelial permeability and is required for dynamic regulation of the endothelial barrier. *J Cell Sci*. 2018;131.
222. Livak KJ and Schmittgen TD. Analysis of relative gene expression data using real-time quantitative PCR and the 2(-Delta Delta C(T)) Method. *Methods*. 2001;25:402-8.
223. Goodman SL and Picard M. Integrins as therapeutic targets. *Trends Pharmacol Sci*. 2012;33:405-12.
224. Tucci M, Stucci S and Silvestris F. Does cilengitide deserve another chance? *Lancet Oncol*. 2014;15:e584-e585.
225. Stupp R, Hegi ME, Gorlia T, Erridge SC, Perry J, Hong YK, Aldape KD, Lhermitte B, Pietsch T, Grujicic D, Steinbach JP, Wick W, Tarnawski R, Nam DH, Hau P, Weyerbrock A, Taphoorn MJ,

Shen CC, Rao N, Thurzo L, Herrlinger U, Gupta T, Kortmann RD, Adamska K, McBain C, Brandes AA, Tonn JC, Schnell O, Wiegel T, Kim CY, Nabors LB, Reardon DA, van den Bent MJ, Hicking C, Markivskyy A, Picard M, Weller M, European Organisation for R, Treatment of C, Canadian Brain Tumor C and team Cs. Cilengitide combined with standard treatment for patients with newly diagnosed glioblastoma with methylated MGMT promoter (CENTRIC EORTC 26071-22072 study): a multicentre, randomised, open-label, phase 3 trial. *Lancet Oncol*. 2014;15:1100-8.
226. Eisele G, Wick A, Eisele AC, Clement PM, Tonn J, Tabatabai G, Ochsenbein A, Schlegel U, Neyns B, Krex D, Simon M, Nikkhah G, Picard M, Stupp R, Wick W and Weller M. Cilengitide treatment of newly diagnosed glioblastoma patients does not alter patterns of progression. *J Neurooncol*. 2014;117:141-5.
227. Turley TN, Theis JL, Sundsbak RS, Evans JM, O'Byrne MM, Gulati R, Tweet MS, Hayes SN and Olson TM. Rare Missense Variants in TLN1 Are Associated With Familial and Sporadic Spontaneous Coronary Artery Dissection. *Circ Genom Precis Med*. 2019;12:e002437.
228. Becam IE, Tanentzapf G, Lepesant JA, Brown NH and Huynh JR. Integrin-independent repression of cadherin transcription by talin during axis formation in Drosophila. *Nat Cell Biol*. 2005;7:510-6.
229. Kragl M, Schubert R, Karsjens H, Otter S, Bartosinska B, Jeruschke K, Weiss J, Chen C, Alsteens D, Kuss O, Speier S, Eberhard D, Muller DJ and Lammert E. The biomechanical properties of an epithelial tissue determine the location of its vasculature. *Nat Commun*. 2016;7:13560.
230. Mahabeleshwar GH, Chen J, Feng W, Somanath PR, Razorenova OV and Byzova TV. Integrin affinity modulation in angiogenesis. *Cell Cycle*. 2008;7:335-47.
231. Camilleri M. Leaky gut: mechanisms, measurement and clinical implications in humans. *Gut*. 2019;68:1516-1526.
232. Dong JM, Tay FP, Swa HL, Gunaratne J, Leung T, Burke B and Manser E. Proximity biotinylation provides insight into the molecular composition of focal adhesions at the nanometer scale. *Sci Signal*. 2016;9:rs4.
233. Branon TC, Bosch JA, Sanchez AD, Udeshi ND, Svinkina T, Carr SA, Feldman JL, Perrimon N and Ting AY. Efficient proximity labeling in living cells and organisms with TurboID. *Nat Biotechnol*. 2018;36:880-887.
234. Dumbauld DW, Lee TT, Singh A, Scrimgeour J, Gersbach CA, Zamir EA, Fu J, Chen CS, Curtis JE, Craig SW and Garcia AJ. How vinculin regulates force transmission. *Proc Natl Acad Sci U S A*. 2013;110:9788-93.